Distribution and Behavior of the Lithogenic Tracers Aluminium and Titanium in the Upper Water Column of the Atlantic Ocean

Dissertation

zur Erlangung des Doktorgrades

an der Mathematisch-Naturwissenschaftlichen Fakultät

der Christian-Albrechts-Universität zu Kiel

vorgelegt von

Anna Dammshäuser

Kiel, 2012

Referent:	Prof. Dr. A. Körtzinger
Koreferent:	Prof. Dr. D. W. R. Wallace
Tag der mündlichen Prüfung:	10.02.2012
Zum Druck genehmigt:	10.02.2012

gez. Prof. Dr. Lutz Kipp, Dekan

Hiermit erkläre ich, dass ich die vorliegende Doktorarbeit - abgesehen von der Beratung durch meine Betreuer - selbstständig und ohne Zuhilfenahme unerlaubter Hilfsmittel erstellt habe. Alle benutzten Quellen habe ich vollständig angeben. Weder diese noch eine ähnliche Arbeit wurden an einer anderen Abteilung oder Hochschule im Rahmen eines Prüfungsverfahrens vorgelegt, veröffentlicht oder zur Veröffentlichung vorgelegt. Ferner versichere ich, dass die Arbeit unter Einhaltung der Regeln guter wissenschaftlicher Praxis der Deutschen Forschungsgemeinschaft entstanden ist.

Kiel,.....

Anna Dammshäuser

Contents

Kurzfassung **3**

Abstract **7**

1 Scientific Background **9**

1.1 Atmospheric transport of material to the ocean 9

1.2 Oceanic distributions of Al and Ti 11

1.3 Input pathways of Al and Ti to the surface ocean 13

1.3.1 Fluvial inputs 14

1.3.2 Inputs from shelf sources 14

1.3.3 Atmospheric inputs 15

1.4 Surface Ocean processes of Al and Ti 16

1.4.1 Speciation and size distribution 17

1.4.2 Removal processes 17

1.5 Objectives and thesis outline 19

1.6 References 20

2 Study Area **27**

3 Surface Water Dissolved Aluminium and Titanium: Tracers for Specific Time Scales of Dust Deposition to the Atlantic? **31**

3.1 Introduction 32

3.2 Methods 32

3.3 Results and discussion 33

3.3.1 Residence times of dAl and dTi 35

3.3.2 Relationship between dAl and dTi surface water concentrations and dust deposition 36

3.4 Conclusions 40

3.5 References 40

3.6 Auxiliary material 43

4 Low Colloidal Associations of Aluminium and Titanium in Surface Waters of the Tropical Atlantic **47**

4.1 Introduction 48

4.2 Methods ... 49
4.2.1 Sampling ... 50
4.2.2 Size fractionation by cross-flow ultrafiltration ... 51
4.2.3 Analytical procedures ... 52
4.2.4 Calculation of the colloidal fraction and mass balance ... 53
4.3 Results and method evaluation ... 54
4.3.1 Size fractionation by cross-flow ultrafiltration ... 54
4.3.2 Mass balance and calculation of colloidal Al ... 55
4.3.3 Calculation of colloidal Ti ... 58
4.3.4 Spatial distributions of Al and Ti ... 60
4.4 Discussion ... 60
4.4.1 Spatial distributions of Al and Ti ... 60
4.4.2 Size distributions of Al and Ti in seawater ... 64
4.4.3 Residence times of Al and Ti in surface waters and role of the colloidal pool ... 67
4.5 Conclusions ... 70
4.6 References ... 71

5 Particulate and Dissolved Aluminium and Titanium in the Upper Water Column of the Atlantic Ocean ... 77

5.1 Introduction ... 78
5.2 Methods ... 80
5.2.1 Dissolved fractions ... 81
5.2.2 Particulate fractions ... 81
5.2.3 Ancillary data ... 85
5.3 Results ... 85
5.3.1 Aluminium ... 85
5.3.2 Titanium ... 88
5.4 Discussion ... 89
5.4.1 Distributions of Al and Ti in the Atlantic Ocean ... 89
5.4.2 Residence times ... 93
5.4.3 Partitioning between the particulate and dissolved fractions ... 96
5.5 Conclusions ... 98
5.6 References ... 99

6 Synthesis ... 103

Acknowledgements ... 105

Curriculum Vitae ... 107

Kurzfassung

In vielen Regionen des offenen Ozeans werden biogeochemische Prozesse in der oberen Wassersäule maßgeblich durch den Eintrag von mineralischen Partikeln aus der Atmosphäre (Staub) beeinflusst. Diese atmosphärischen Einträge sind bislang jedoch schlecht quantifiziert. In früheren Studien wurde gelöstes Aluminium (Al) als Tracer für Staubeinträge verwendet, wobei räumliche Unterschiede in den Verweilzeiten und in der Löslichkeit von Al eine genaue Abschätzung des Eintrags erschwerten. Diese Dissertation untersucht die potentielle Eignung des lithogenen Elements Titan (Ti) als komplementärer Staubtracer zu Al. Zu diesem Zweck ist ein detailliertes Verständnis des ozeanischen Verhaltens von Al und Ti während und nach dem Eintrag durch Staub notwendig. Die Ziele der Arbeit liegen daher darin, die Zusammenhänge zwischen Staubeinträgen und den Verteilungen von Al und Ti, sowie Entfernungsprozesse und Verweilzeiten der beiden Metalle in der oberen Schicht des Ozeans (200 m) besser zu verstehen.

Das erste Manuskript dieser Dissertation beschäftigt sich mit den Konzentrationen von gelöstem Al und Ti entlang eines meridionalen Transekts im Atlantik (Kapitel 3). Trotz ihres gemeinsamen Vorkommens im Staub waren beide Metalle spezifisch im Oberflächenwasser verteilt, was auf unterschiedliche Prozesse während und nach dem Eintrag hinweist. Im Fall von Al wurden Hinweise darauf gefunden, dass sich die Löslichkeit aus Saharastaub während des Eintrags durch nasse Deposition erhöht. Im Fall von Ti stimmten die gelösten Konzentrationen im nordatlantischen Oberflächenwasser gut mit dem Muster des mittleren jährlichen Staubeintrags überein. Im Südatlantik zeigten nur die gelösten Ti, nicht aber die Al Konzentrationen den Eintrag von Staub aus Patagonien an. Niedrige Konzentrationen an gelöstem Al können hier auf die schnelle Entfernung durch Scavenging an biogenen Partikeln zurückgeführt werden. Die spezifischen Verteilungen und Verweilzeitabschätzungen deuten darauf hin, dass die Konzentrationen von Al und Ti Staubeinträge über unterschiedliche Zeitskalen widerspiegeln. Gelöste Al Konzentrationen könnten als Tracer für saisonale Variationen im Staubeintrag dienen, wohingegen gelöste Ti Konzentrationen Aufschluss über Variationen im Staubeintrag über längere Zeitskalen geben könnten.

Im zweiten Manuskript wird die Verteilung von gelöstem (<0,2 µm), echt gelöstem (<10 kDa) und kolloidalem (10 kDa - 0,2 µm) Al und Ti in der oberen Wassersäule des

östlichen tropischen Nordatlantiks untersucht (Kapitel 4). Beide Metalle lagen zum Großteil in der echt gelösten Phase vor und es wurden nur in sehr geringem Maße kolloidale Assoziationen gefunden. Diese Ergebnisse stehen im Gegensatz zu früheren Schätzungen für Ti und zum vorwiegenden Vorkommen beider Metalle als hydrolysierte und hoch partikelreaktive Spezies in Seewasser. Die Größenverteilung kann dadurch erklärt werden, dass Al und Ti geringe Tendenz dazu aufweisen anorganische oder organische Kolloide zu bilden, da sie innerhalb ihrer Löslichkeitsgrenzen in Seewasser vorliegen und bisher auch keine Affinität zur Bildung von organischen Komplexen bekannt ist. Die vertikalen Verteilungen von gelöstem (und echt gelöstem) Al und Ti spiegelten den vorwiegenden Eintrag aus atmosphärischen Quellen sowie schnelle Entfernung aus der oberen Wassersäule wider. Im Fall von Al wurde eine Abnahme um 80 - 90 % zwischen den Oberflächenmaxima und den Minima unterhalb der Oberfläche festgestellt. Die Verweilzeiten in den oberen 100 m der Wassersäule lagen zwischen 1,6 und 4 Jahren bei gelöstem Al und zwischen 14 und 17 Jahren bei gelöstem Ti. Diese kurzen Verweilzeiten stehen im Gegensatz zur geringen kolloidalen Assoziation von Al und Ti, wenn man die angenommene Rolle von Kolloiden als Zwischenprodukt im Entfernungsprozess berücksichtigt. Dies legt nahe, dass der Transfer von der echt gelösten in die partikuläre Phase entweder durch schnellen Umsatz der kolloidalen Phase oder durch direkte Adsorption an Partikeloberflächen geschieht.

Das dritte Manuskript dieser Dissertation beschäftigt sich schließlich mit der Verteilung von Al und Ti zwischen der gelösten und partikulären Phase in den oberen 200 m des tropischen und subtropischen Atlantik (Kapitel 5). In beiden Größenfraktionen spiegelte die räumliche und vertikale Verteilung Al und Ti den Eintrag durch atmosphärische Quellen wider. Des Weiteren konnten verstärkte Entfernungsprozesse von Al und Ti mit erhöhter biologischer Produktivität in Verbindung gebracht werden. In der gelösten Phase kann solche verstärkte Entfernung durch Adsorptions- und Aggregationsmechanismen an biogenen Partikeloberflächen begründet sein. In der partikulären Phase kann biologische Produktivität die Entfernungsraten durch die Bildung von großen, schnell sinkenden Partikeln erhöhen. Die Verweilzeiten in der partikulären Phase lagen im tropischen und subtropischen Nordatlantik zwischen 3 und 22 Tagen bei Al und zwischen 4 und 37 Tagen bei Ti. In der gelösten Phase stimmten die Verweilzeiten mit vorhergehend abgeschätzten Werten überein. Im Südatlantik wurden deutlich längere Verweilzeiten in beiden Größenfraktionen gefunden, in Übereinstimmung mit der zu erwartenden niedrigeren biologischen Produktivität in dieser Region. Insgesamt unterschied sich die Verteilung

zwischen der gelösten und partikulären Phase deutlich für Al und Ti. Der Großteil des Al lag gelöst vor, wohingegen Ti vorwiegend partikulär vorkam. Im Oberflächenwasser deuteten die Elementverhältnisse von gelöstem und partikulärem Al und Ti außerdem auf eine erhöhte Löslichkeit von Al aus atmosphärischen mineralischen Partikeln hin, und damit auf erhöhten Eintrag von Al in gelöster Form im Vergleich zu Ti.

Ein wichtiges Ergebnis dieser Dissertation ist die potentielle Eignung von gelösten Ti Konzentrationen im Oberflächenwasser als komplementärer Staubtracer zu Al. Beide Metalle spiegeln unterschiedliche Zeitskalen des Staubeintrags wider. Des Weiteren beleuchtet diese Dissertation die Entfernungsprozesse und Verweilzeiten von Al und Ti in verschiedenen Regionen des Atlantischen Ozeans, die sich hinsichtlich der atmosphärischen Einträge und biologischen Produktivität deutlich unterscheiden. Dieses Wissen bietet eine Basis für zukünftige Abschätzungen der Staubdeposition anhand von Oberflächenwasserkonzentrationen beider Metalle. Eine große Unsicherheit in derartigen Abschätzungen ist allerdings nach wie vor die Löslichkeit von Al und Ti aus atmosphärischen mineralischen Partikeln. Die Bestimmung der löslichen Fraktionen von Al und Ti in Proben von atmosphärischen mineralischen Partikeln sollte daher das Ziel zukünftiger Studien sein.

Abstract

Inputs of atmospheric mineral particles (dust) are known to strongly influence biogeochemical processes in many regions of the ocean. However, dust inputs to the ocean are yet poorly quantified. In previous studies, dissolved aluminium (Al) concentrations have been utilized as dust tracer, but poorly constrained oceanic residence times and soluble dust fractions of Al complicate an exact estimation of dust inputs. This thesis examines the potential suitability of the lithogenic element titanium (Ti) as dust tracer, analog or complementary to Al. For this purpose, detailed knowledge of the behavior of Al and Ti during and after their input from the dust is required. The aims of this work are to better constrain the relationship between Al and Ti concentrations and atmospheric inputs, as well as their removal processes and residence times in the surface ocean.

The first manuscript focuses on surface water concentrations of dissolved Al and Ti along a meridional Atlantic transect (Chapter 3). The distributions of both metals reveal distinct relationships to dust inputs. For Al, evidence was found for increased dissolution from Saharan dust during wet deposition. In the case of Ti, the distribution in the North Atlantic was closely related to the pattern of annual dust deposition. In the South Atlantic, dissolved Ti concentrations reflected the input of Patagonian dust whereas Al concentrations did not. Here, for dissolved Al evidence was found for fast scavenging removal onto biogenic particles. The specific distributions and residence time estimates indicate that Al and Ti concentrations are related to dust inputs over different time scales. Dissolved Al concentrations may serve to trace seasonal variations in dust deposition, while dissolved Ti concentrations may serve to trace the dust deposition over longer temporal scales.

In the second manuscript, the distributions of dissolved (<0.2 μm), soluble (<10 kDa) and colloidal (10 kDa - 0.2 μm) Al and Ti in the upper water column of the eastern tropical North Atlantic are examined (Chapter 4). The size distributions of both metals were clearly dominated by the soluble phase, and very little colloidal associations were found. The results are in contrast to previous estimates for Ti and to the predominant occurrence of both metals as hydrolyzed and highly particle reactive species in seawater. The size distributions can be explained by low tendencies to form organic or inorganic colloids, as Al and Ti occurred within their inorganic solubility levels and are not known to form organic complexes in seawater. The vertical distributions of dissolved (and soluble) Al and

Ti reflected the predominant supply from atmospheric sources and extensive removal processes in the upper water column. Dissolved Al concentrations decreased by 80 - 90 % from the surface maxima to the subsurface minima. Residence times in the upper 100 m of the ocean were 1.6 - 4 years for dissolved Al and 14 - 17 years for dissolved Ti. These short residence times are in contrast to the low colloidal associations of Al and Ti, given the assumed role of colloids as intermediates in scavenging processes. This suggests that the transfer from the soluble into the particulate phase occurs either via rapid turnover of the colloidal phase or via direct adsorption onto particle surfaces.

Finally, the third manuscript focuses on the partitioning of Al and Ti between the dissolved and the particulate phase in the upper 200 m of the tropical and subtropical Atlantic (Chapter 5). In both size fractions, the spatial and vertical distributions of Al and Ti reflected their input from atmospheric sources. Moreover, decreased concentrations of Al and Ti can be related to elevated biological productivity. In the dissolved phase, this relation is likely due to increased removal via adsorption and aggregation processes on biogenic particle surfaces. In the particulate phase, biological productivity may increase removal rates via the formation of large, rapidly sinking biogenic particles. Estimated residence times in the tropical and subtropical North Atlantic were 3 - 22 days for particulate Al and 4 - 37 days for particulate Ti. Those in the dissolved phase agreed with previously estimated values. In the South Atlantic, significantly longer residence times were found in both size fractions, in agreement with the expected lower biological productivity in this region. The partitioning between the dissolved and particulate phase was markedly different for Al and Ti, with Al occurring predominantly in the dissolved phase and Ti being mostly present in the particulate phase. In surface waters, elemental ratios of dissolved and particulate Al and Ti indicate elevated dissolution of Al from atmospheric mineral particles and thus elevated input of dissolved Al compared to Ti.

A major finding of this thesis is the potential suitability of surface water dissolved Ti concentrations as complementary dust tracer to Al, with both metals reflecting different time scales of dust deposition. Moreover, this thesis provides detailed insights into removal processes and residence times of Al and Ti in regions of the Atlantic Ocean that largely differ in atmospheric inputs and biological productivity. This knowledge provides a basis for future estimations of dust deposition from surface water concentrations of both metals. However, the solubilities of Al and Ti from atmospheric mineral particles remain a major uncertainty in such estimations. Determining the fractional dissolution of Al and Ti from sampled atmospheric mineral particles should thus be an aim of future studies.

1 Scientific Background

The present thesis focuses on the relationship between aluminium (Al) and titanium (Ti) concentrations and atmospheric inputs to the surface ocean, and examines the behavior of both metals upon their atmospheric delivery into the upper water column. This general introduction first gives an overview of the mechanisms and the relevance of atmospheric inputs to the surface ocean. In the following chapters, the present knowledge of the oceanic distributions and the input and removal processes of Al and Ti in the surface ocean are recapitulated. Finally, the objectives of this thesis and an outline of the included manuscripts are presented.

1.1 Atmospheric transport of material to the ocean

The ocean receives inputs from its adjacent reservoirs, being the oceanic crust, the continental crust and the atmosphere. Atmospheric transport may occur in great distance from the coast and is thus a significant input pathway of material into the open ocean on a global scale. The atmosphere can supply essential nutrients for organisms into the surface ocean (such as Fe, Si, P and N) and is thus particularly important for biological processes in remote oceanic regions [e.g. Duce et al., 1991; Jickells, 1995; Jickells et al., 2005; Duce et al., 2008; Baker et al., 2010]. In the last two decades, the atmospheric delivery of iron has been a focus of intensive research, as iron has been found to limit primary productivity in large areas of the ocean [e.g. Martin et al., 1994; Behrenfeld and Kolber, 1999; Boyd et al., 2000; Krishnamurthy et al., 2009; Okin et al., 2011]. Iron inputs thus have been suggested to influence the global climate at geological time scales [Martin, 1990].

The transport of trace metals in the atmosphere occurs in the particulate form, or dissolved in cloud droplets. Iron and other trace metals such as Al and Ti are predominantly associated with the mineral particle phase [Duce et al., 1991]. Mineral particles mainly originate from large arid areas, where wind friction may lift easily erodible particles into the air [Mahowald et al., 2005]. On a global scale, the most relevant source regions of mineral particles are situated in the Northern Hemisphere, mainly in the large arid regions of North Africa, Asia and the Arabian peninsula [Chester, 2000; Jickells and Spokes, 2001; Prospero et al., 2002]. From their source, mineral particles can be transported in the

atmosphere over thousands of kilometers to remote oceanic regions, as has been illustrated via satellite images. The input to the surface ocean eventually occurs via dry and wet deposition. Dry deposition affects particles in the marine boundary layer and has the strongest influence close to the source regions due to the preferential gravitational settling of larger particles [Prospero, 1996; Mahowald et al., 2005]. Wet deposition is related to precipitation rates and is the more important removal mechanism in open ocean regions [Prospero, 1996]. Overall, dust deposition into the ocean occurs in sporadic and highly variable episodes. Field observations of both wet and dry deposition over the ocean are sparse due to the technical challenges of long term dust deposition measurements in oceanic regions. Given the spatial and temporal variability of deposition events, the supply of dust into the surface ocean is thus still poorly quantified [e.g. Duce et al., 1991; Prospero, 1996; Mahowald et al., 2005]. Global estimates of dust distribution and deposition are assessed in a number of different modeling approaches [Duce et al., 1991; Tegen and Fung, 1994; Luo et al., 2003; Ginoux et al., 2004]. Figure 1.1 shows the flux of mineral particles to the surface ocean for a 10-year average, derived from a recent composite model [Ginoux et al., 2001; Mahowald and Luo, 2003; Tegen et al., 2004; Jickells et al., 2005]. The results are in broad agreement with other model estimates and suggest that the major part of the global dust deposition occurs in the tropical and subtropical North Atlantic.

In an alternative approach to better assess the deposition, surface water dissolved Al (dAl) concentrations have been suggested as a tracer for dust inputs. Aluminium is a major and relatively invariant component of the earth's crust, with short residence times in the surface ocean [Orians and Bruland, 1986; Jickells, 1999; McLennan, 2001] and is not known to have essential biological functions. In previous studies, reasonable agreement has been observed between the surface ocean distribution of dAl and different dust deposition estimates [e.g. Measures and Vink, 2000; Gehlen et al., 2003; Han et al., 2008]. However, spatial variations in the residence times and in the dissolution of Al from the supplied mineral particles have to be considered if the dust deposition is inferred from surface water concentrations of dAl [Gehlen et al., 2003; Han et al., 2008]. In particular, the influence of biological productivity on the removal of dAl [e.g. Moran and Moore, 1988; Hydes, 1989; Gehlen et al., 2002; Koning et al., 2007] may bias the quantification of atmospheric inputs. This suggests that alternative or complementary tracers may provide more appropriate approaches to assess the dust deposition to the surface ocean. Titanium is similarly a major and relatively invariant component of the earth's crust [McLennan, 2001]

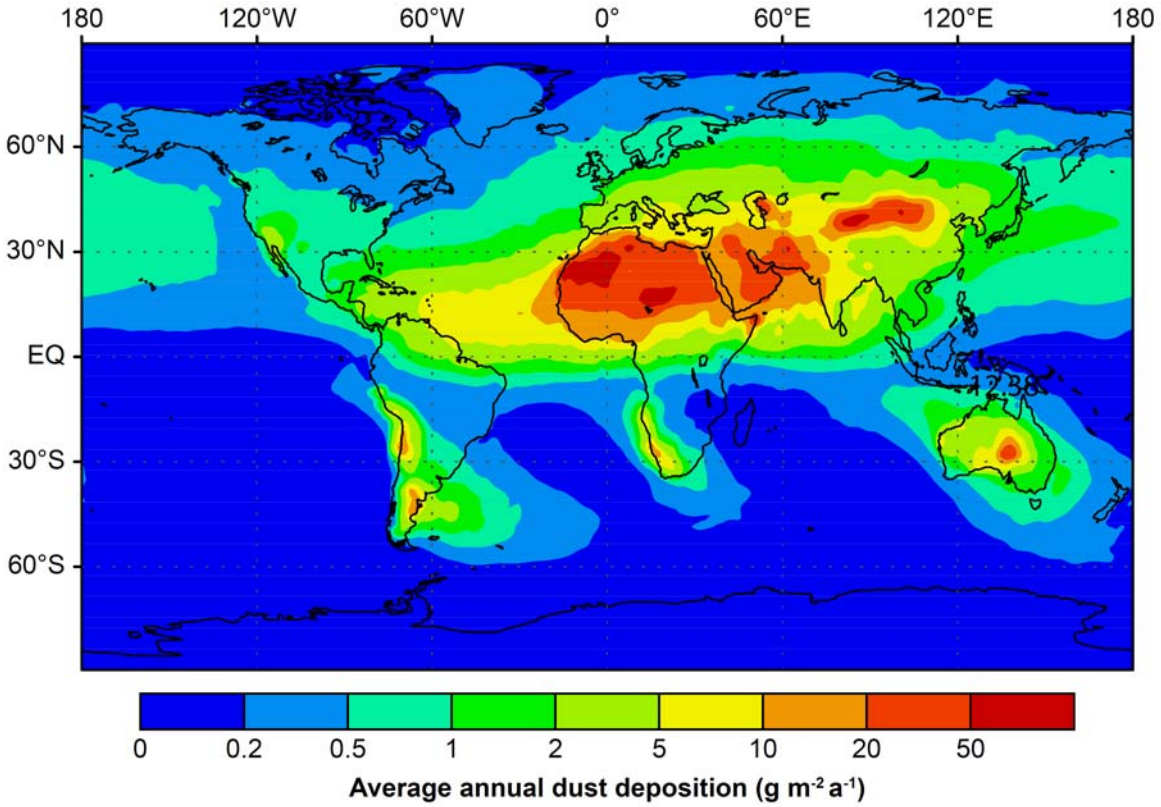

Fig. 1.1: Average annual dust deposition to the surface ocean (g m^{-2} a^{-1}; reprinted from Jickells et al., [2005]). The dust fluxes are based on a composite of three published modeling studies [Ginoux et al., 2001; Mahowald and Luo, 2003; Tegen et al., 2004].

and is not known as bioactive metal in the ocean. However, very little information is available on the oceanic distribution and behavior of Ti so far. The general aim of this thesis is therefore to better constrain the processes that affect the distribution, speciation and residence times of Al and Ti in the surface ocean and to evaluate their potential utilization as complementary dust tracers.

1.2 Oceanic distributions of Al and Ti

Aluminium and Ti are abundant elements in the earth's upper crust (Al: 8.04 %, Ti: 0.41 %) [McLennan, 2001], but yet present at very low concentrations in open ocean seawater. Concentrations of dAl are in the higher nM-range, whereas dissolved Ti (dTi) is present in the pM-range in the ocean [Bruland and Lohan, 2003]. Both elements go through related processes in the surface ocean, with their distributions being controlled by

the predominant input from atmospheric sources and the removal by scavenging mechanisms. This chapter gives an overview of the oceanic distributions of dAl and dTi, before sources, surface ocean processes and removal mechanisms are summarized in more detail in the Chapters 1.3 and 1.4.

Highest concentrations of dAl occur in regions of elevated dust input, with up to 100 nM in the Mediterranean [Hydes et al., 1988; Chou and Wollast, 1997] and up to 70 nM in the tropical North Atlantic [Measures, 1995]. By contrast, in regions receiving low dust deposition, e.g. the surface waters of the eastern Pacific [Duce et al., 1991], dAl concentrations lie below 5 nM [Orians and Bruland, 1986; Kaupp et al., 2011]. Depth profiles of dAl (Fig. 1.2) show typical scavenging type distributions with highest concentrations at the surface, mid-depth minima and increasing concentrations towards the sediment water interface [Hydes, 1979; Orians and Bruland, 1986]. As a consequence of the pronounced differences in the atmospheric supply and the increasing removal by scavenging processes with water mass age, the spatial distribution of dAl shows a strong inter-ocean fractionation, with 8 - 40 times higher concentrations in North Atlantic than in the North Pacific [Orians and Bruland, 1985]. In bottom waters, elevated concentrations of dAl can be explained by the release of dAl during remineralization processes [Orians and Bruland, 1986] or the supply of dAl from sediment resuspension [Moran and Moore, 1991]. In the upper water column, elevated dAl signals resulting from elevated benthic or atmospheric input may be laterally transported to regions with lower dAl supply [Measures et al., 2008; Slemons et al., 2010; Kaupp et al., 2011].

Very limited information is available on the oceanic distribution of dTi so far. Reported data are restricted to a few observations in the North Pacific [Orians et al., 1990], the western North Atlantic [Orians et al., 1990; Skrabal et al., 1992; Skrabal, 1995; Skrabal and Terry, 2002; Skrabal, 2006] and the Mediterranean [van den Berg et al., 1994]. This study adds new information on the distribution of dTi in the eastern tropical North Atlantic and in the South Atlantic. Similar to dAl, the distribution of dTi reflects its atmospheric supply to the open ocean [Orians et al., 1990; Skrabal, 2006]. Observed open ocean surface water concentrations are 100 - 200 pM in regions that receive elevated dust inputs [van den Berg et al., 1994; Skrabal, 2006] whereas dTi concentrations are much lower in regions that receive lower dust inputs, e.g. the subtropical gyres of the South Atlantic and Pacific [Orians et al., 1990]. Surface water concentrations in the North Pacific (4 - 8 pM) are significantly lower than in the North Atlantic [Orians et al., 1990]. The depth profiles of dTi (Fig. 1.2) from the North Pacific and North Atlantic show

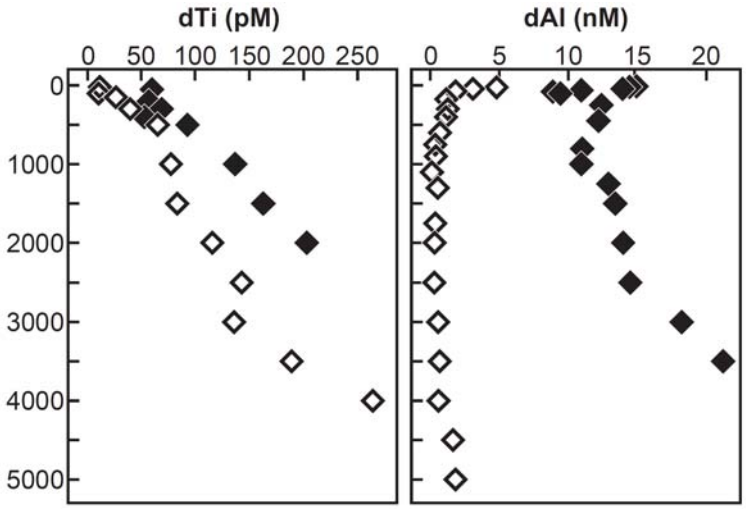

Fig. 1.2: Representative depth profiles of dTi and dAl in the Atlantic (black diamonds) and Pacific (open diamonds) Oceans. The distribution of dTi was reprinted from Orians et al. [1990] and shows stations at 32°N, 64°W and 50°N, 155°W. The distribution of dAl is displayed for stations at 28°N, 155°W (reprinted from Orians et al., [1986]) and 18 °N, 24 °W (determined during ANTXXVI-4, May 2010).

continuously increasing concentrations from the surface to the bottom waters [Orians et al., 1990]. However, despite the untypical depth profiles, the inter-ocean fractionation between Atlantic and Pacific waters suggests that the dTi distribution is controlled by scavenging processes. The elevated deep water concentrations of dTi indicate a strong benthic source [Orians et al., 1990], e.g. through resuspension or diagenetic processes. Evidence for the benthic supply of dTi has also been found for shelf sediments [Skrabal and Terry, 2002].

1.3 Input pathways of Al and Ti to the surface ocean

Major input processes that deliver trace metals to the surface ocean comprise fluvial inputs, the supply from shelf sources and atmospheric inputs. For riverine and shelf sources, a strong influence can be expected close to the land-ocean interface, whereas atmospheric inputs also occur in remote oceanic regions. An overview of the fluxes into and out of the oceanic reservoir is given in Fig. 1.3. Flux magnitudes are displayed only for Al, as few data are available for Ti so far. The specific supply mechanisms of Al and Ti are discussed below.

1.3.1 Fluvial inputs

In river water, the abundances of Al and Ti are two to three orders of magnitude higher than in seawater [e.g. Yokoi and Van den Berg, 1991; Skrabal et al., 1992; Chester, 2000; Upadhyay et al., 2002]. The major transport of Al and Ti in rivers occurs in the particulate form, with less than 1 % of the total Al and Ti being dissolved [Martin and Meybeck, 1979]. The riverine fractions of dissolved Al and Ti are to a large part present as colloids [Skrabal et al., 1992; Sañudo-Wilhelmy et al., 1996; Neal et al., 2011]. During estuarine mixing, the dissolved concentrations of Al and Ti significantly decrease due to the flocculation of the colloidal material with increasing salinity [e.g. Sholkovitz, 1978; Yokoi and Van den Berg, 1991; Skrabal et al., 1992; Skrabal, 1995; Sañudo-Wilhelmy et al., 1996]. During this process also the colloidal fractions of Al and Ti within the dissolved phase disappear [Sañudo-Wilhelmy et al., 1996; Skrabal and Terry, 2002]. The riverine particulate material is to a large part deposited in the estuarine and coastal zone [Bewers and Yeats, 1989; Brown and Bruland, 2009]. Therefore, the majority of the total riverine trace metal load is removed at the land-ocean interface before it actually reaches the open ocean. The estimation of net total river transport to the global ocean is complicated due to few available data and the complex processes occurring at the land-ocean interface [Bruland and Lohan, 2003]. Overall, the gross total river transport dominates the supply of trace metals to the global ocean [Chester, 2000]. For Al, it is estimated to be one to three orders of magnitude higher than the total atmospheric input [Chester, 2000; Rauch and Pacyna, 2009]. For Ti, no estimates are available so far; however similar relations to those of Al are likely. Assuming a removal of 90 % of the gross total riverine input to the coastal zone [Bewers and Yeats, 1989; Skrabal, 1995], the net total riverine flux can then be expected to still exceed atmospheric inputs. In addition, parts of the material deposited in coastal regions may be remobilized from the shelf and transported further offshore.

1.3.2 Inputs from shelf sources

The supply of trace metals from sedimentary sources occurs through resuspension of deposited material and fluxes across the benthic boundary. Both mechanisms have been suggested to contribute to increasing concentrations of Al and Ti in bottom waters and in shelf regions [e.g. Moran and Moore, 1991; Skrabal, 2002, Skrabal, 2006; Ussher et al., 2007]. In contrast to redox senitive trace metals such as Fe, Al and Ti do not experience redox transitions in the marine environment and their input from sedimentary sources is

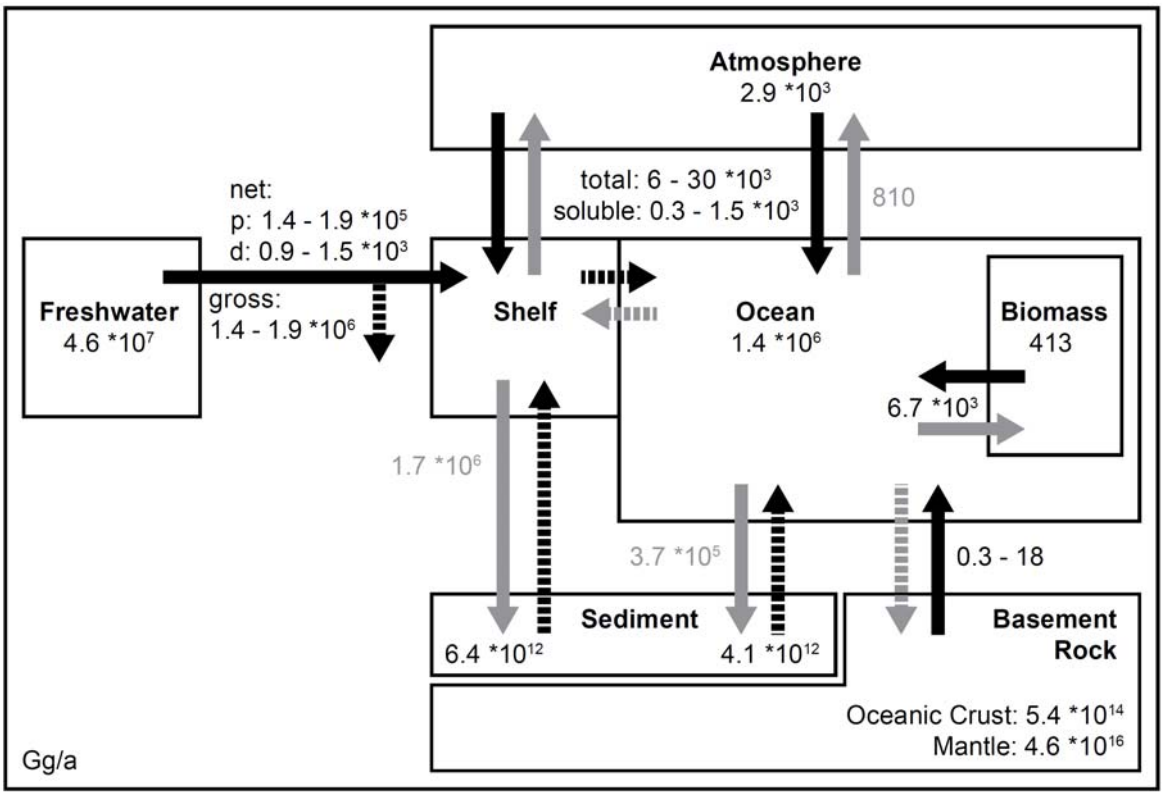

Fig. 1.3: Schematic overview of trace metal fluxes between the Ocean and adjacent reservoirs. For Al, estimates of flux magnitudes and reservoir inventories are given (dotted lines depict fluxes of unknown magnitudes). The given values are based on estimates compiled by Chester [2000] and Rauch and Pacyna [2009]. The soluble atmospheric flux was estimated as 5 % of the total atmospheric flux. The net riverine flux denominates the flux after estuarine removal, p = particulate, d = dissolved.

thus unlikely to be influenced by redox conditions in the water column. However, the supply of dAl and dTi may additionally be enhanced by upwelling processes, and onshore-offshore gradients of dAl and dTi suggest that the mobilized trace metals may be laterally transported from the shelf to open ocean regions [Skrabal, 2006; Slemons et al., 2010; Kaupp et al., 2011]. Driving physical mechanisms of such offshore transport may include tidal currents, eddies, Ekman transport and internal waves [Chester, 2000; Cullen et al., 2009]. The input of Al and Ti from shelf sources can be expected to have particular relevance in regions where low atmospheric inputs occur, e.g. the eastern Pacific. For surface waters, however, sedimentary inputs will have decreasing influence with distance from the coast.

1.3.3 Atmospheric inputs

Major carriers for the atmospheric transport of Al and Ti are mineral particles (also

referred to as mineral aerosols or dust) that derive from terrestrial origin [Duce et al., 1991]. Common mineral phases of Al are aluminosilicates and oxyhydroxides, whereas Ti mostly occurs in the form of oxides and silicates. The flux of trace metals into the water column is controlled by both the composition of the deposited particles and their soluble trace metal fractions. The composition of atmospheric mineral particles depends on their source region [e.g. Guieu et al., 2002; Moreno et al., 2006; Gaiero et al., 2007] and changes with physical and chemical processing during the atmospheric transport [Prospero, 1996; Shi et al., 2009]. In estimations of atmospheric inputs, the mineral particle composition is frequently assumed to equal the average crustal abundance, with 8.04 % of Al and 0.41 % of Ti [McLennan, 2001]. The soluble trace metal fractions are related to specific atmospheric and oceanic controls and are still poorly constrained. For example, the solubility of Al was found to increase with chemical processing during the atmospheric transport [Spokes et al., 1994; Measures et al., 2010] and with wet deposition, likely due to the lower pH in rainwater [Prospero et al., 1987]. In addition, the solubility may differ with the source region of the mineral particles [Baker et al., 2006]. Results from dissolution experiments and modeling studies indicate average solubilities between 1.5 % and 5 % for Al [e.g. Prospero et al., 1987; Measures and Vink, 2000; Gehlen et al., 2003; Baker et al., 2006; Han et al., 2008; Measures et al., 2010]. For Ti, the information is restricted to observations in ultrapure deionized water; Buck et al. [2010] report Ti solubilities of 0.3 - 15.3 % for Aerosol collected over the Atlantic Ocean. The large uncertainties in both, the soluble trace metal fractions and the total dust deposition complicate the quantification of atmospheric inputs of Al and Ti. A similar situation exists in the case of the potentially limiting nutrient Fe. Overall, there is still a clear need to better constrain the processes of atmospheric trace metal inputs to the surface ocean.

1.4 Surface Ocean processes of Al and Ti

Upon delivery to the surface ocean, the fate of trace metals is coupled to complex geochemical and biological processes, including adsorption-desorption, aggregation, redox processes, ligand complex formation, biological uptake and recycling within the upper water column [Chester, 2000; Bruland and Lohan, 2003; Baker and Croot, 2010]. These processes are closely related to the oceanic speciation, solubility and size distribution of the trace metal and finally control the export from the surface waters. The specific mechanisms for Al and Ti are discussed in the following.

1.4.1 Speciation and size distribution

In seawater, the inorganic speciation of Al and Ti is dominated by the hydrolyzed forms, $Al(OH)_4^-$ and $TiO(OH)_2$ [Turner et al., 1981; Bruland, 1983; Byrne et al., 1988]. These hydroxyl species are highly particle reactive [Turner et al., 1981] and have comparably low solubilities. For Al, the solubility in seawater is suggested to range between ~1.8 µM [Savenko and Savenko, 2011] and ~18.5 µM [Willey, 1975]. For Ti, no seawater data are available so far. In 0.1 M NaCl, the solubility of crystalline TiO_2 is about 1 nM in the pH range of 3 - 11 [Schmidt and Vogelsberger, 2009]. Other studies with saturated Ti solutions report solubilities of up to ~3 µM related to amorphous TiO_2 [Sugimoto et al., 2002].

Weak evidence exists for the occurrence of organically complexed species of Al and Ti in seawater [van den Berg et al., 1994]. Some Al was found to bind to terrestrial fulvic acids at seawater pH [Sutheimer and Cabaniss, 1997]. However, under seawater conditions Ca and Mg may outcompete Al for binding sites. Titanium is believed to form strongly bound organo-Ti complexes similar to Fe siderophores [Uppal et al., 2009], but these complexes have not been examined or detected in seawater. Overall it may be assumed that Al and Ti predominantly occur as inorganic species in seawater.

The size distributions of Al and Ti are poorly investigated in seawater so far. For Al, very low colloidal fractions have been observed, with most of the dAl being present in the soluble form [Moran and Moore, 1989; Reitmeyer et al., 1996]. This observation is in contrast to the occurrence of Al as strongly hydrolyzed and highly particle reactive species in the ocean. Colloidal associations of Ti were only reported in the context of general elemental compositions of oceanic colloidal material [Bertine and Vernonclark, 1996; Guo et al., 2000]. However, these studies do not report concentrations of colloidal or dissolved Ti, or colloidal fractions of Ti in seawater.

1.4.2 Removal processes

The removal of trace metals from the water column generally can be described as a process that involves the transfer from the dissolved into the particulate phase, followed by the final settling of the particulate species through the water column [Turekian, 1977]. The transfer from the dissolved into the particulate species may occur via active or passive biological uptake and via passive scavenging processes [Chester, 2000].

Aluminium and Ti are so far not known to have essential biological functions, yet this does

not necessarily preclude biological uptake. A number of studies found evidence for the removal of Al with diatoms [Deuser et al., 1983; Moran and Moore, 1988; van Bennekom et al., 1989; Moran and Moore, 1992] and some general relation between the removal of Ti and biological activity has been suggested [Orians et al., 1990; Skrabal et al., 1992]. However, these relations could be due to uptake as well as to surface adsorption processes. For Al, two recent studies observed the incorporation in the frustules of diatoms in living cultures [Gehlen et al., 2002] as well as post-mortem [Koning et al., 2007], suggesting that both processes, biological uptake and the formation of alumino-silicate phases on the diatom surfaces take place [Koning et al., 2007].

Passive scavenging comprises the transfer from the dissolved trace metal to the particulate phase via surface adsorption and aggregation processes. Adsorption may occur on both inorganic and organic surfaces [e.g. Turekian, 1977; Balistrieri et al., 1981; Li, 1981; Hunter, 1983] mostly in the colloidal and smaller sized (<10 μm) particulate fraction [Chester, 2000]. Therefore, biological productivity may enhance the removal of trace metals from the water column not only through active uptake but also by providing additional adsorption surfaces. The overall transfer from the dissolved to the particulate fraction is controlled to the abundance of particles in the water column [Honeyman et al., 1988; Chester, 2000]. In addition, the association with the colloidal phase is assumed to play an important role in trace metal scavenging. Studies on the removal of Th suggest that scavenging occurs as a two step process, including first the formation of colloidal intermediates, e.g. through surface adsorption, and second the coagulation to larger particles [e.g. Honeyman and Santschi, 1989; Moran and Buesseler, 1993; Moran et al., 1996]. Adsorptive and aggregative processes are generally reversible and may thus also release trace metals from the particulate to the dissolved phase [Moran et al., 1996; Chester, 2000]. The final settling and removal of particles from the surface to deeper waters predominantly occurs in the larger (>50 μm) particulate fraction [Chester, 2000]. The aggregation to larger particles is considered to be rate-limiting [Honeyman et al., 1988; Honeyman and Santschi, 1989; Chester, 2000], and before the final removal takes place trace metals may repeatedly cycle between the dissolved and particulate phase [Bruland and Lohan, 2003].

The susceptibility of trace metals to scavenging processes is closely coupled to their speciation. Highest particle reactivities and scavenging rates are suggested for hydroxyl species in seawater [Turner et al., 1981; Li, 1991], and therefore Al and Ti can be expected to be strongly influenced by scavenging processes. This generally agrees with the oceanic

distributions of the two metals [Hydes, 1979; Orians and Bruland, 1986; Orians et al., 1990; Kramer et al., 2004]. Furthermore, observations of increased Al/Ti ratios in sediments and sediment traps indicate that Al is preferentially scavenged over Ti, likely in association with the settling of biogenic particles (e.g. opal rain) [Murray et al., 1993; Murray and Leinen, 1996; Dymond et al., 1997].

1.5 Objectives and thesis outline

The above given considerations highlight the following important issues: 1) atmospheric inputs have strong influence on biogeochemical processes in the surface ocean but are yet poorly quantified; 2) the estimation of dust inputs from surface water dAl concentrations is complicated by spatial variations in oceanic residence times and soluble dust fractions of Al; 3) the lithogenic element Ti could serve as alternative or even complementary dust tracer to Al; and 4) not much is yet known about the behavior of Ti in the surface ocean. Consequently, in order to evaluate the potential utilization of dTi concentrations as tracer for dust inputs, a better understanding of its surface ocean processes is essential. In this work, the distribution and the behavior of both Al and Ti are investigated in regions of the Atlantic that differ largely in the magnitude and characteristics of dust inputs. A principal aim is to identify controls on the relationship between dust inputs and surface water concentrations of Al and Ti. Particular attention is given to the removal processes of both metals upon the atmospheric supply, and their residence times in the surface ocean are constrained.

The following chapters represent stand-alone manuscripts that are published in, submitted to or in preparation for submission to peer-reviewed scientific journals. Figure 1.4 gives a general overview of the contents and relations of the different chapters. In Chapter 3, surface water concentrations of dAl and dTi are reported from stations along an Atlantic meridional transect and the relationship to atmospheric inputs is discussed. The particular focus lies on the specific supply mechanisms and residence times of both metals. Chapter 4 deals with the size distributions of Al and Ti in the upper water column of the eastern tropical North Atlantic. The dissolved fractions of both metals were size fractionated by ultra-filtration and the soluble (<10 kDa) and colloidal fractions of Al and Ti were determined. The results are discussed with regard to the oceanic speciation and solubilities of both metals and provide insights into the general role of the colloidal phase in oceanic scavenging processes. In Chapter 5, the distributions of Al and Ti between the dissolved

and

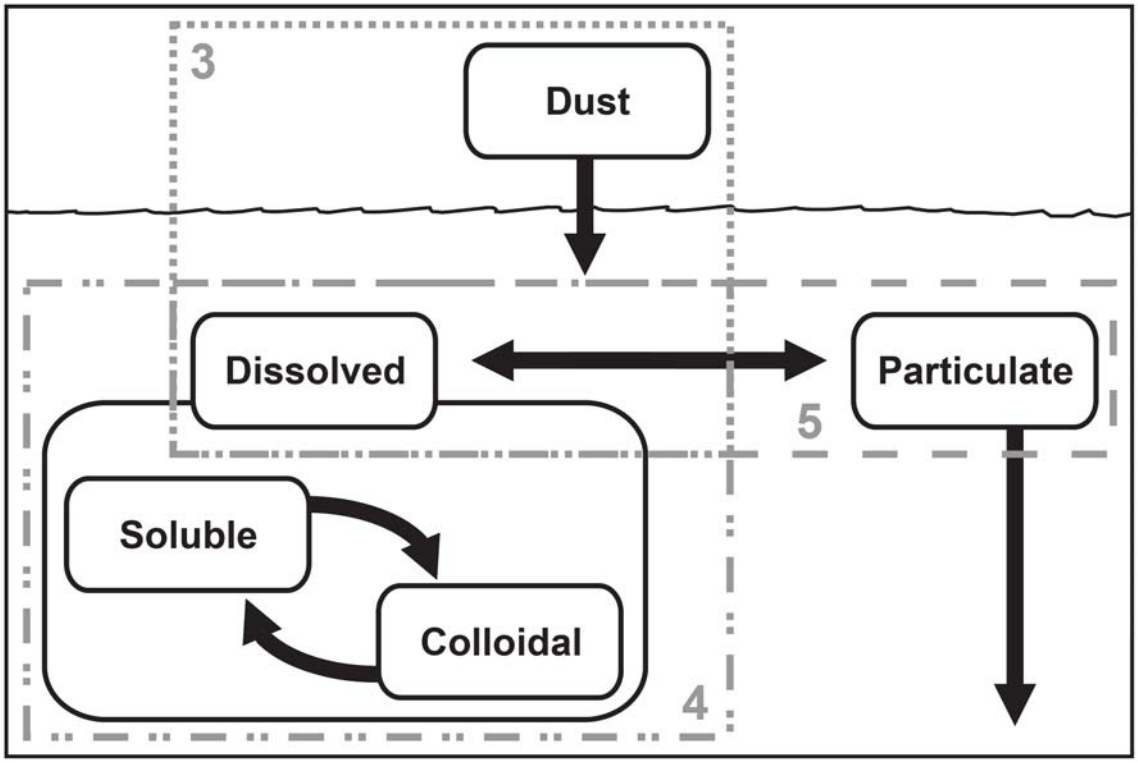

Fig. 1.4: Schematic overview of the contents and relationships of the different studies during this work. Details are given in the following Chapters 3 - 5.

the particulate phase are examined. Trace metal concentrations were determined in upper water column samples from ten stations in the tropical and subtropical North and South Atlantic. The discussion focuses on the behavior of both metals upon their delivery from atmospheric particles, and the removal processes of both metals via scavenging mechanisms are better constrained. Finally, in Chapter 6 the findings of this work are concluded against the background of the above raised questions.

1.6 References

Baker A. R. and Croot P. L. (2010) Atmospheric and marine controls on aerosol iron solubility in seawater. *Marine Chemistry* **120**, 4-13.

Baker A. R., Jickells T. D., Witt M. and Linge K. L. (2006) Trends in the solubility of iron, aluminium, manganese and phosphorus in aerosol collected over the Atlantic Ocean. *Marine Chemistry* **98**, 43-58.

Baker A. R., Lesworth T., Adams C., Jickells T. D. and Ganzeveld L. (2010) Estimation of atmospheric nutrient inputs to the Atlantic Ocean from 50 °N to 50 °S based on large-scale field sampling: Fixed nitrogen and dry deposition of phosphorus. *Global Biogeochemical Cycles* **24**, GB3006, doi:10.1029/2009gb003634.

Balistrieri L., Brewer P. G. and Murray J. W. (1981) Scavenging residence times of trace metals and surface chemistry of sinking particles in the deep ocean. *Deep Sea Research Part A. Oceanographic Research Papers* **28**, 101-121.

Behrenfeld M. J. and Kolber Z. S. (1999) Widespread iron limitation of phytoplankton in the South Pacific Ocean. *Science* **283**, 840-843.

Bertine K. K. and Vernonclark R. (1996) Elemental composition of the colloidal phase isolated by cross-flow filtration from coastal seawater samples. *Marine Chemistry* **55**, 189-204.

Bewers J. M. and Yeats P. A. (1989) Transport of river-derived trace metals through the coastal zone. *Netherlands Journal of Sea Research* **23**, 359-368.

Boyd P. W., Watson A. J., Law C. S., Abraham E. R., Trull T., Murdoch R., Bakker D. C. E., Bowie A. R., Buesseler K. O., Chang H., Charette M., Croot P., Downing K., Frew R., Gall M., Hadfield M., Hall J., Harvey M., Jameson G., LaRoche J., Liddicoat M., Ling R., Maldonado M. T., McKay R. M., Nodder S., Pickmere S., Pridmore R., Rintoul S., Safi K., Sutton P., Strzepek R., Tanneberger K., Turner S., Waite A. and Zeldis J. (2000) A mesoscale phytoplankton bloom in the polar Southern Ocean stimulated by iron fertilization. *Nature* **407**, 695-702.

Brown M. T. and Bruland K. W. (2009) Dissolved and particulate aluminum in the Columbia River and coastal waters of Oregon and Washington: Behavior in near-field and far-field plumes. *Estuarine, Coastal and Shelf Science* **84**, 171-185.

Bruland K. (1983) Trace elements in seawater. In *Chemical Oceanography* (eds. Riley J. P. and Chester R.). Academic Press, London.

Bruland K. W. and Lohan M. C. (2003) Controls of trace metals in seawater. In *Treatise on Geochemistry* (eds. Holland H. D. and Turekian K. K.). Elsevier, London, pp. 23-49.

Buck C. S., Landing W. M., Resing J. A. and Measures C. I. (2010) The solubility and deposition of aerosol Fe and other trace elements in the North Atlantic Ocean: Observations from the A16N CLIVAR/CO_2 repeat hydrography section. *Marine Chemistry* **120**, 57-70.

Byrne R. H., Kump L. R. and Cantrell K. J. (1988) The influence of temperature and pH on trace metal speciation in seawater. *Marine Chemistry* **25**, 163-181.

Chester R. (2000) *Marine Geochemistry*. Blackwell Science Ltd, Oxford.

Chou L. and Wollast R. (1997) Biogeochemical behavior and mass balance of dissolved aluminum in the western Mediterranean Sea. *Deep Sea Research Part II: Topical Studies in Oceanography* **44**, 741-768.

Cullen J. T., Chong M. and Ianson D. (2009) British Columbian continental shelf as a source of dissolved iron to the subarctic northeast Pacific Ocean. *Global Biogeochemical Cycles* **23**, GB4012, doi:10.1029/2008GB003326.

Deuser W. G., Brewer P. G., Jickells T. D. and Commeau R. F. (1983) Biological control of the removal of abiogenic particles from the surface ocean. *Science* **219**, 388-391.

Duce R. A., Liss P. S., Merrill J. T., Atlas E. L., Buat-Menard P., Hicks B. B., Miller J. M., Prospero J. M., Arimoto R., Church T. M., Ellis W., Galloway J. N., Hansen L., Jickells T. D., Knap A. H., Reinhardt K. H., Schneider B., Soudine A., Tokos J. J., Tsunogai S., Wollast R. and Zhou M. (1991) The atmospheric input of trace species to the World Ocean. *Global Biogeochemical Cycles* **5**, 193-259.

Duce R. A., LaRoche J., Altieri K., Arrigo K. R., Baker A. R., Capone D. G., Cornell S., Dentener F., Galloway J., Ganeshram R. S., Geider R. J., Jickells T., Kuypers M. M., Langlois R., Liss P. S., Liu S. M., Middelburg J. J., Moore C. M., Nickovic S., Oschlies A., Pedersen T., Prospero J., Schlitzer R., Seitzinger S., Sorensen L. L., Uematsu M., Ulloa O., Voss M., Ward B. and Zamora L. (2008) Impacts of Atmospheric Anthropogenic Nitrogen on the Open Ocean. *Science* **320**, 893-897.

Dymond J., Collier R., McManus J., Honjo S. and Manganini S. (1997) Can the aluminium and titanium contents of ocean sediments be used to determine the paleoproductivity of the oceans? *Paleoceanography* **12**, 586-593.

Gaiero D. M., Brunet F., Probst J.-L. and Depetris P. J. (2007) A uniform isotopic and chemical signature of dust exported from Patagonia: Rock sources and occurrence in southern environments. *Chemical Geology* **238**, 107-120.

Gehlen M., Beck L., Calas G., Flank A. M., van Bennekom A. J. and van Beusekom J. E. E. (2002) Unraveling the atomic structure of biogenic silica: Evidence of the structural association of Al and Si in diatom frustules. *Geochimica et Cosmochimica Acta* **66**, 1601-1609.

Gehlen M., Heinze C., Maier-Reimer E. and Measures C. I. (2003) Coupled Al-Si geochemistry in an ocean general circulation model: A tool for the validation of oceanic dust deposition fields? *Global Biogeochemical Cycles* **17**, 1028, doi:10.1029/2001gb001549.

Ginoux P., Chin M., Tegen I., Prospero J. M., Holben B., Dubovik O. and Lin S.-J. (2001) Sources and distributions of dust aerosols simulated with the GOCART model. *Journal of Geophysical Research* **106**, 20255-20273.

Ginoux P., Prospero J. M., Torres O. and Chin M. (2004) Long-term simulation of global dust distribution with the GOCART model: Correlation with North Atlantic Oscillation. *Environmental Modelling & Software* **19**, 113-128.

Guieu C., Loÿe-Pilot M. D., Ridame C. and Thomas C. (2002) Chemical characterization of the Saharan dust end-member: Some biogeochemical implications for the western Mediterranean Sea. *Journal of Geophysical Research* **107**, 4258, doi:10.1029/2001JD000582.

Guo L., Santschi P. H. and Warnken K. W. (2000) Trace metal composition of colloidal organic material in marine environments. *Marine Chemistry* **70**, 257-275.

Han Q., Moore J. K., Zender C., Measures C. I. and Hydes D. J. (2008) Constraining oceanic dust deposition using surface ocean dissolved Al. *Global Biogeochemical Cycles* **22**, GB2003, doi:10.1029/2007gb002975.

Honeyman B. D. and Santschi P. H. (1989) A Brownian-pumping model for oceanic trace metal scavenging: Evidence from Th isotopes. *Journal of Marine Research* **47**, 951-992.

Honeyman B. D., Balistrieri L. S. and Murray J. W. (1988) Oceanic trace metal scavenging: The importance of particle concentration. *Deep Sea Research Part A. Oceanographic Research Papers* **35**, 227-246.

Hunter K. A. (1983) The adsorptive properties of sinking particles in the deep ocean. *Deep Sea Research Part A. Oceanographic Research Papers* **30**, 669-675.

Hydes D. J. (1979) Aluminum in seawater: Control by inorganic processes. *Science* **205**, 1260-1262.

Hydes D. J. (1989) Seasonal variation in dissolved aluminium concentrations in coastal waters and biological limitation of the export of the riverine input of aluminium to the deep sea. *Continental Shelf Research* **9**, 919-929.

Hydes D. J., de Lange G. J. and de Baar H. J. W. (1988) Dissolved aluminium in the Mediterranean. *Geochimica et Cosmochimica Acta* **52**, 2107-2114.

Jickells T. D. (1995) Atmospheric inputs of metals and nutrients to the oceans: Their magnitude and effects. *Marine Chemistry* **48**, 199-214.

Jickells T. D. (1999) The inputs of dust derived elements to the Sargasso Sea; A synthesis. *Marine Chemistry* **68**, 5-14.

Jickells T. D. and Spokes L. J. (2001) Atmospheric iron inputs to the oceans. In *The Biogeochemistry of Iron in Seawater* (eds. Turner D. R. and Hunter K. A.). John Wiley & Sons Ltd., pp. 85-121.

Jickells T. D., An Z. S., Andersen K. K., Baker A. R., Bergametti G., Brooks N., Cao J. J., Boyd P. W., Duce R. A., Hunter K. A., Kawahata H., Kubilay N., laRoche J., Liss P. S., Mahowald N., Prospero J. M., Ridgwell A. J., Tegen I. and Torres R. (2005) Global iron connections between desert dust, ocean biogeochemistry, and climate. *Science* **308**, 67-71.

Kaupp L. J., Measures C. I., Selph K. E. and Mackenzie F. T. (2011) The distribution of dissolved Fe and Al in the upper waters of the Eastern Equatorial Pacific. *Deep Sea Research Part II: Topical Studies in Oceanography* **58**, 296-310.

Koning E., Gehlen M., Flank A. M., Calas G. and Epping E. (2007) Rapid post-mortem incorporation of aluminum in diatom frustules: Evidence from chemical and structural analyses. *Marine Chemistry* **106**, 208-222.

Kramer J., Laan P., Sarthou G., Timmermans K. R. and de Baar H. J. W. (2004) Distribution of dissolved aluminium in the high atmospheric input region of the subtropical waters of the North Atlantic Ocean. *Marine Chemistry* **88**, 85-101.

Krishnamurthy A., Moore J. K., Mahowald N., Luo C. and Zender C. S. (2009) Impacts of atmospheric nutrient inputs on marine biogeochemistry. *Journal of Geophysical Research* **115**, G01006, doi:10.1029/2009JG001115.

Li Y.-H. (1981) Ultimate removal mechanisms of elements from the ocean. *Geochimica et Cosmochimica Acta* **45**, 1659-1664.

Li Y.-H. (1991) Distribution patterns of the elements in the ocean: A synthesis. *Geochimica et Cosmochimica Acta* **55**, 3223-3240.

Luo C., Mahowald N. and del Corral J. (2003) Sensitivity study of meteorological parameters on mineral aerosol mobilization, transport, and distribution. *Journal of Geophysical Research* **108**, 4447, doi:10.1029/2003jd003483.

Mahowald N. M. and Luo C. (2003) A less dusty future? *Geophysical Research Letters* **30**, 1903, doi:10.1029/2003gl017880.

Mahowald N. M., Baker A. R., Bergametti G., Brooks N., Duce R. A., Jickells T. D., Kubilay N., Prospero J. M. and Tegen I. (2005) Atmospheric global dust cycle and iron inputs to the ocean. *Global Biogeochemical Cycles* **19**, GB4025, doi:10.1029/2004GB002402.

Martin J. H. (1990) Glacial-interglacial CO_2 change: The iron hypothesis. *Paleoceanography* **5**, 1-13.

Martin J.-M. and Meybeck M. (1979) Elemental mass-balance of material carried by major world rivers. *Marine Chemistry* **7**, 173-206.

Martin J. H., Coale K. H., Johnson K. S., Fitzwater S. E., Gordon R. M., Tanner S. J., Hunter C. N., Elrod V. A., Nowicki J. L., Coley T. L., Barber R. T., Lindley S., Watson A. J., Vanscoy K., Law C. S., Liddicoat M. I., Ling R., Stanton T., Stockel J., Collins C., Anderson A., Bidigare R., Ondrusek M., Latasa M., Millero F. J., Lee K., Yao W., Zhang J. Z., Friederich G., Sakamoto C., Chavez F., Buck K., Kolber Z., Greene R., Falkowski P., Chisholm S. W., Hoge F., Swift R., Yungel J., Turner S., Nightingale P., Hatton A., Liss P. and Tindale N. W. (1994) Testing the iron hypothesis in ecosystems of the equatorial Pacific Ocean. *Nature* **371**, 123-129.

McLennan S. M. (2001) Relationships between the trace element composition of sedimentary rocks and upper continental crust. *Geochemistry Geophysics Geosystems* **2**, 1021, doi:10.1029/2000gc000109.

Measures C. I. (1995) The distribution of Al in the IOC stations of the eastern Atlantic between 30 °S and 34 °N. *Marine Chemistry* **49**, 267-281.

Measures C. I. and Vink S. (2000) On the use of dissolved aluminum in surface waters to estimate dust deposition to the ocean. *Global Biogeochemical Cycles* **14**, 317-327.

Measures C. I., Landing W. M., Brown M. T. and Buck C. S. (2008) High-resolution Al and Fe data from the Atlantic Ocean CLIVAR-CO2 repeat hydrography A16N transect: Extensive linkages between atmospheric dust and upper ocean geochemistry. *Global Biogeochemical Cycles* **22**, GB1005, doi:10.1029/2007gb003042.

Measures C. I., Sato T., Vink S., Howell S. and Li Y. H. (2010) The fractional solubility of aluminium from mineral aerosols collected in Hawaii and implications for atmospheric deposition of biogeochemically important trace elements. *Marine Chemistry* **120**, 144-153.

Moran S. B. and Moore R. M. (1988) Evidence from mesocosm studies for biological removal of dissolved aluminum from sea water. *Nature* **335**, 706-708.

Moran S. B. and Moore R. M. (1989) The distribution of colloidal aluminum and organic carbon in coastal and open ocean waters off Nova Scotia. *Geochimica et Cosmochimica Acta* **53**, 2519-2527.

Moran S. B. and Moore R. M. (1991) The potential source of dissolved aluminum from resuspended sediments to the North Atlantic Deep Water. *Geochimica et Cosmochimica Acta* **55**, 2745-2751.

Moran S. B. and Moore R. M. (1992) Kinetics of the removal of dissolved aluminum by diatoms in seawater: A comparison with thorium. *Geochimica et Cosmochimica Acta* **56**, 3365-3374.

Moran S. B. and Buesseler K. O. (1993) Size-fractionated ^{234}Th in continental shelf waters off New England: Implications for the role of colloids in oceanic trace metal scavenging. *Journal of Marine Research* **51**, 893-922.

Moran S. B., Yeats P. A. and Balls P. W. (1996) On the role of colloids in trace metal solid-solution partitioning in continental shelf waters: A comparison of model results and field data. *Continental Shelf Research* **16**, 397-408.

Moreno T., Querol X., Castillo S., Alastuey A., Cuevas E., Herrmann L., Mounkaila M., Elvira J. and Gibbons W. (2006) Geochemical variations in aeolian mineral particles from the Sahara-Sahel Dust Corridor. *Chemosphere* **65**, 261-270.

Murray R. W. and Leinen M. (1996) Scavenged excess aluminum and its relationship to bulk titanium in biogenic sediment from the central equatorial Pacific Ocean. *Geochimica et Cosmochimica Acta* **60**, 3869-3878.

Murray R. W., Leinen M. and Isern A. R. (1993) Biogenic flux of Al to sediment in the central equatorial Pacific Ocean: Evidence for increased productivity during glacial periods. *Paleoceanography* **8**, 651-670.

Neal C., Jarvie H., Rowland P., Lawler A., Sleep D. and Scholefield P. (2011) Titanium in UK rural, agricultural and urban/industrial rivers: Geogenic and anthropogenic colloidal/sub-colloidal sources and the significance of within-river retention. *Science of The Total Environment* **409**, 1843-1853.

Okin G. S., Baker A. R., Tegen I., Mahowald N. M., Dentener F. J., Duce R. A., Galloway J. N., Hunter K., Kanakidou M., Kubilay N., Prospero J. M., Sarin M., Surapipith V., Uematsu M. and Zhu T. (2011) Impacts of atmospheric nutrient deposition on marine productivity: Roles of nitrogen, phosphorus, and iron. *Global Biogeochemical Cycles* **25**, GB2022, doi:10.1029/2010gb003858.

Orians K. J. and Bruland K. W. (1985) Dissolved aluminium in the central North Pacific. *Nature* **316**, 427-429.

Orians K. J. and Bruland K. W. (1986) The biogeochemistry of aluminum in the Pacific Ocean. *Earth and Planetary Science Letters* **78**, 397-410.

Orians K. J., Boyle E. A. and Bruland K. W. (1990) Dissolved titanium in the open ocean. *Nature* **348**, 322-325.

Prospero J. M. (1996) The atmospheric transport of particles to the ocean. In *Particle Flux in the Ocean* (eds. Ittekkot V., Schäfer P., Honjo S. and Depetris P. J.). John Wiley & Sons Ltd., U.K., pp. 19-53.

Prospero J. M., Nees R. T. and Uematsu M. (1987) Deposition rate of particulate and dissolved aluminium derived from Saharan dust in precipitation at Miami, Florida. *Journal of Geophysical Research* **92**, 14723-14731.

Prospero J. M., Ginoux P., Torres O., Nicholson S. E. and Gill T. E. (2002) Environmental characterization of global sources of atmospheric soil dust identified with the NIMBUS 7 Total Ozone Mapping Spectrometer (TOMS) absorbing aerosol product. *Reviews of Geophysics* **40**, 1002, doi:10.1029/2000rg000095.

Rauch J. N. and Pacyna J. M. (2009) Earth's global Ag, Al, Cr, Cu, Fe, Ni, Pb, and Zn cycles. *Global Biogeochemical Cycles* **23**, GB2001, doi:10.1029/2008GB003376.

Reitmeyer R., Powell R. T., Landing W. M. and Measures C. I. (1996) Colloidal aluminum and iron in seawater: An intercomparison between various cross-flow ultrafiltration systems. *Marine Chemistry* **55**, 75-91.

Sañudo-Wilhelmy S. A., Rivera-Duarte I. and Russell Flegal A. (1996) Distribution of colloidal trace metals in the San Francisco Bay estuary. *Geochimica et Cosmochimica Acta* **60**, 4933-4944.

Savenko A. V. and Savenko V. S. (2011) Aluminum hydroxide's solubility and the forms of dissolved aluminum's occurrence in Seawater. *Oceanology* **51**, 231-234.

Schmidt J. and Vogelsberger W. (2009) Aqueous long-term solubility of titania nanoparticles and titanium(IV) hydrolysis in a sodium chloride system studied by adsorptive stripping voltammetry. *Journal of Solution Chemistry* **38**, 1267-1282.

Shi Z. B., Krom M. D., Bonneville S., Baker A. R., Jickells T. D. and Benning L. G. (2009) Formation of iron nanoparticles and increase in iron reactivity in mineral dust during simulated cloud processing. *Environmental Science and Technology* **43**, 6592-6596.

Sholkovitz E. R. (1978) The flocculation of dissolved Fe, Mn, Al, Cu, Ni, Co and Cd during estuarine mixing. *Earth and Planetary Science Letters* **41**, 77-86.

Skrabal S. A. (1995) Distributions of dissolved titanium in Chesapeake Bay and the Amazon River Estuary. *Geochimica et Cosmochimica Acta* **59**, 2449-2458.

Skrabal S. A. (2006) Dissolved titanium distributions in the Mid-Atlantic Bight. *Marine Chemistry* **102**, 218-229.

Skrabal S. A. and Terry C. M. (2002) Distributions of dissolved titanium in porewaters of estuarine and coastal marine sediments. *Marine Chemistry* **77**, 109-122.

Skrabal S. A., Ullman W. J. and Luther III G. W. (1992) Estuarine distributions of dissolved titanium. *Marine Chemistry* **37**, 83-103.

Slemons L. O., Murray J. W., Resing J., Paul B. and Dutrieux P. (2010) Western Pacific coastal sources of iron, manganese, and aluminum to the Equatorial Undercurrent. *Global Biogeochemical Cycles* **24**, GB3024, doi:10.1029/2009GB003693.

Spokes L. J., Jickells T. D. and Lim B. (1994) Solubilisation of aerosol trace metals by cloud processing: A laboratory study. *Geochimica et Cosmochimica Acta* **58**, 3281-3287.

Sugimoto T., Zhou X. and Muramatsu A. (2002) Synthesis of uniform anatase TiO_2 nanoparticles by gel-sol method: 1. Solution chemistry of $Ti(OH)_n^{(4-n)+}$ complexes. *Journal of Colloid and Interface Science* **252**, 339-346.

Sutheimer S. H. and Cabaniss S. E. (1997) Aluminum binding to humic substances determined by high performance cation exchange chromatography. *Geochimica et Cosmochimica Acta* **61**, 1-9.

Tegen I. and Fung I. (1994) Modeling of mineral dust in the atmosphere: Sources, transport, and optical thickness. *Journal of Geophysical Research* **99**, 22897-22914.

Tegen I., Werner M., Harrison S. P. and Kohfeld K. E. (2004) Relative importance of climate and land use in determining present and future global soil dust emission. *Geophysical Research Letters* **31**, L05105, doi:10.1029/2003gl019216.

Turekian K. K. (1977) The fate of metals in the oceans. *Geochimica et Cosmochimica Acta* **41**, 1139-1144.

Turner D. R., Whitfield M. and Dickson A. G. (1981) The equilibrium speciation of dissolved components in freshwater and sea water at 25 °C and 1 atm pressure. *Geochimica et Cosmochimica Acta* **45**, 855-881.

Upadhyay S., Liss P. S. and Jickells T. D. (2002) Sorption model for dissolved aluminium in freshwaters. *Aquatic Geochemistry* **8**, 255-275.

Uppal R., Israel H. P., Incarvito C. D. and Valentine A. M. (2009) Titanium(IV) complexes with N,N'-dialkyl-2,3-dihydroxyterephthalamides and 1-hydroxy-2(1H)-pyridinone as siderophore and tunichrome analogues. *Inorganic Chemistry* **48**, 10769-10779.

Ussher S. J., Worsfold P. J., Achterberg E. P., Laes A., Blain S., Laan P. and De Baar H. J. W. (2007) Distribution and redox speciation of dissolved iron on the European continental margin. *Limnology and Oceanography* **52**, 2530-2539.

van Bennekom A. J., Fred Jansen J. H., van der Gaast S. J., van Iperen J. M. and Pieters J. (1989) Aluminium-rich opal: An intermediate in the preservation of biogenic silica in the Zaire (Congo) deep-sea fan. *Deep Sea Research Part A. Oceanographic Research Papers* **36**, 173-190.

van den Berg C. M. G., Boussemart M., Yokoi K., Prartono T. and Campos M. L. A. M. (1994) Speciation of aluminium, chromium and titanium in the NW Mediterranean. *Marine Chemistry* **45**, 267-282.

Willey J. D. (1975) Reactions which remove dissolved alumina from seawater. *Marine Chemistry* **3**, 227-240.

Yokoi K. and Van den Berg C. M. G. (1991) Determination of titanium in sea water using catalytic cathodic stripping voltammetry. *Analytica Chimica Acta* **245**, 167-176.

2 Study Area

During this work, the upper water column distributions of Al and Ti were examined in different regions of the Atlantic Ocean. Samples were collected in in maximum water depths of 800 m in the tropical northeast Atlantic during the cruise M80-2 aboard RV Meteor (November-December 2009) and along a meridional Atlantic transect during the cruise ANTXXVI-4 aboard RV Polarstern (April - May 2010). All sampling stations are displayed in Fig. 2.1. Hydrological and atmospheric characteristics of the study area are outlined below.

The major surface currents in the Atlantic Ocean are illustrated in Fig. 2.1. Transport in the upper water column of the subtropical northeast Atlantic is dominated by the Canary Current, with southward flowing temperate waters in a broad region along the African coast that originate from the Azores Current [Stramma, 1984]. Under the influence of the northeast trade winds, the Canary Current upwelling system develops, extending south to 12 °N during boreal winter [Marcello et al., 2011]. Around the Cape Verde Islands, the Canary Current deflects to the west and feeds the North Equatorial Current covering the region between 25 °N and 10 °N in the boreal summer and between 25 °N and 5 °N in boreal winter [Tchernia, 1980]. Similarly, in the tropical southwest Atlantic the Benguela Current deflects to the west and feeds the South Equatorial current extending between 20 °S and ~3 °N [Tchernia, 1980]. At the western boundary of the Atlantic Ocean, the North Equatorial Current continues towards the Caribbean [Tchernia, 1980; Tomczak and Godfrey, 1994]. The South Equatorial Current develops two branches; one crosses the Equator and feeds the North Brazil Current flowing to the northwest, the other inflects to the South and forms the Brazil Current [Tchernia, 1980; Tomczak and Godfrey, 1994; Schott et al., 2004]. Parts of both Equatorial currents also supply the North Equatorial Counter Current between 5 °N and 8 °N, the North Equatorial Undercurrent between 3 °N and 5 °N, the Equatorial Undercurrent, and the South Equatorial Undercurrent between 3 °S and 4 °S that circulate towards the east [Schott et al., 2004]. The undercurrents are located at depths of 100 to 200 m and feed the cyclonic Guinea and Angola Domes at the eastern boundary of the equatorial Atlantic through upwelling [Schott et al., 2004; Stramma et al., 2005]. The zone between the equatorial current system and the North

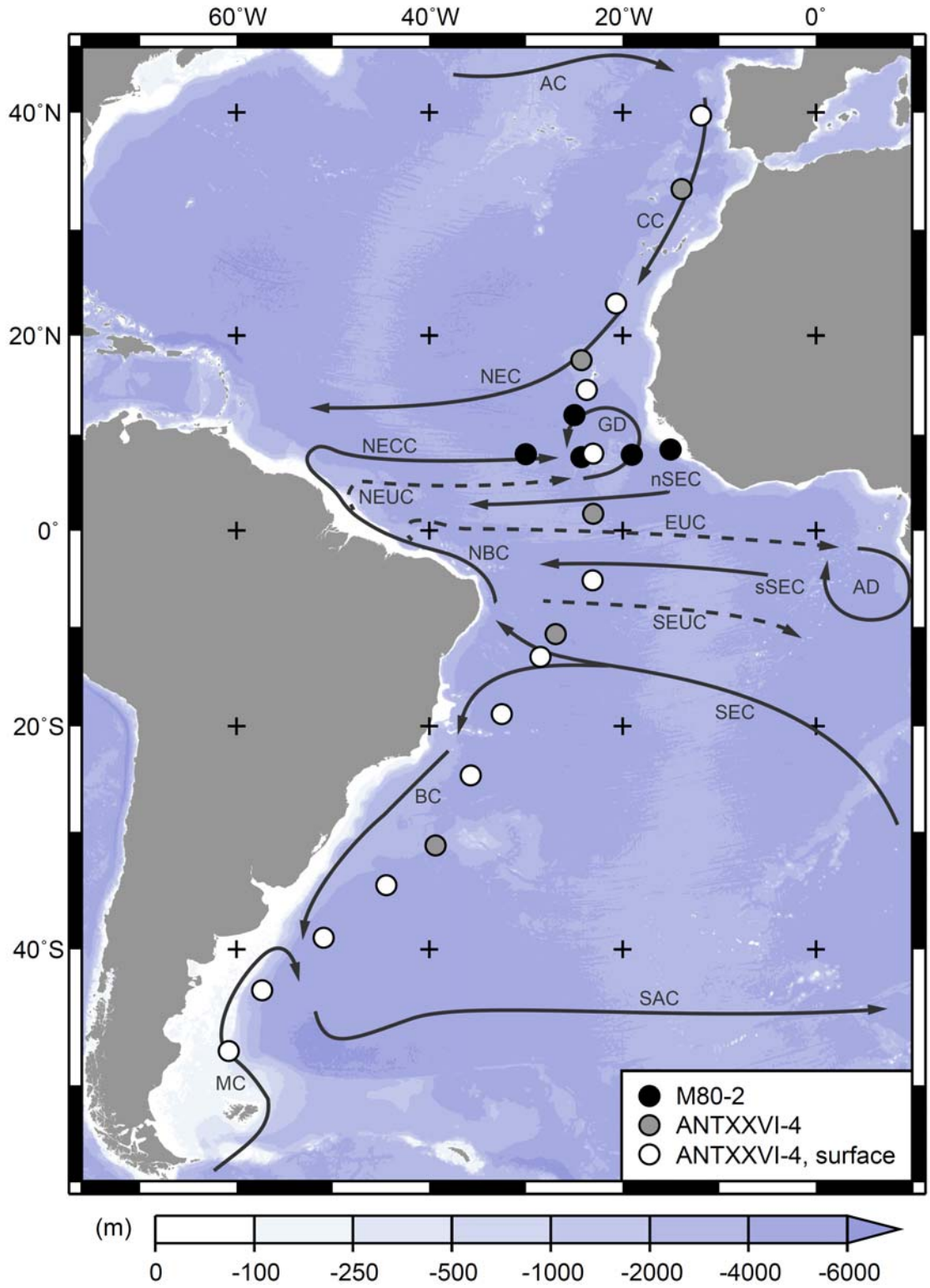

Fig. 2.1: Location of sampling stations discussed in this work. During M80-2 depth profiles between 20 and 800 m were sampled. During ANTXXVI-4 either depths profiles between 20 m and 400 m were sampled, or single surface seawater samples were taken at 20 m. Also displayed are major surface (dark grey arrows) and subsurface (dotted arrows) currents in the study regions, based on publications by Tomczak and Godfrey [1994], Stramma and England [1999] and Schott et al., [2004]. AC: Azores Current, CC: Canary Current, NEC: North Equatorial Current, NECC: North Equatorial Countercurrent, GD: Guinea Dome, NEUC: North Equatorial Undercurrent, SEC: South Equatorial Current, EUC: Equatorial Undercurrent, AD: Angola Dome, NBC: North Brazil Current, SEUC: South Equatorial Undercurrent, BC: Brazil Current, MC: Malvinas Current, SAC: South Atlantic Current.

Equatorial Current is characterized by an oxygen minimum that is most pronounced at water depths of 400 m to 500 m, with westward transport of the low-oxygen waters occurring at and north of the Guinea Dome [Stramma et al., 2008]. In the western South Atlantic, the Brazil Current flows to the south along the South American coast and defines the western boundary of the South Atlantic Gyre [Stramma and England, 1999]. Between 33 °S and 38 °S, the Brazil Current forms a front with the Malvinas Current that transports Antarctic Intermediate Water to the north, and deflects to the east [Tchernia, 1980; Tomczak and Godfrey, 1994]. With some admixture in the Brazil Malvinas Confluence Zone, the Brazil Current then continues as the South Atlantic Current that finally splits up close to South Africa and partly feeds the Benguela and South Equatorial Currents [Stramma and England, 1999]. The northern boundary of the South Atlantic Gyre is located at 16 °S - 20 °S in the upper water column [Stramma and England, 1999].

Precipitation and dust deposition vary widely over the Atlantic Ocean. Highest rainfalls occur within the Inter-Tropical Convergence Zone (ITCZ), resulting in a tropical salinity minimum, and within the Westerlies over the North and South Atlantic [Tchernia, 1980; Tomczak and Godfrey, 1994]. Low precipitation occurs in the subtropical regions, particularly in the subtropical gyres, where the combination with high evaporation causes high sea surface salinities [Tchernia, 1980]. The dust inputs to the Atlantic Ocean are displayed in Fig. 1.1. Highest dust deposition occurs in the tropical Atlantic, due to the transport of particles originating from the Sahara region with the northeast trade winds [Chester, 2000; Jickells et al., 2005]. The zone of dust deposition in the tropical Atlantic is located further north during the boreal summer than during the boreal winter months. Highest dust deposition can be expected during boreal summer [Moulin et al., 1997]. Elevated dust deposition also occurs in the western South Atlantic due to the transport of atmospheric particles from Patagonian Sources [Chester, 2000; Jickells et al., 2005], with most pronounced dust inputs during austral summer [Johnson et al., 2010]. By contrast, the region of the South Atlantic Gyre receives very low dust inputs [Chester, 2000; Jickells et al., 2005]

References

Chester R. (2000) *Marine Geochemistry*. Blackwell Science Ltd, Oxford.

Jickells T. D., An Z. S., Andersen K. K., Baker A. R., Bergametti G., Brooks N., Cao J. J., Boyd P. W., Duce R. A., Hunter K. A., Kawahata H., Kubilay N., laRoche J., Liss P. S., Mahowald N., Prospero J. M., Ridgwell A. J., Tegen I. and Torres R. (2005) Global iron connections between desert dust, ocean biogeochemistry, and climate. *Science* **308**, 67-71.

Johnson M. S., Meskhidze N., Solmon F., Gassó S., Chuang P. Y., Gaiero D. M., Yantosca R. M., Wu S., Wang Y. and Carouge C. (2010) Modeling dust and soluble iron deposition to the South Atlantic Ocean. *Journal of Geophysical Research* **115**, D15202, doi:10.1029/2009JD013311.

Marcello J., Hernandez-Guerra A., Eugenio F. and Fonte A. (2011) Seasonal and temporal study of the northwest African upwelling system. *International Journal of Remote Sensing* **32**, 1843-1859.

Moulin C., Lambert C. E., Dulac F. and Dayan U. (1997) Control of atmospheric export of dust from North Africa by the North Atlantic Oscillation. *Nature* **387**, 691-694.

Schott F. A., McCreary J. P. and Johnson G. C. (2004) Shallow overturning circulations of the tropical-subtropical oceans. In *Earth's climate: The Ocean-Atmosphere Interaction* (eds. Wang C., Xie S.-P. and Carton J. A.). AGU, Washington, D. C., pp. 261-304.

Stramma L. (1984) Geostrophic transport in the Warm Water Sphere of the eastern subtropical North Atlantic. *Journal of Marine Research* **42**, 537-558.

Stramma L. and England M. (1999) On the water masses and mean circulation of the South Atlantic Ocean. *Journal of Geophysical Research* **104**, 20863-20883.

Stramma L., Hüttl S. and Schafstall J. (2005) Water masses and currents in the upper tropical northeast Atlantic off northwest Africa. *Journal of Geophysical Research* **110**, C12006, doi:10.1029/2005jc002939.

Stramma L., Brandt P., Schafstall J., Schott F., Fischer J. and Körtzinger A. (2008) Oxygen minimum zone in the North Atlantic south and east of the Cape Verde Islands. *Journal of Geophysical Research* **113**, C04014, doi:10.1029/2007JC004369.

Tchernia P. (1980) *Descriptive Regional Oceanography*. Pergamon Press Ltd., Oxford.

Tomczak M. and Godfrey J. S. (1994) *Regional Oceanography: An Introduction*. Elsevier Science Ltd., Oxford.

3 Surface Water Dissolved Aluminium and Titanium: Tracers for Specific Time Scales of Dust Deposition to the Atlantic?

Anna Dammshäuser[1], Thibaut Wagener[1, 2], Peter L. Croot[1, 3, 4]

Geophysical Research Letters 38, L24601, doi:10.1029/2011GL049847, 2011[5]

Abstract

Surface water distributions of dissolved aluminium (dAl) and dissolved titanium (dTi) were investigated along a meridional Atlantic transect and related to dust deposition estimates. In the zone of Saharan dust deposition, highest dAl concentrations occurred in the tropical salinity minimum and suggest increasing Al dissolution from Saharan aerosols with wet deposition. By contrast, the dTi distribution is not related to precipitation but agrees with the pattern of annual dust deposition. In the zone of Patagonian dust deposition, elevated dTi concentrations contrasted with decreased dAl concentrations, indicating excess dAl scavenging onto biogenic particles in surface waters. Estimated residence times range from months to years for dAl and are ~10 times higher for dTi. This suggests that dAl reflects seasonal changes in dust deposition, while dTi is related to longer temporal scales. However, spatial variations in input and removal processes complicate the quantification of dust deposition from surface water concentrations.

[1] Helmholtz Centre for Ocean Research Kiel (GEOMAR), Germany

[2] now at: Mediterranean Institute of Oceanography (MIO), UMR 7294 - CNRS - Univ. Aix-Marseille - IRD, Marseille, France

[3] Plymouth Marine Laboratory, PML, United Kingdom

[4] now at: Earth and Ocean Sciences, National University of Ireland - Galway, NUIG, Ireland

[5] Copyright 2011 by the American Geophysical Union, reproduced by permission

3.1 Introduction

The deposition and dissolution of atmospheric lithogenic particles from continental sources (hereafter referred to as dust) is a major input path of trace elements into the open ocean. In recent years, the atmospheric supply of the potentially limiting nutrient iron has been a focus of intensive research [e.g. Jickells et al., 2005], yielding a better understanding of dust dissolution processes and surface water residence times [e.g. Baker and Croot, 2010]. However, dust deposition to the open ocean is still poorly constrained and restricted to few direct observations [Duce et al., 1991; e.g. Luo et al., 2003 and references therein] and estimates based on model outputs [e.g. Luo et al., 2003; Jickells et al., 2005]. Dissolved Al (dAl) concentrations have been introduced as tracer to assess the supply of dust particles to the surface ocean [e.g. Measures and Vink, 2000]. By contrast, very little is known about the potential application of dissolved Ti (dTi) concentrations to trace dust inputs. The utilization of a certain element as a tracer for dust supply requires some estimations of its input, depending on the dust composition and solubility in surface seawater, and of its removal from the surface ocean. Surface water residence times constrain the time frame of dust deposition that can be inferred from the trace metal concentrations. Both Al and Ti are abundant, relatively invariant components of the earth's crust [McLennan, 2001] and are predominantly delivered to the open ocean by dust deposition [Orians and Bruland, 1986; Orians et al., 1990]. In seawater, dAl and dTi have scavenging type distributions and so far are not known to have essential biological functions. However, both elements also behave specifically in their dissolution from dust and have different residence times in the surface ocean [e.g. Orians and Bruland, 1986; Orians et al., 1990; Buck et al., 2010]. Therefore, Al and Ti may provide complementary approaches to assess the dust deposition to the surface ocean.

In this study, the distributions of dAl and dTi are investigated on a meridional Atlantic transect through ocean regions covering a wide range of dust deposition fluxes. The aim of this work was to identify controls on the relationship between surface water concentrations of dAl and dTi and dust deposition and thus to better constrain the potential utilization of dAl and dTi to trace dust inputs to the surface ocean.

3.2 Methods

Surface seawater samples (20 - 25 m depth) were collected aboard the RV Polarstern (ANTXXVI-4, Punta Arenas - Bremerhaven) during April and May 2010. Water samples

were collected using trace metal clean GO-FLO samplers (General Oceanics) and filtered through 0.2 µm cartridge filters (Sartobran® P, Sartorius) under slight nitrogen overpressure (0.2 bar). All sample handling and processing was conducted in the IFM-GEOMAR clean container (ISO 5, class 100). The samples were acidified with sub-boiled quartz distilled HCl to pH <2 at least 24 h before analysis and analyzed directly on board. Dissolved Al concentrations were determined using the method described by Hydes and Liss [1976]. In short, the reagent lumogallion is added, the samples are buffered to pH 5 with ammonium-acetate and heated to 50 °C for 3 h to improve the complex formation. The fluorescence was measured with a Hitachi FL 2700 Fluorescence Spectrophotometer (excitation wavelength 497 nm, emission wavelength 572 nm). The detection limit was 0.1 - 0.3 nM for dAl, the blank values ranged between 0.4 - 0.6 nM on different days of analysis. Analysis of the SAFe reference seawater S1 resulted in 1.70 ± 0.21 nM of dAl (n = 14, consensus value 1.74 ± 0.09 nM). Dissolved Ti concentrations were determined by catalytic cathodic stripping voltammetry (µAutolab III with 663VA stand, Metrohm), using cupferron as the complexing ligand and bromate as an auxiliary oxidant [Croot, 2011]. The detection limit was 9 pM and the blank value 24 ± 3 pM for dTi. Supporting oceanographic data were obtained from continuous thermosalinograph measurements and the CTD system and are available in the Pangaea data management system [Rohardt, 2010; Rohardt and Bracher, 2011].

3.3 Results and discussion

Figure 3.1 displays dAl and dTi surface water concentrations over the cruise transect. The hydrographic regions were classified according to the variations in salinity and temperature [Tchernia, 1980]. Dissolved Al concentrations gradually increased from 5 nM in the Malvinas Current (MC) and the Canary Current (CC) towards 30 nM in the tropical salinity minimum (TSM), in agreement with previous observations [Vink and Measures, 2001; Measures et al., 2008]. Dissolved Ti concentrations showed two maxima, with concentrations of up to 90 pM in the MC and 110 pM in the CC at 15 °N. Lowest concentrations of dTi (~30 pM) occurred in the South Atlantic Gyre (SAG). Few other studies report surface water concentrations of dTi in the Atlantic Ocean. Our results lay in the same range as earlier observations in the western North Atlantic [Orians et al., 1990; Skrabal, 2006].

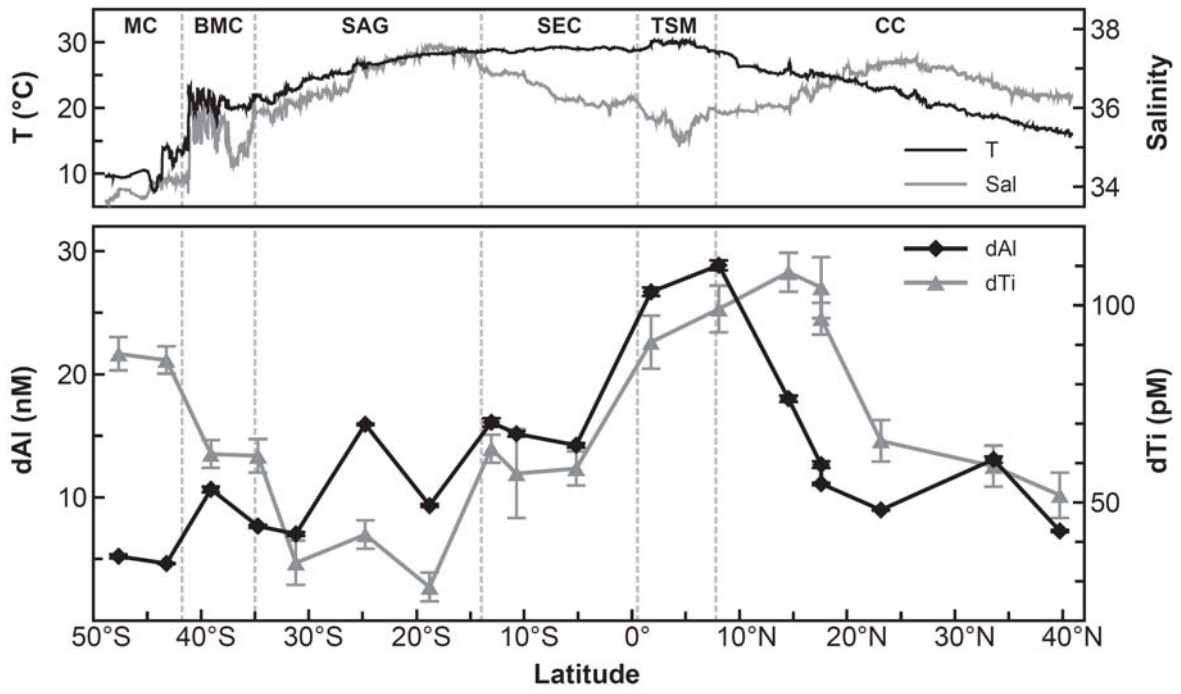

Fig. 3.1: Surface seawater concentrations of dAl, dTi, salinity and temperature over the cruise transect. Dotted lines define the hydrographic regions encountered during the cruise (MC: Malvinas Current, BMC: Brazil Malvinas Confluence, SAG: South Atlantic Gyre, SEC: South Equatorial Current, TSM: Tropical Salinity Minimum, CC: Canary Current). Exact values and station locations are given in Table A1 (section 3.6).

In the tropical and subtropical North Atlantic, elevated concentrations of dAl and dTi agree with increased dust deposition [e.g. Duce et al., 1991; Jickells et al., 2005]. The additionally elevated concentrations of dAl at 33 °N can be attributed to the propagation of Al-rich subtropical mode water from the western Atlantic basin [Measures et al., 2008]. Maximum concentrations of dTi occurred north of the highest dAl concentrations and are more in line with the location of highest annual dust deposition [Jickells et al., 2005]. In the South Atlantic, elevated dTi concentrations indicate the input of dust from Patagonian sources [Johnson et al., 2010]. However, in this region dAl concentrations were decreased, with exception of elevated concentrations in the confluence of the Brazil and the Malvinas Currents (BMC) that can be attributed to the delivery of Al-rich equatorial waters with the Brazil Current (BC) [Vink and Measures, 2001]. Overall, our data suggest that specific input and/or removal processes determine the distributions of dAl and dTi in the different regions.

3.3.1 Residence times of dAl and dTi

In order to better assess the specific processes influencing dAl and dTi distributions, elemental residence times were calculated at each sampling station. The objective is to determine differences in the residence times of dAl and dTi rather than absolute values. For this calculation it was assumed that input solely occurs via dust deposition and that input and removal processes are balanced in the mixed layer. The residence time is thus given as quotient between soluble atmospheric flux and inventory of the dissolved metal. The inventory was estimated as integrated dissolved metal concentration over a mixed layer of 30 m (all samples originated from the mixed layer; see Table A1 in section 3.6). The atmospheric flux was estimated from the average annual dust deposition given in the model composite by Jickells et al. [2005 and references therein], assuming that over the Atlantic transect this estimate adequately reflects the spatial and temporal variations in dust deposition. The soluble flux was calculated assuming dust fractions of 8.04 % and 0.41 % for Al and Ti [McLennan, 2001] and solubilities of 5 % and 0.1 % respectively. The elemental fractions in the dust are well established [Formenti et al., 2003; e.g. Gaiero et al., 2007], however, the solubilities are key uncertainties in the residence time calculation. For Al, the solubility estimate is based on average values reported for the Atlantic [Prospero et al., 1987; Baker et al., 2006]. For Ti, an intermediate value was chosen based on results in seawater incubations with Saharan dust (Text A2 in section 3.6) and aerosol filter leachings with deionized water [Buck et al., 2010]. The observed variations in the Ti solubilities may reflect higher Ti solubility in deionized water, specific properties of aerosol and dust samples, or the experimental setup.

Table 3.1: Residence times of dAl and dTi calculated from the annual average dust deposition estimates by Jickells et al. [2005]. For details see section 3.3.1.

	Residence time (years)		Residence time
Region	**Al**	**Ti**	**Ti:Al**
Malvinas Current	0.4 - 0.6	12 - 17	29 - 32
Brazil Malvinas Confluence	1.4 - 2.9	14 - 40	10 - 14
South Atlantic Gyre	4.6 - 17.2	39 - 78	5 - 9
South Equatorial Current	3.5 - 15.7	25 - 108	7
Tropical Salinity Minimum	0.7 - 1.8	4 - 10	6
Canary Current	0.2 - 1.1	3 - 14	5 - 18

In the regions of high dust deposition, the estimated residence times vary between months for dAl and several years for dTi (Table 3.1). Longer residence times occurred in the SAG, most likely due to decreased biological activity and slower removal by scavenging processes. For Al, the observed ranges agree with previous estimations, in the Sargasso Sea [Jickells, 1999], the North Pacific [Orians and Bruland, 1986] and from modelling approaches [Gehlen et al., 2003; Han et al., 2008]. For dTi, to our knowledge these are the first residence time estimates in Atlantic surface waters. The residence times of dTi clearly exceed those of dAl, on average by a factor of ~10. This generally indicates higher reactivity of dAl in the surface ocean. Specific differences occurred in the MC and the TSM, and could be related to spatial variations in both inventories and/or atmospheric fluxes of dAl and dTi in these regions.

3.3.2 Relationship between dAl and dTi surface water concentrations and dust deposition

Surface water dAl concentrations have been previously suggested as tracer to estimate the dust supply to the ocean, giving reasonable agreement to model based estimates of dust deposition [Measures and Vink, 2000; Han et al., 2008]. Our observed dAl concentrations similarly agree with the deposition of Saharan dust in the tropical North Atlantic. However, the dAl concentrations do not reflect the deposition of dust from Patagonian sources that is suggested in a more recent estimate [Jickells et al., 2005], whereas dTi concentrations were elevated in both regions. Furthermore, dAl and dTi were specifically distributed within the Saharan dust input region. These observations are in contrast to the expected common atmospheric supply of both metals. Potentially influencing factors for the different regions are discussed below.

Patagonian dust input region

In the MC, decreased dAl concentrations contrast with increased dTi concentrations, and the difference between dAl and dTi residence times is more pronounced than in other regions (Fig. 3.1, Table 3.1). The differences could result either from additional supply of dTi, or increased removal of dAl in this region. The input of excess dTi from atmospheric sources is unlikely, since Ti/Al ratios from Patagonian and Saharan dust are similar [Formenti et al., 2003; Gaiero et al., 2007] and solubility experiments by Baker et al. [2006] rather indicate higher solubility of Al for Patagonian than for Saharan dust. The sampling stations in the MC were located at the edge of the Patagonian shelf (300 - 400 km

offshore), suggesting that additional supply of dTi might have occurred via coastal erosion or resuspension of shelf sediments [Pierce and Siegel, 1979; Gaiero et al., 2003]. Suspended material may be transported offshore with surface currents [Pierce and Siegel, 1979], however, previous studies showed only small release of dTi through sediment resuspension [Skrabal and Terry, 2002] compared to considerable release of dAl [Moran and Moore, 1991; Skrabal and Terry, 2002]. Similarly, pore water profiles indicate the benthic supply of both metals to bottom waters [Skrabal and Terry, 2002]. The supply of excess dTi over dAl in the MC is thus unlikely, suggesting that the deviating distributions and residence times of dAl and dTi rather result from the preferential removal of dAl over dTi. The removal of dAl is strongly influenced by surface adsorption on biogenic particles and/or biological uptake, and is thus coupled to biological productivity [e.g. Moran and Moore, 1988; Gehlen et al., 2002; Middag et al., 2009]. Observations in sediment cores indicate that dTi is less susceptible to such removal than dAl [e.g. Murray and Leinen, 1996]. SeaWiFS images show high chlorophyll *a* concentrations in the MC in the two months preceding the sampling (see Fig. A3 in section 3.6). This suggests that the removal with biogenic particles may indeed have resulted in excess removal of dAl over dTi. The high reactivity of dAl would also explain why dAl concentrations in April do not reflect the Patagonian dust deposition that occurs predominantly in austral summer [Johnson et al., 2010].

Saharan dust input region

In the North Atlantic, the dAl maximum concurred with the TSM as well as with the southward shifted zone of maximum Saharan dust transport during boreal winter [Moulin et al., 1997]. In agreement with short residence times, the dAl concentrations may thus reflect the seasonal dust deposition pattern in the months preceding the sampling. However, previous studies (Table 3.2) similarly found highest dAl concentrations in the TSM in boreal summer [Measures et al., 2008], that do not agree with the seasonal dust deposition pattern. In contrast to this, the maximum concentrations of total dissolvable Al reflected the seasonal movement of the maximum dust transport between boreal sping and autumn (Table 3.2) [Helmers and Rutgers van der Loeff, 1993; Bowie et al., 2002]. This suggests that, due to increased solubility of Al with the lower pH in rainwater [Prospero et al., 1987; Losno et al., 1993], dAl is predominantly supplied by wet deposition within the Inter-Tropical Convergence Zone. The underestimated solubility of Al in rainwater could have resulted in an overestimation of the residence times in the TSM.

Table 3.2: Observations of maximum Al concentrations in the tropical and subtropical Atlantic.

Study	Sampling period	Location of maximum
total dissolvable Al		
Helmers and R. v. d. Loeff, 1993	May	7 °S - 10 °N
Helmers and R. v. d. Loeff, 1993	Oct	2 °S - 20 °N
Bowie et al., 2002	May - Jun	8 °S - 10 °N
Bowie et al., 2002	Sep - Oct	10 °N - 25 °N
dissolved Al		
Measures et al., 2008	Jul - Aug	0 - 10 °N
this study	April - May	0 - 10 °N

By contrast to dAl, the distribution of dTi in the North Atlantic agreed with the annual dust deposition average [Jickells et al., 2005] and the estimated longer residence times for dTi. The absence of elevated dTi concentrations in the TSM suggests that potential solubility differences between rainwater and seawater are less pronounced for Ti than for Al. Overall, the different distributions of dAl and dTi in the North Atlantic can be explained by two processes that may also be complementary: a) due to different residence times the dAl and dTi concentrations reflect the variations between seasonal and annual dust deposition and b) the difference between the dust solubilities in rainwater and seawater is more pronounced for dAl, resulting in a stronger influence of wet deposition for dAl than for dTi.

Relationship over the Atlantic transect

Figure 3.2 shows the relationship between the surface water concentrations of dAl and dTi and dust deposition estimates given in the model composite by Jickells et al. [2005 and references therein] for both the annual and the sampling period (April-May) average. For dAl the correlation improves if the seasonal dust deposition is considered (Fig. 3.2 a, b), suggesting that dAl concentrations are stronger related to integrations of the dust deposition over shorter time scales. By contrast, dTi concentrations are reasonably correlated with both the annual and the seasonal dust deposition estimate (Fig. 3.2 c, d). These observations support the idea that dAl concentrations reflect seasonal variations in the dust deposition, whereas dTi concentrations rather reflect interannual variations in the dust deposition. This suggests that dAl and dTi concentrations may serve as tracers for dust deposition variations over different time scales. However, in addition to the general

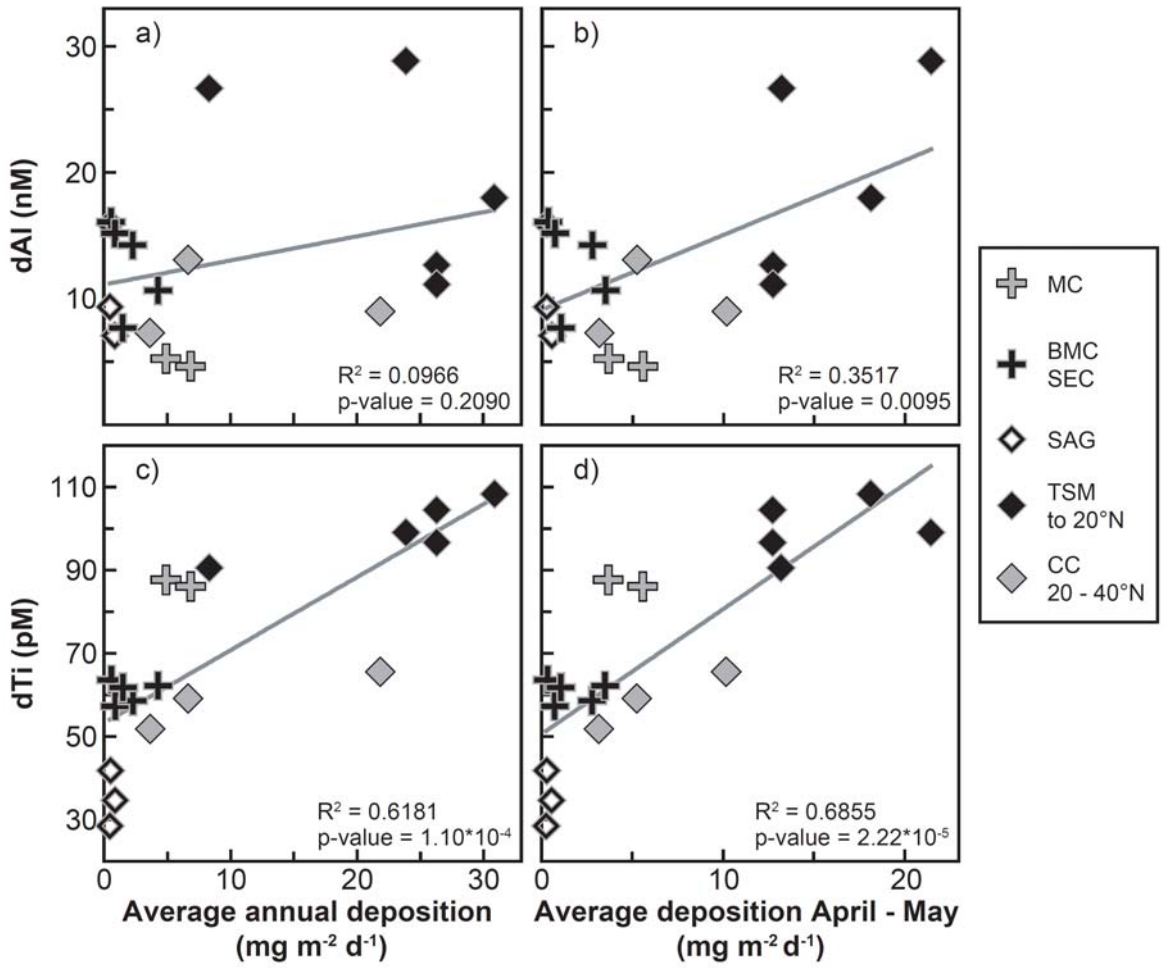

Fig. 3.2: Dissolved Al and dTi concentrations versus average dust deposition estimates from the model composite by Jickells et al., [2005]. Figures 2 a and 2 c show the average annual dust deposition, Figures 2 b and d the average dust deposition during the sampling period (April - May). The grey lines indicate the correlation functions. For further details refer to section 3.3.2.

relationship, dAl and dTi distributions show specific spatial variations over the Atlantic transect (see data points from MC in Fig. 3.2). As discussed above, additional differences between both metals can be attributed to the excess removal of dAl in the MC and to the elevated supply of only dAl with wet deposition in the TSM. Previous studies suggested the simple estimation of dust inputs from dAl concentrations with the assumption of invariant values for both residence times (5 years) and soluble dust fractions of Al (1.5 - 5 %) [e.g. Measures and Vink, 2000; Vink and Measures, 2001; Measures et al., 2008]. However, our data indicate variations in both factors in different regions of the Atlantic Ocean. Considering the observed residence times (Table 3.1), such calculation would likely overestimate dust inputs in the SAG (dAl residence times >5 years) and

underrestimate inputs in the MC, TSM and CC (dAl residence times <5 years). Similarly, underestimated solubilities of dust Al in regions with strong influence of wet deposition would result in overestimated dust inputs.

3.4 Conclusions

Despite the common source of dAl and dTi we observed distinct differences in the distributions of both metals in Atlantic surface waters. Patagonian dust input was only reflected in dTi concentrations, most likely due to fast removal of dAl onto biogenic particles. In the North Atlantic, highest dAl concentrations indicate the increased dissolution and supply of dust derived Al with wet deposition. By contrast, the distribution of dTi was not related to wet deposition but reflected the pattern of the average annual dust deposition [Jickells et al., 2005]. Residence time estimates and the relation between surface water concentrations and dust deposition suggest that dAl concentrations may serve to trace seasonal variations in the dust deposition, whereas dTi concentrations may serve to trace variations in the dust deposition over longer time scales. However, our data also indicate spatial differences in supply and removal processes of dAl and dTi in the surface ocean. Variations in solubilities and residence times have to be considered if the dust deposition is assessed from surface water concentrations of dAl and dTi.

Acknowledgements: We thank the officers and crew of RV Polarstern and our colleagues D. Gaiero and M. Heller for their help during ANTXXVI-4, and two anonymous reviewers for their constructive comments on the manuscript. Funding for the participation and the work performed during ANTXXVI-4 was provided by the DFG via grants to PLC (CR145/15-1 and CR145/18-1). The financial support by SOPRAN (BMBF FKZ 03F0462A and 03F0611A) is also gratefully acknowledged. T. Wagener was supported by a Marie Curie IEF (Grant agreement No.: PIEF-GA-2009-236694, DAPOP).

3.5 References

Baker A. R. and Croot P. L. (2010) Atmospheric and marine controls on aerosol iron solubility in seawater. *Marine Chemistry* **120**, 4-13.

Baker A. R., Jickells T. D., Witt M. and Linge K. L. (2006) Trends in the solubility of iron, aluminium, manganese and phosphorus in aerosol collected over the Atlantic Ocean. *Marine Chemistry* **98**, 43-58.

Bowie A. R., Whitworth D. J., Achterberg E. P., Mantoura R. F. C. and Worsfold P. J. (2002) Biogeochemistry of Fe and other trace elements (Al, Co, Ni) in the upper Atlantic Ocean. *Deep Sea Research Part I: Oceanographic Research Papers* **49**, 605-636.

Buck C. S., Landing W. M., Resing J. A. and Measures C. I. (2010) The solubility and deposition of aerosol Fe and other trace elements in the North Atlantic Ocean: Observations from the A16N CLIVAR/CO_2 repeat hydrography section. *Marine Chemistry* **120**, 57-70.

Croot P. L. (2011) Rapid determination of picomolar titanium in seawater with catalytic cathodic stripping voltammetry. *Analytical Chemistry* **83**, 6395-6400.

Duce R. A., Liss P. S., Merrill J. T., Atlas E. L., Buat-Menard P., Hicks B. B., Miller J. M., Prospero J. M., Arimoto R., Church T. M., Ellis W., Galloway J. N., Hansen L., Jickells T. D., Knap A. H., Reinhardt K. H., Schneider B., Soudine A., Tokos J. J., Tsunogai S., Wollast R. and Zhou M. (1991) The atmospheric input of trace species to the World Ocean. *Global Biogeochemical Cycles* **5**, 193-259.

Formenti P., Elbert W., Maenhaut W., Haywood J. and Andreae M. O. (2003) Chemical composition of mineral dust aerosol during the Saharan Dust Experiment (SHADE) airborne campaign in the Cape Verde region, September 2000. *Journal of Geophysical Research* **108**, 8576, doi:10.1029/2002JD002648.

Gaiero D. M., Brunet F., Probst J.-L. and Depetris P. J. (2007) A uniform isotopic and chemical signature of dust exported from Patagonia: Rock sources and occurrence in southern environments. *Chemical Geology* **238**, 107-120.

Gaiero D. M., Probst J.-L., Depetris P. J., Bidart S. M. and Leleyter L. (2003) Iron and other transition metals in Patagonian riverborne and windborne materials: Geochemical control and transport to the southern South Atlantic Ocean. *Geochimica et Cosmochimica Acta* **67**, 3603-3623.

Gehlen M., Beck L., Calas G., Flank A. M., van Bennekom A. J. and van Beusekom J. E. E. (2002) Unraveling the atomic structure of biogenic silica: Evidence of the structural association of Al and Si in diatom frustules. *Geochimica et Cosmochimica Acta* **66**, 1601-1609.

Gehlen M., Heinze C., Maier-Reimer E. and Measures C. I. (2003) Coupled Al-Si geochemistry in an ocean general circulation model: A tool for the validation of oceanic dust deposition fields? *Global Biogeochemical Cycles* **17**, 1028, doi:10.1029/2001gb001549.

Han Q., Moore J. K., Zender C., Measures C. I. and Hydes D. J. (2008) Constraining oceanic dust deposition using surface ocean dissolved Al. *Global Biogeochemical Cycles* **22**, GB2003, doi:10.1029/2007gb002975.

Helmers E. and Rutgers van der Loeff M. M. (1993) Lead and aluminum in Atlantic surface waters (50 °N to 50 °S) reflecting anthropogenic and natural sources in the eolian transport. *Journal of Geophysical Research* **98**, 20261-20273.

Hydes D. J. and Liss P. S. (1976) Fluorimetric method for the determination of low concentrations of dissolved aluminum in natural waters. *Analyst* **101**, 922-931.

Jickells T. D. (1999) The inputs of dust derived elements to the Sargasso Sea; A synthesis. *Marine Chemistry* **68**, 5-14.

Jickells T. D., An Z. S., Andersen K. K., Baker A. R., Bergametti G., Brooks N., Cao J. J., Boyd P. W., Duce R. A., Hunter K. A., Kawahata H., Kubilay N., laRoche J., Liss P. S., Mahowald N., Prospero J. M., Ridgwell A. J., Tegen I. and Torres R. (2005) Global iron connections between desert dust, ocean biogeochemistry, and climate. *Science* **308**, 67-71.

Johnson M. S., Meskhidze N., Solmon F., Gassó S., Chuang P. Y., Gaiero D. M., Yantosca R. M., Wu S., Wang Y. and Carouge C. (2010) Modeling dust and soluble iron deposition to the South Atlantic Ocean. *Journal of Geophysical Research* **115**, D15202, doi:10.1029/2009JD013311.

Losno R., Colin J. L., Bris N., Bergametti G., Jickells T. and Lim B. (1993) Aluminium solubility in rainwater and molten snow. *Journal of Atmospheric Chemistry* **17**, 29-43.

Luo C., Mahowald N. and del Corral J. (2003) Sensitivity study of meteorological parameters on mineral aerosol mobilization, transport, and distribution. *Journal of Geophysical Research* **108**, 4447, doi:10.1029/2003jd003483.

McLennan S. M. (2001) Relationships between the trace element composition of sedimentary rocks and upper continental crust. *Geochemistry Geophysics Geosystems* **2**, 1021, doi:10.1029/2000gc000109.

Measures C. I. and Vink S. (2000) On the use of dissolved aluminum in surface waters to estimate dust deposition to the ocean. *Global Biogeochemical Cycles* **14**, 317-327.

Measures C. I., Landing W. M., Brown M. T. and Buck C. S. (2008) High-resolution Al and Fe data from the Atlantic Ocean CLIVAR-CO2 repeat hydrography A16N transect: Extensive linkages between atmospheric dust and upper ocean geochemistry. *Global Biogeochemical Cycles* **22**, GB1005, doi:10.1029/2007gb003042.

Middag R., de Baar H. J. W., Laan P. and Bakker K. (2009) Dissolved aluminium and the silicon cycle in the Arctic Ocean. *Marine Chemistry* **115**, 176-195.

Moran S. B. and Moore R. M. (1988) Evidence from mesocosm studies for biological removal of dissolved aluminum from sea water. *Nature* **335**, 706-708.

Moran S. B. and Moore R. M. (1991) The potential source of dissolved aluminum from resuspended sediments to the North Atlantic Deep Water. *Geochimica et Cosmochimica Acta* **55**, 2745-2751.

Moulin C., Lambert C. E., Dulac F. and Dayan U. (1997) Control of atmospheric export of dust from North Africa by the North Atlantic Oscillation. *Nature* **387**, 691-694.

Murray R. W. and Leinen M. (1996) Scavenged excess aluminum and its relationship to bulk titanium in biogenic sediment from the central equatorial Pacific Ocean. *Geochimica et Cosmochimica Acta* **60**, 3869-3878.

Orians K. J., Boyle E. A. and Bruland K. W. (1990) Dissolved titanium in the open ocean. *Nature* **348**, 322-325.

Orians K. J. and Bruland K. W. (1986) The biogeochemistry of aluminum in the Pacific Ocean. *Earth and Planetary Science Letters* **78**, 397-410.

Pierce J. W. and Siegel F. R. (1979) Supended particulate matter on the southern Argentine shelf. *Marine Geology* **29**, 73-91.

Prospero J. M., Nees R. T. and Uematsu M. (1987) Deposition rate of particulate and dissolved aluminium derived from Saharan dust in precipitation at Miami, Florida. *Journal of Geophysical Research* **92**, 14723-14731.

Rohardt G. (2010), Continuous thermosalinograph oceanography along POLARSTERN cruise track ANT-XXVI/4, Alfred Wegener Institute for Polar and Marine Research, Bremerhaven, doi:10.1594/PANGAEA.753224.

Rohardt G. and Bracher A. (2011), Physical oceanography during POLARSTERN cruise ANT-XXVI/4, Alfred Wegener Institute for Polar and Marine Research, Bremerhaven, doi:10.1594/PANGAEA.758127.

Skrabal S. A. (2006) Dissolved titanium distributions in the Mid-Atlantic Bight. *Marine Chemistry* **102**, 218-229.

Skrabal S. A. and Terry C. M. (2002) Distributions of dissolved titanium in porewaters of estuarine and coastal marine sediments. *Marine Chemistry* **77**, 109-122.

Tchernia P. (1980) *Descriptive Regional Oceanography.* Pergamon Press Ltd., Oxford.

Vink S. and Measures C. I. (2001) The role of dust deposition in determining surface water distributions of Al and Fe in the South West Atlantic. *Deep Sea Research Part II: Topical Studies in Oceanography* **48**, 2787-2809.

3.6 Auxiliary material

Table A1: Station Information and dAl and dTi concentrations

Table A1: Station information and determined dAl and dTi concentrations in surface seawater samples during ANTXXVI-4 (presented in Fig. 3.1). MLD is mixed layer depth, SD is standard deviation.

Station	Date	Time (UTC)	Latitude	Longitude	Depth (m)	MLD (m)	dAl (nM)	SD dAl (nM)	dTi (pM)	SD dTi (pM)
PS75/264-2	2010-04-10	04:36	47° 39.61' S	60° 44.90' W	20	32	5.23	0.15	87.67	4.20
PS75/266-4	2010-04-11	17:58	43° 13.38' S	57° 17.83' W	20	60	4.63	0.03	86.08	3.48
PS75/268-1	2010-04-13	15:20	39° 05.59' S	50° 56.02' W	20	40	10.66	0.22	62.24	3.54
PS75/270-1	2010-04-15	15:19	34° 42.96' S	44° 26.43' W	20	61	7.67	0.12	61.79	4.26
PS75/272-4	2010-04-17	15:44	31° 12.53' S	39° 22.06' W	20	53	7.04	0.16	34.68	5.62
PS75/274-1	2010-04-19	14:17	24° 45.24' S	35° 42.76' W	25	66	15.93	0.06	41.83	3.60
PS75/276-1	2010-04-21	14:14	18° 47.27' S	32° 31.37' W	25	82	9.34	0.13	28.52	3.64
PS75/278-1	2010-04-23	14:22	13° 03.38' S	28° 30.59' W	25	36	16.09	0.33	63.63	3.51
PS75/279-6	2010-04-24	16:16	10° 42.47' S	26° 55.75' W	25	48	15.17	0.22	57.35	11.23
PS75/281-1	2010-04-26	14:17	5° 09.77' S	23° 06.58' W	25	56	14.23	0.18	58.60	4.31
PS75/283-5	2010-04-28	14:25	1° 46.47' N	23° 00.07' W	20	32	26.68	0.34	90.61	6.72
PS75/285-1	2010-04-30	13:19	8° 03.90' N	22° 59.99' W	25	37	28.84	0.4	99.04	5.88
PS75/286-2	2010-05-02	13:43	14° 33.19' N	23° 40.98' W	25	31	18.01	0.24	108.36	4.94
PS75/287-4	2010-05-04	07:55	17° 35.34' N	24° 15.65' W	20	41	12.66	0.28	104.47	7.76
PS75/289-1	2010-05-04	13:16	17° 36.53' N	24° 45.03' W	25	34	11.12	0.09	96.63	4.02
PS75/292-1	2010-05-06	11:32	23° 07.35' N	20° 39.21' W	25	27	8.97	0.03	65.61	5.27
PS75/294-5	2010-05-09	13:23	33° 35.66' N	13° 51.43' W	20	30	13.08	0.25	59.17	5.23
PS75/296-1	2010-05-11	11:47	39° 45.75' N	11° 50.75' W	25	49	7.28	0.08	51.83	5.79

Text A2: Dissolution of Ti from Saharan dust: Methodology and results of incubation experiments during ANTXXVI-4

Methods

The solubility of aerosol Ti in surface seawater was assessed in dissolution experiments with Saharan dust. Details of the dust preparation and its chemical composition are given in Guieu et al. [2010]. Surface seawater samples from three stations (268, 278 and 289, see Table A1) were incubated with 10 mg/l of evapocondensed dust in Teflon bottles. The bottles were kept in the dark and subsamples were taken at the beginning and at days 1, 3, 5 and 7 of the incubation. The subsamples were vacuum filtered on 0.2 µm polycarbonate membranes (Nuclepore™, 47 mm, Whatman) using Teflon filtration devices and subsequently analyzed for dTi.

Results

The observed solubilities of Ti closely agreed for the three dissolution experiments and insignificantly varied with the different intial seawaters utilized. In general, the concentrations of dTi did not further increase after 3 days. Within 3 to 7 days after beginning of the incubation on average 0.0071 ± 0.0008 % of Ti were dissolved from the Saharan dust samples.

References

Guieu C., Dulac F., Desboeufs K., Wagener T., Pulido-Villena E., Grisoni J. M., Louis F., Ridame C., Blain S., Brunet C., Nguyen E. B., Tran S., Labiadh M. and Dominici J. M. (2010) Large clean mesocosms and simulated dust deposition: A new methodology to investigate responses of marine oligotrophic ecosystems to atmospheric inputs, *Biogeosciences* **7**, 2765-2784.

Figure A3: SeaWiFS chlorophyll a concentrations in April - May 2010

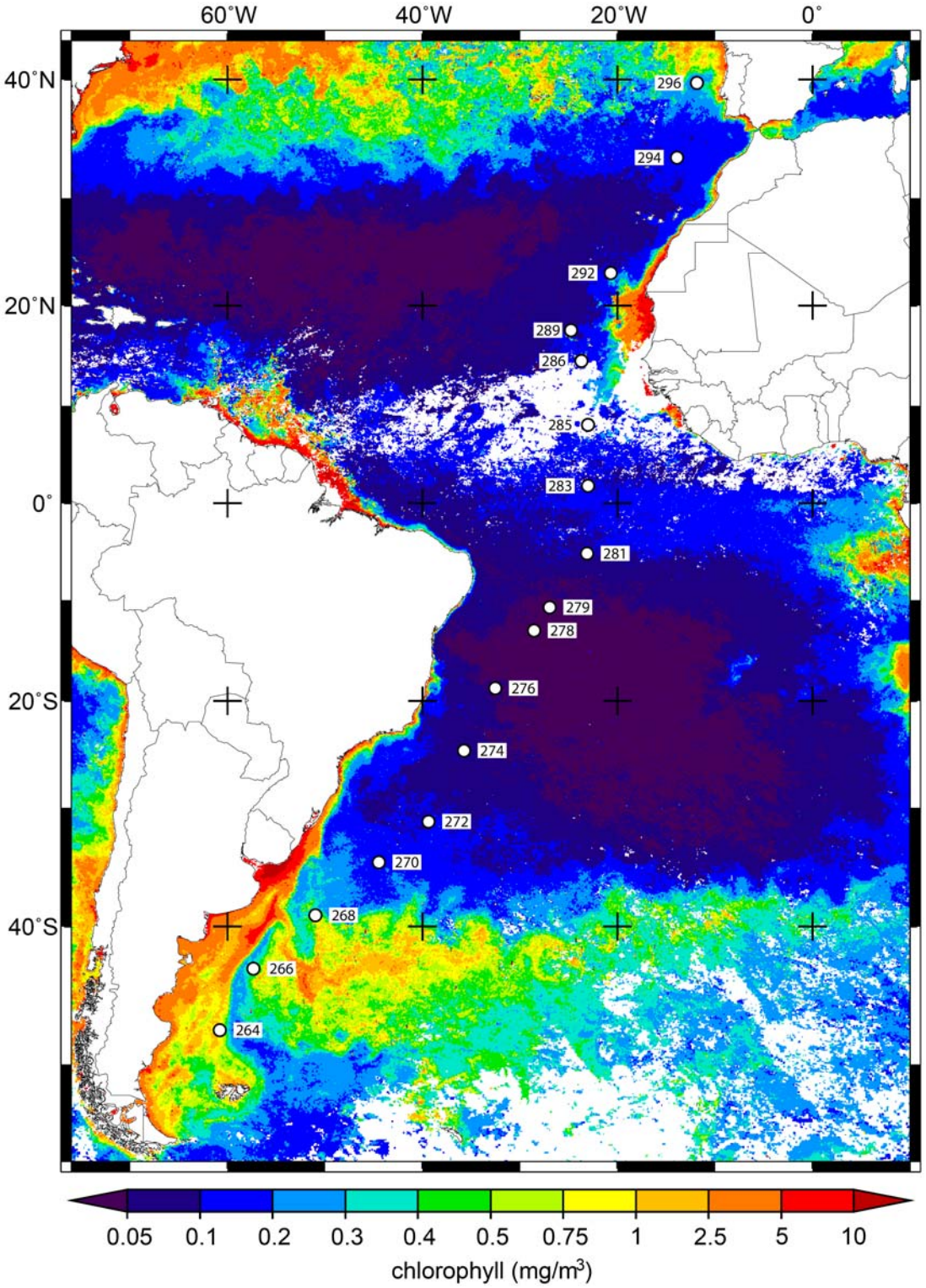

Fig. A3: Average chlorophyll *a* concentrations (mg/m³) obtained from SeaWiFS images in April and May 2010. Cirles and associated numbers denote the sampling stations during ANTXXVI-4. Analyses and visualizations of chlorophyll *a* concentrations were produced with the Giovanni online data system, developed and maintained by the NASA GES DISC.

4 Low Colloidal Associations of Aluminium and Titanium in Surface Waters of the Tropical Atlantic

Anna Dammshäuser[1], Peter L. Croot[1, 2, 3]

Submitted to Geochimica et Cosmochimica Acta, 12 December 2011

Abstract

The distributions of dissolved, soluble and colloidal aluminium (Al) and titanium (Ti) were assessed by ultrafiltration studies in the upper water column of the eastern tropical North Atlantic. The dissolved fractions of both metals were found to be dominated by the soluble phase smaller than 10 kDa. The colloidal associations were very low (0.2 - 3.4 %) for Al and not detectable for Ti. These findings are in some contrast to previous estimations for Ti and to the predominant occurrence of both metals as hydrolyzed species in seawater. However, low tendencies to form inorganic colloids can be expected, as in seawater dissolved Al and dissolved Ti are present within their inorganic solubility levels. In addition, the association with functional organic groups in the colloidal phase is unlikely for both metals. The vertical distributions of the dissolved fractions showed surface maxima with up to 43 nM of Al and 157 pM of Ti, reflecting their predominant supply from atmospheric sources to the open ocean. In the surface waters, excess dissolved Al over dissolved Ti was present compared to the crustal source, indicating higher solubility and thus elevated inputs of dissolved Al from atmospheric mineral particles. At most stations, subsurface minima of Al and Ti were observed and can be ascribed to scavenging processes and/or biological uptake. The dissolved Al concentrations decreased by

[1] Helmholtz Centre for Ocean Research Kiel (GEOMAR), Germany

[2] Plymouth Marine Laboratory, PML, United Kingdom

[3] now at: Earth and Ocean Sciences, National University of Ireland-Galway, NUIG, Ireland

80 - 90 % from the surface maximum to the subsurface minimum. Estimated residence times in the upper 100 m of the water column were 1.6 - 4 years for dissolved Al and 14 - 17 years for dissolved Ti. These short residence times are in some contrast to the low colloidal associations of Al and Ti and the assumed role of colloids as intermediates in scavenging processes. This suggests that either the removal of both metals occurs predominantly via adsorption of the hydrolyzed species on the particulate fraction or that the colloidal phase is rapidly turned over in the upper water column.

4.1 Introduction

Aluminium (Al) and Titanium (Al) are abundant elements in the earth's crust [McLennan, 2001] but are found in comparably low concentrations (pM to nM) in seawater. Their delivery to the open ocean occurs predominantly via the deposition and dissolution of atmospherically transported mineral particles from terrestrial origin (also referred to as dust) [Orians and Bruland, 1986; Orians et al., 1990]. As a consequence, the surface water concentrations of dissolved Al (dAl) and dissolved Ti (dTi) are clearly related to atmospheric inputs [e.g. Helmers and Rutgers van der Loeff, 1993; Measures, 1995; Measures and Vink, 2000; Dammshäuser et al., 2011]. The material input via the deposition of dust into the open ocean is yet poorly constrained, with flux estimations based on few direct observations [Duce et al., 1991; Luo et al., 2003 and references therein] and modeling approaches [e.g. Luo et al., 2003; Jickells et al., 2005]. Dissolved Al concentrations have been suggested as tracer to estimate the dust supply [e.g. Measures and Vink, 2000; Gehlen et al., 2003; Han et al., 2008]. However, an accurate quantification is complicated by spatial and temporal variations in both the soluble Al fractions in the mineral particles and in the residence times of dAl in the surface waters [Han et al., 2008; Dammshäuser et al., 2011]. Recent observations along a meridional Atlantic transect suggest that dTi concentrations may be complementary utilized to trace the dust deposition [Dammshäuser et al., 2011]. However, the oceanic distribution of Ti is still poorly constrained and further information is required about its behavior in the surface ocean.

In seawater, both Al and Ti predominantly occur as hydrolyzed species [Turner et al., 1981] and are highly particle reactive [Li, 1991]. The distributions of both elements are thus expected to be strongly influenced by abiotic scavenging processes in the upper water column [e.g. Hydes, 1979; Orians et al., 1990]. For Al, additional evidence has been found for biological removal mechanisms [Deuser et al., 1983; Moran and Moore, 1988; van

Bennekom et al., 1989; Moran and Moore, 1992], via the inclusion of Al in the silicate frustules of diatoms [Gehlen et al., 2002; Koning et al., 2007]. In the case of Ti, nothing is yet known about incorporation or utilization in marine biological materials. The process of abiotic scavenging includes the transfer from the dissolved to the particulate phase via surface adsorption and/or aggregation mechanisms [e.g. Li, 1981], with colloidal associations likely acting as an intermediate species [e.g. Honeyman and Santschi, 1989; Moran et al., 1996]. Thus, the removal of trace metals can be expected to be related to their distributions between the colloidal and the soluble phase in seawater. Accordingly, the strong influence of scavenging mechanisms on the oceanic distributions of dAl and dTi also suggests their association with colloidal species. However, for Al low colloidal fractions were observed [Moran and Moore, 1989; Reitmeyer et al., 1996], and for Ti, there is to our knowledge no information on colloidal associations published so far.

In this study, the dissolved, colloidal and soluble fractions of Al and Ti were determined in surface waters of the eastern tropical North Atlantic. The size fractionation was conducted simultaneously by cross-flow ultrafiltration with a membrane cut-off of 10 kDa. The colloidal fraction is thus defined as the size fraction between 10 kDa and 0.2 μm. Since the size fractionation of Al has been reported to be hampered by contamination problems [Reitmeyer et al., 1996] and no information is available on the size fractionation of Ti so far, we provide a thorough evaluation of the ultrafiltration process and compare different approaches to determine the colloidal fraction. The study area is characterized by the elevated supply of atmospheric mineral particles originating from the Sahara region. Therefore, pronounced input signals and extensive removal processes can be expected for dAl and dTi in the upper water column. The aim of this study was to better constrain the behavior of dAl and dTi upon their supply via dust deposition. The particular focus lies on identifying potential relationships between the size distributions and the removal processes of both metals. A deeper understanding of the oceanic behavior of Al and Ti will eventually help to better constrain their complementary utilization as tracers for dust deposition to the open ocean.

4.2 Methods

Seawater samples were collected aboard RV Meteor during the SFB 754 cruise M80-2 (Mindelo - Dakar) in November and December 2009. The study area is located in the eastern tropical North Atlantic. The sampled stations are displayed in Fig. 4.1. Four

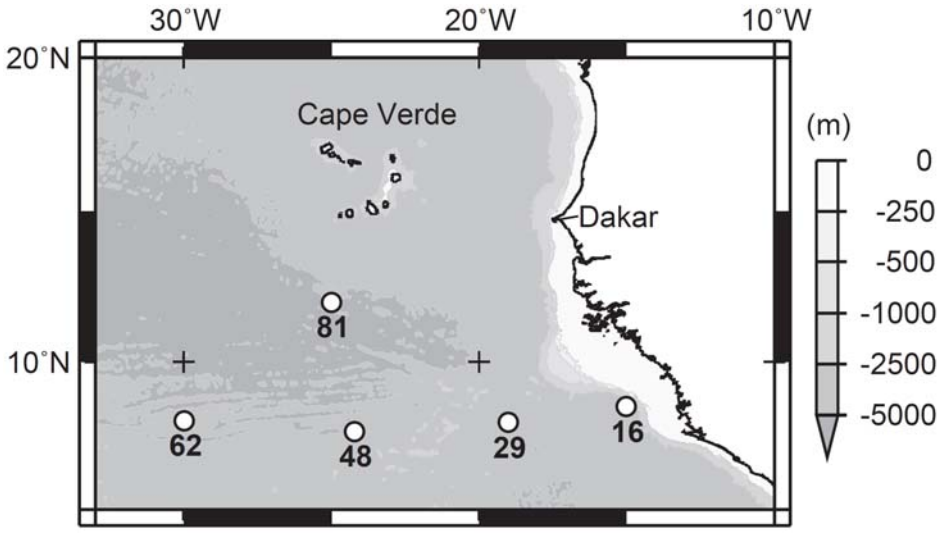

Fig. 4.1: Map of the study area. Circles denote the sampled stations

stations (16, 29, 48, 62) were located on an E - W transect (15 - 30 °W) close to 8 °N. An additional station (81) was sampled north of this transect at 12 °N and 25 °W.

4.2.1 Sampling

Seawater samples were collected in PTFE coated 8 l GO-FLO bottles (General Oceanics) individually mounted on a Kevlar wire. At each station, seawater was sampled from eight depths in two casts (shallow cast to maximum 200 m, deep cast to maximum 800 m). Immediately after recovery the GO-FLO bottles were transferred into a clean container (ISO 5, class 100, IFM-GEOMAR). In line filtration (0.2 µm) was conducted by applying overpressure of 0.2 bar (N_2 - grade 5.5) to the GO-FLO bottle and filtering the sample into a previously acid cleaned sampling bottle [Kremling et al., 2007]. Two different filter types were applied, cellulose acetate membrane filter capsules (Sartobran® P, Sartorius Stedim Biotech S.A.) and track-etched polycarbonate membrane disk filters (Nuclepore™, 47 mm, Whatman). The filtration on polycarbonate (PC) disk filters was conducted in order to collect particulate material (not discussed here) and the filtrate from the PC filtration was further size fractionated by cross flow ultrafiltration. The filtrate from the cellulose acetate (CA) membrane filter capsules was sampled as part of a standard sampling routine for trace metal analysis in the shore-based laboratory. In order to identify potential contamination or filtration effects during the 0.2 µm filtration, both filtrates were analyzed for Al and Ti concentrations. The different filtration steps are illustrated in Fig. 4.2.

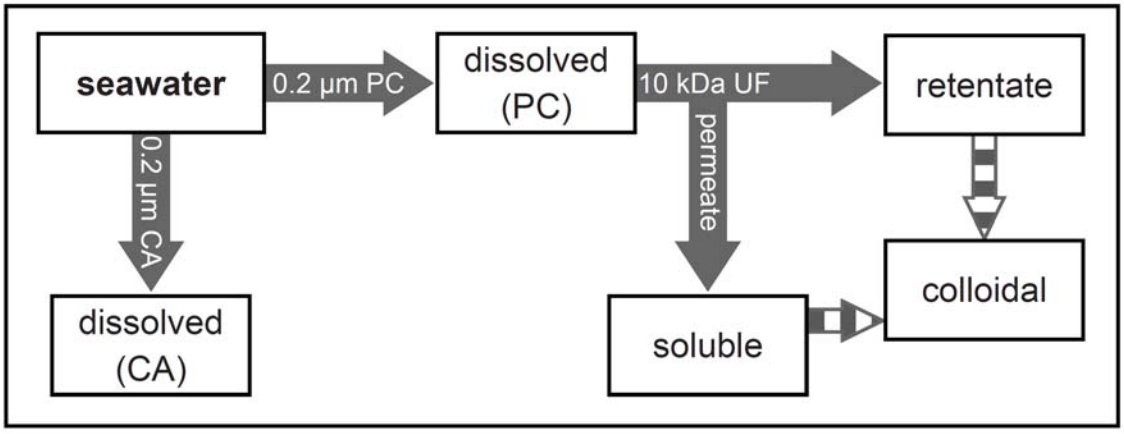

Fig. 4.2: Filtration and ultrafiltration steps during the size fractionation of Al and Ti. Note that the PC filtrate is further size fractionated by ultrafiltration. The CA filtrate was analyzed for Al and Ti and served as reference. The dissolved fraction is here defined as smaller than 0.2 µm, the soluble fraction as smaller than 10 kDa (ultrafiltration permeate). A detailed description of the ultrafiltration process and the calculation of the colloidal fraction are given in sections 4.2.2 and 4.2.4.

4.2.2 Size fractionation by cross-flow ultrafiltration

A detailed discussion of cross-flow ultrafiltration and its application for the sampling of colloidal material is provided in previous studies [e.g. Buesseler et al., 1996; Reitmeyer et al., 1996; Dahlqvist et al., 2004; Guo and Santschi, 2007; Schlosser and Croot, 2008]. In brief, a pre-filtered seawater sample flows parallel to the filtration membrane and is recycled through a reservoir. Compounds smaller than the nominal molecular weight cut-off (MWCO) of the membrane pass the membrane (permeate) and are herein referred to as soluble fraction. The remaining retentate contains both the colloidal fraction which has been rejected by the membrane and some part of the soluble fraction. Over filtration time, the retentate becomes increasingly concentrated and the concentration factor (CF) is given by the ratio between the initial sample volume and the retentate volume:

$$CF = \frac{Vol_{initial}}{Vol_{retentate}} \quad (1)$$

In this study, the ultrafiltration was conducted on polyethersulfone cross flow membranes with a nominal MWCO of 10 kDa (Vivaflow 50, active membrane area 50 cm², Sartorius Stedim Biotech S.A.). Schlosser and Croot [2008] have extensively evaluated the performance of this membrane type for the size fractionation of Fe. The retentate reservoir (PTFE, Savillex) was connected to the membranes with C-FLEX® tubing (Cole-Parmer) and the recirculation flow of the retentate was set to approximately 300 ml/min. The

resulting permeate flow reached 5 ml/min and the integrated permeate sample was collected in a 1 l Teflon bottle.

Prior to utilization, the ultrafiltration membranes were rinsed with 18 MΩ deionized ultrapure water (MQ), 0.1 M HCl and 0.1 M EDTA solution in the following sequence: MQ, HCl, MQ, EDTA, MQ, HCl (200 ml each). After a final rinse with 300 ml of MQ the membranes were conditioned with 200 ml of the respective seawater (recirculation of permeate and retentate). Finally, 1 l of pre-filtered seawater (0.2 µm) was ultrafiltered and subsamples from the retentate and from the integrated permeate were taken at a CF 4 and at the end of the ultrafiltration, when CF 8 - 10 was achieved. The cleaning procedure minimized contamination of the membranes with Al and Ti and was repeated before each filtration of new samples. This allowed the reuse of the membranes for several seawater samples.

4.2.3 Analytical procedures

Aluminium and Ti concentrations were analyzed directly on board. All samples were acidified with sub-boiled quartz distilled HCl [Kuehner et al., 1972] to pH <2 for at least 24 h. Blank values were determined by comparing the analysis results of a duplicate sample that was both normally treated and spiked with double amounts of all reagents. The limits of detection were defined as three times the standard deviation of the blank [de Jong et al., 1998].

Aluminium concentrations were measured as a complete mass balance (analysis of <0.2 µm filtrate, permeate and retentate) in all samples at both subsampled CF. The analysis was conducted using the fluorometric method described by Hydes and Liss [1976]. In short, the reagent lumogallion is added to the sample, which is then buffered to pH 5 with ammonium-acetate, and heated to 40 - 50 °C for 3 h to accelerate complex formation. The fluorescence of the sample was measured with a Hitachi FL 2700 Fluorescence Spectrophotometer (excitation wavelength 497 nm, emission wavelength 572 nm). The detection limit varied between 0.1 and 0.3 nM for Al and blank values lay between 0.4 and 0.6 nM for the different days of analysis. In the SAFe reference seawater S1 (S1 543, S1 474) 1.81 ± 0.24 nM of Al (n = 4) were determined (consensus value is 1.74 ± 0.09 nM).

Titanium concentrations were determined in the <0.2 µm fraction and in the final permeate sample by a new voltammetric method [Croot, 2011]. In brief, Ti is analyzed by catalytic cathodic stripping voltammetry (CSV) on a hanging mercury drop electrode (HMDE,

Metrohm model 663VA). Cupferron (ammonium N-nitrosophenylhydroxylamine) is used as a ligand and bromate serves to enhance catalysis and to improve the sensitivity. The detection limit was 9 pM and the blank value 24 ± 3 pM for Ti. The standard deviation of multiple measurements of Ti in the same sample (n = 5) was smaller than 5 %.

Chlorophyll *a* concentrations were measured from each GO-FLO bottle and also served to calibrate the fluorescence data from the CTD sensor. Seawater samples (250 ml) were filtered onto Whatman 25 mm glass fiber filters (GF/F Whatman) and subsequently the filters were extracted in 90 % acetone. The chlorophyll *a* concentrations were determined fluorometrically (Turner AU-10). Supporting oceanographic data including fluorescence data were obtained from the CTD system.

4.2.4 Calculation of the colloidal fraction and mass balance

In this study, the colloidal fraction is operationally defined as the size fraction between 0.2 µm and 10 kDa. Consequently, the colloidal fractions of the different metals can be calculated from the CF and the measured concentrations in permeate, retentate and dissolved fraction. Several calculation methods have been applied for the calculation of the colloidal fractions [e.g. Reitmeyer et al., 1996; Wen et al., 1999; Dahlqvist et al., 2004]. Frequently, the colloidal fraction is calculated from the retentate concentration by correcting for the presence of some part of the soluble fraction and the extent of sample concentration [Buesseler et al., 1996; Reitmeyer et al., 1996]:

$$c_{colloidal} = \frac{\left(c_{retentate} - c_{permeate}\right)}{CF} \tag{2}$$

However, using this equation assumes ideal behavior of the permeable species and the membrane during the ultrafiltration process. Schlosser and Croot [2008] suggest the more accurate calculation of the colloidal fraction by also considering the permeation coefficient (P_c) and the loss during the ultrafiltration:

$$c_{colloidal} = c_{initial} - \frac{c_{permeate}}{V_{initial}} \cdot \left(\frac{V_{retentate}}{P_c} + V_{permeate} \right) \tag{3}$$

The experimental determination of the permeation coefficient necessitates the analysis of the instantaneous permeate outflow at multiple time steps during the ultrafiltration [e.g. Guo et al., 2001; Schlosser and Croot, 2008]. In this study the labor intensive analysis procedures limited the amount of subsamples that could be analyzed; and the permeate was thus collected as an integrated sample [Reitmeyer et al., 1996; Wen et al., 1996]. If ideal permeation behavior ($P_c = 1$) is assumed Eq. 3 reduces to the following:

$$c_{colloidal} = c_{initial} - c_{permeate} \quad (4)$$

The performance of the ultrafiltration process can be evaluated by calculating a mass balance. Ideally, contamination and adsorptive losses during the ultrafiltration are negligible and the sum of the colloidal and soluble fraction equals the dissolved fraction [Buesseler et al., 1996; Reitmeyer et al., 1996]:

$$c_{initial} = \frac{c_{retentate}}{CF} + c_{permeate} \cdot \left(1 - \frac{1}{CF}\right) \quad (5)$$

Loss or contamination during the ultrafiltration can be experimentally determined from the deviation between the calculated initial concentration and the measured initial concentration of the investigated species. The recovery is then given as the ratio of calculated initial concentration to measured initial concentration:

$$\text{Rec.}\,(\%) = \frac{c_{initial,\,calculated}}{c_{initial,\,measured}} \cdot 100 \quad (6)$$

Both equations to calculate the colloidal fractions (Eqs. 2 and 4) can also be connected via the mass balance. Subtracting the deviation between the calculated initial concentration (Eq. 5) and the measured initial concentration from the colloidal fraction calculated by Eq. 2 equals the colloidal fraction calculated by Eq. 4:

$$c_{initial} - c_{permeate} = \frac{\left(c_{retentate} - c_{permeate}\right)}{CF} - \left(\frac{c_{retentate}}{CF} + c_{permeate} \cdot \left(1 - \frac{1}{CF}\right) - c_{initial}\right) \quad (7)$$

With ideal filtration behavior both equations would give similar results for the colloidal fractions. If the filtration behavior is not ideal, Eq. 4 entirely attributes the potential losses or contamination from the ultrafiltration to the colloidal fraction. However, loss or contamination may also affect the permeable species. In this study ideal filtration behavior is assumed (P_c = 1), and both calculation methods, Eqs. 2 and 4, are compared for the determination of the colloidal fractions. In addition, the permeation coefficient was estimated and the colloidal fraction was also calculated using the approach described in Schlosser and Croot [2008].

4.3 Results and method evaluation

4.3.1 Size fractionation by cross-flow ultrafiltration

The concentrations of dAl and dTi and the measured and calculated values from the ultrafiltration process are given in the Tables 4.1 and 4.2. The dissolved fractions were

determined in the filtrates of both filtration procedures, filtration through cellulose acetate (CA) filter capsules and through polycarbonate (PC) disk filters. The dAl and dTi concentrations in the two filtrates agreed well, with exception of three samples (station 16, 80 m, station 29, 60 m; station 48, 80 m). These samples are considered as contaminated for Ti. Applying a paired t-test to the corresponding data sets gives $|t| < t_{(0.95;\ 19)}$ and p-values higher than 0.05, showing no statistically significant differences ($t_{(0.95;\ 19)}$ = 2.1; for Al is $|t|$ = 1.29 and p = 0.47, for Ti is $|t|$ = 1.40 and p = 0.2). The performance of the ultrafiltration process was generally satisfying for Al and Ti. In the following, the mass balances and the determination of the colloidal fractions are evaluated.

4.3.2 Mass balance and calculation of colloidal Al

Aluminium concentrations were determined in all size fractions at both CF (Table 4.1) and in most samples mass balances of 100 ± 10 % were achieved. In general, Al contamination during the ultrafiltration process was significantly decreased compared to the results reported by Reitmeyer et al. [1996]. However, recoveries above 120 % were found in some samples (stations 16 and 29) and can be ascribed to both elevated permeate and retentate concentrations. One sample (station 16, 120 m) showed a strong increase in the retentate concentration and recovery from CF 4 to CF final. This sample is suspected to be contaminated with Al, probably due to improper cleaning and/or sample handling and is not further considered. Aluminium contamination was also observed during preparatory tests with less extensive cleaning steps. Therefore, a thorough cleaning procedure (see 3.2) prior to the sample filtration is strongly recommended. Decreased recoveries were observed in three samples (stations 62 and 81) and indicate some loss of Al during the ultrafiltration. In those samples the recovery was balanced with increasing CF, suggesting initial but limited adsorption processes on the ultrafiltration membrane and/or other chromatographic effects. With exception of the sample suspected to be contaminated, the average recoveries are 100.25 % (± 13.28 %) at CF 4 and 102.45 % (± 10.18 %) at CF final. The permeate concentrations of Al increased from CF 4 to CF final in most of the samples, indicating permeation coefficients (P_c) <1 [Guo and Santschi, 2007 and references therein]. Similar results have been previously reported for Al [Reitmeyer et al., 1996] and other trace metals [Wen et al., 1996; Schlosser and Croot, 2008]. Estimations of P_c from the change in retentate and permeate concentrations between the two CF suggest a mean value of 0.94 ± 0.04 for Al.

Table 4.1: Analyzed and calculated values for the different size fractions of Al. Standard deviations are given in parentheses, CF is concentration factor. See section 4.2.4 for definitions of equations.

			CF 4					CF final				
Depth	**dAl CA**	**dAl PC**	**sAl**	**rAl**	**cAl Eq. 2**	**cAl Eq. 4**	**Rec.**	**sAl**	**rAl**	**cAl Eq. 2**	**cAl Eq. 4**	**Rec.**
(m)	**(nM)**	**(nM)**	**(nM)**	**(nM)**	**(%)**	**(%)**	**(%)**	**(nM)**	**(nM)**	**(%)**	**(%)**	**(%)**
Station 16												
20	30.52	33.31	37.04	32.52	b.d.	b.d.	107.8	31.23	31.84	0.2	6.2	94.0
	(0.07)	(0.47)	(0.36)	(0.10)			(8.1)	(0.21)	(0.30)	(0.1)	(1.6)	(9.3)
50	11.93	8.70	8.67	8.51	b.d.	0.3	99.6	9.34	10.45	1.5	b.d.	109.0
	(0.11)	(0.02)	(0.03)	(0.09)		(0.5)	(7.9)	(0.01)	(0.08)	(0.2)		(8.8)
80	6.32	5.69	8.39	6.52	b.d.	b.d.	139.3	6.80	8.32	2.6	b.d.	122.1
	(0.02)	(0.07)	(0.10)	(0.07)			(8.3)	(0.08)	(0.02)	(0.3)		(9.0)
120 *	8.05	9.32	10.83	19.70	23.8	b.d.	140.0	9.98	47.50	50.3	b.d.	157.4
	(0.06)	(0.20)	(0.17)	(0.06)	(2.5)		(7.3)	(0.06)	(0.05)	(5.1)		(8.4)
Station 29												
20	42.68	44.56	46.27	43.91	b.d.	b.d.	102.5					
	(0.27)	(0.42)	(0.75)	(1.06)			(8.1)					
40	7.36	7.84	9.50	10.48	3.2	b.d.	124.3	9.53	10.51	1.5	b.d.	123.2
	(0.10)	(0.15)	(0.06)	(0.22)	(0.8)		(7.8)	(0.15)	(0.17)	(0.4)		(8.8)
60	6.26	5.42	5.48	5.79	1.5	b.d.	102.5	5.91	5.82	b.d.	b.d.	108.8
	(0.08)	(0.11)	(0.02)	(0.07)	(0.4)		(7.9)	(0.10)	(0.04)			(9.1)
100	10.10	9.50	9.08	9.79	1.9	4.4	97.5	9.63	8.94	b.d.	b.d.	100.8
	(0.27)	(0.12)	(0.15)	(0.18)	(0.7)	(2.1)	(7.9)	(0.23)	(0.14)			(9.5)
Station 48												
20	35.26	36.61	35.95	36.84	0.6	1.8	98.8	34.57	36.77	0.6	5.6	95.0
	(0.17)	(0.86)	(0.61)	(0.11)	(0.4)	(2.9)	(8.0)	(0.04)	(0.32)	(0.1)	(2.4)	(9.3)
50	13.16	14.24	13.45	13.88	0.8	5.5	95.2	13.76	15.40	1.7	3.4	98.3
	(0.10)	(0.11)	(0.04)	(0.10)	(0.2)	(0.8)	(7.9)	(0.08)	(0.03)	(0.2)	(0.9)	(8.8)
80	7.31	7.55	7.44	8.74	4.3	1.5	102.8	8.17	10.63	3.0	b.d.	111.2
	(0.12)	(0.02)	(0.08)	(0.10)	(0.6)	(1.2)	(7.8)	(0.09)	(0.03)	(0.3)		(9.0)
120	9.55	9.74	10.67	9.67	b.d.	b.d.	106.9	9.74	10.96	1.2	0.1	101.2
	(0.09)	(0.20)	(0.22)	(0.13)			(8.2)	(0.15)	(0.18)	(0.3)	(2.6)	(9.2)
Station 62												
20	30.93	31.05	29.75	30.99	1.0	4.2	96.8	36.49	30.63	b.d.	b.d.	115.1
	(0.41)	(0.19)	(0.39)	(0.19)	(0.4)	(1.4)	(7.9)	(0.22)	(0.23)			(9.4)
50	25.66	26.85	24.81	26.21	1.3	7.6	93.7	25.20	27.66	1.2	6.2	95.0
	(0.45)	(0.29)	(0.44)	(0.26)	(0.5)	(2.0)	(8.0)	(0.37)	(0.09)	(0.2)	(1.7)	(9.2)
80	15.24	14.80	12.86	13.16	0.5	13.1	87.4	13.29	13.49	0.2	10.1	90.0
	(0.29)	(0.33)	(0.14)	(0.07)	(0.3)	(2.4)	(7.9)	(0.17)	(0.12)	(0.2)	(2.5)	(8.9)
200	9.09	9.66	8.65	8.40	b.d.	10.5	88.9	8.81	12.25	3.3	8.8	94.5
	(0.05)	(0.25)	(0.12)	(0.19)		(2.9)	(8.0)	(0.01)	(0.07)	(0.4)	(2.6)	(8.9)
Station 81												
20	28.58	30.20	28.13	29.40	1.1	6.9	94.2	28.31	29.13	0.2	6.3	94.0
	(0.24)	(0.44)	(0.12)	(0.16)	(0.2)	(1.5)	(7.9)	(0.23)	(0.20)	(0.1)	(1.6)	(9.4)
50	3.30	3.45	2.69	2.82	0.9	22.0	78.9	3.31	3.49	0.6	3.9	96.6
	(0.06)	(0.08)	(0.14)	(0.03)	(1.0)	(4.7)	(8.8)	(0.05)	(0.02)	(0.2)	(2.7)	(9.0)
80	5.59	5.34	4.69	5.93	5.8	12.3	93.6	4.95	5.05	0.2	7.3	92.9
	(0.05)	(0.13)	(0.04)	(0.01)	(0.6)	(2.5)	(7.7)	(0.04)	(0.03)	(0.1)	(2.5)	(9.2)
200	9.42	8.94	8.02	9.70	4.7	10.3	94.4	8.86	11.45	3.4	0.9	102.6
	(0.05)	(0.14)	(0.08)	(0.07)	(0.6)	(1.8)	(7.7)	(0.04)	(0.07)	(0.4)	(1.6)	(8.7)

dAl CA: dissolved Al, CA filtrate
dAl PC: dissolved Al, PC filtrate
sAl: soluble Al, ultra-filtration permeate
rAl: retentate Al, ultra-filtration retentate
cAl: colloidal Al, calculated from Eqs. 2 and 4 and dAl PC filtrate
Rec.: Recovery, calculated from Eq. 6
b.d.: below detection limit, calculation gives negative value
* ultra-filtration samples considered as contaminated

The calculation of colloidal Al (cAl) from the Eqs. 2 and 4 produced considerably different results. The calculation by Eq. 2 yielded colloidal fractions of Al ranging from 0.5 % to 5.8 % at CF 4 and from 0.2 % to 3.4 % at CF final (Table 4.1). By contrast, the colloidal fractions of Al calculated by Eq. 4 (PC filtrate as initial dissolved concentration) are strongly scattered, ranging from 0.3 % to 22 % at CF 4 and from 0.1 % to 10.1 % at CF final (Table 4.1). In Eq. 4 the results strongly depend on the filtration behavior of the permeable species, as the loss/gain from the mass balance is entirely added to the colloidal fraction (see section 4.2.4 and Eq. 7). By contrast, in Eq. 2 the retentate concentrations and concentration factors are considered in the calculation which explains the smaller range in the derived colloidal fractions. Some of our data show reductions in both, retentate and permeate concentrations during the ultrafiltration. In those samples the calculation by Eq. 4 results in an overestimation of the colloidal fractions compared to the calculation by Eq. 2 (e.g. stations 62 and 81). Similar deviations were reported by Moran and Moore [1989]. On the other hand, contamination of the retentate could result in an overestimation of the colloidal fractions calculated by Eq. 2 (station 16, 120 m). However, if ideal filtration behavior has to be assumed, the calculation from both retentate and permeate concentrations (Eq. 2) should provide a more reliable estimation of the colloidal fraction than the simple calculation by difference. In addition, the mass balance serves to assess the data quality. Excluding all samples with recoveries exceeding 100 ± 10 % and with

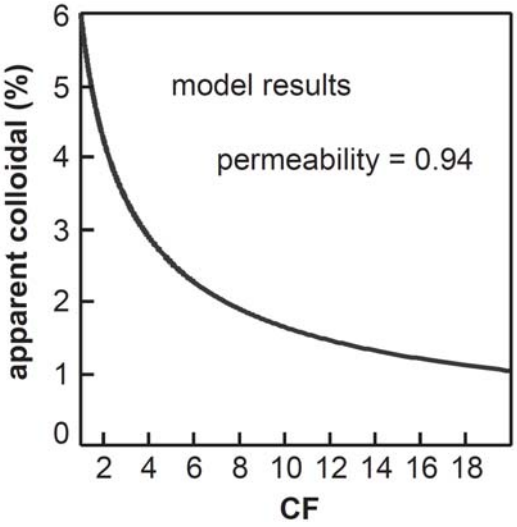

Fig. 4.3: Results from a modeling study based on the theory developed by Schlosser and Croot (2008) for the case of a single soluble component with no colloidal contribution, but with a less than ideal permeation coefficient (in this example set to 0.94). The apparent percentage colloidal contribution is calculated using the Eqs. 2 or 4 (they give the same result) as a function of the CF.

permeate concentrations higher than the initial seawater, results in colloidal fractions of Al between 0.2 and 3.4 % for Eq. 2 at the final CF.

In order to investigate the effect of the permeation behavior on the calculated colloidal concentration we additionally performed modeling studies based on the work of Schlosser and Croot (2008), using the estimated permeation coefficient of 0.94 ± 0.04 for Al. The model results show no difference between the two approaches (Eqs. 2 and 4) but give an apparent colloidal content of 1 - 6 %, simply based on the permeance of the ultrafilter to the analyte (Fig. 4.3). The overestimate of the colloidal content decreases with increasing CF but approaches a non-zero asymptote at higher CF. This suggests that for studied substances with a permeation behavior less than ideal, the colloidal fraction will generally be overestimated, complicating the issue of determining the true colloidal concentration.

4.3.3 Calculation of colloidal Ti

The Ti concentrations in the PC filtrate and in the ultrafiltration permeate are not significantly different (Table 4.2). Applying a paired t-test to the dissolved (PC) and soluble concentrations of Ti gives $|t| < t_{(0.95;\ 19)}$ and a p-value above 0.05 ($t_{(0.95;\ 19)} = 2.1$, $|t| = 1.45$, $p = 0.16$). Therefore, our data do not show any association of Ti with the colloidal phase. Preparatory work in our laboratory showed that for Ti the P_c is ~1, similar to Al; and that the Ti concentration in the initial sample, retentate and permeate change insignificantly as a function of CF, indicating no colloidal component of Ti. In the present work we similarly found close agreement between the initial and the permeate samples. As a consideration for time saving on the analysis, Ti concentrations were thus not determined in the retentate fraction and a full mass balance was not evaluated for the ultrafiltration. With exception of two samples (station 16, 80 m, station 48, 80 m) the results of the dissolved and soluble Ti fractions indicate that negligible contamination or loss of Ti occurred during the size fractionation.

It is possible, however, that our applied voltammetric method does not detect nano-particulate TiO_2, as has been observed for a similar electrochemical detection method [Schmidt and Vogelsberger, 2006]. Nano-particulate crystalline TiO_2 (brookite, anatase and rutile) is a major product of industry at present and can be found in the terrestrial environment [Reyes-Coronado et al., 2008; Boncagni et al., 2009]. Amorphous TiO_2 colloids readily dissolve at low pH, however, more crystalline phases of TiO_2 are not [Kormann et al., 1988]. It is thus likely that both the electrochemical and the ICP-MS method for dTi [Orians and Boyle, 1993] do not detect nano-particulate TiO_2.

Table 4.2: Analyzed and calculated values for the different size fractions of Ti. Standard deviations are given in parentheses. See section 4.2.4 for definitions of equations.

Depth (m)	dTi CA (pM)	dTi PC (pM)	sTi (pM)	cTi Eq. 4 (%)
Station 16				
20	155.0 (10.9)	173.8 (11.3)	164.2 (9.8)	9.7 (15.0)
50	101.9 (10.7)	91.5 (5.2)	97.6 (8.1)	b.d.
80	114.4 (12.7)	224.0 *	542.7 *	*
120	128.3 (12.9)	128.2 (11.6)	132.3 (5.3)	b.d.
Station 29				
20	157.3 (7.0)	140.0 (6.1)	157.0 (9.7)	b.d.
40	68.7 (7.4)	64.4 (6.6)	72.2 (6.9)	b.d.
60	116.8 (12.8)	148.1 *	147.1 *	*
100	137.2 (8.3)	123.2 (6.9)	117.3 (7.1)	5.9 (9.9)
Station 48				
20	139.2 (10.8)	132.8 (5.2)	143.5 (6.7)	b.d.
50	77.0 (6.3)	71.6 (6.3)	69.6 (6.7)	1.9 (9.2)
80	116.3 (13.8)	164.6 *	240.6 *	*
120	126.7 (6.8)	125.9 (12.6)	147.3 (8.9)	b.d.
Station 62				
20	101.1 (6.3)	95.2 (7.1)	102.2 (9.1)	b.d.
50	74.1 (6.6)	79.9 (8.5)	86.0 (6.0)	b.d.
80	90.2 (9.1)	112.4 (8.6)	105.4 (5.7)	7.0 (10.3)
200	111.7 (4.9)	106.3 (12.1)	114.1 (6.4)	b.d.
Station 81				
20	97.1 (5.5)	105.2 (3.6)	105.4 (3.1)	b.d.
50	72.7 (4.6)	72.7 (6.1)	74.8 (4.7)	b.d.
80	110.2 (6.1)	113.3 (4.2)	119.1 (4.5)	b.d.
200	134.8 (5.1)	137.0 (7.6)		

dTi CA: dissolved Ti, CA filtrate
dTi PC: dissolved Ti, PC filtrate
sTi: soluble Al, ultra-filtration permeate
cTi: colloidal Ti, calculated from Eq 4 and dTi PC filtrate
b.d.: below detection limit, calculation gives negative value
*samples considered as contaminated

4.3.4 Spatial distributions of Al and Ti

The profiles of dAl and dTi share some essential features in the upper water column (Fig. 4.4). At most stations elevated surface concentrations were observed, with up to 43 nM of dAl and 157 pM of dTi (CA filtrates). The surface water concentrations of dTi decreased from the stations 16 and 29 towards the more remote stations 48 and 62 and were also lower at station 81. Similarly, dAl concentrations were elevated at the stations 29 and 48 compared to the stations 62 and 81. With depth, the dissolved concentrations decreased to subsurface minima and then again increased to concentrations of around 9 nM of dAl and 130 pM of dTi (CA filtrates). The subsurface minima of dTi were located at the same depth as the chlorophyll *a* maxima. For dAl, the locations of the subsurface minima agreed with those of dTi at the stations 29 and 81, whereas deeper locations were observed at the stations 16 and 48. At station 62, the subsurface minima were little pronounced for both dAl and dTi, and lower surface concentrations of dTi were found. At this station also the chlorophyll *a* maximum was less pronounced and the mixed layer was deeper than at the other stations.

The distributions of sAl and sTi mostly agreed with the dissolved fractions. Figure 4.5 displays the distributions of cAl. At the stations 16, cAl increased with depth, whereas at station 48, the distribution of cAl was quite uniform in the upper 80 m but lower in the 120 m sample. At the stations 62 and 81, a minimum of cAl was found at 80 m depth and the cAl concentrations were elevated at 200 m depth. Overall, the colloidal fractions ranged between 0.2 and 3.4 %.

4.4 Discussion

4.4.1 Spatial distributions of Al and Ti

The elevated surface concentrations at most stations reflect the input of dAl and dTi via the deposition of atmospheric aerosols. The observed values of dAl agree well with previously reported concentrations in high dust input areas of the eastern tropical North Atlantic [Helmers and Rutgers van der Loeff, 1993; Measures, 1995; Kramer et al., 2004; Rijkenberg et al., 2008]. For dTi, sparse literature data is available. Our observations lie in the range of 100 - 200 pM found in the Mediterranean [van den Berg et al., 1994] and in the Mid-Atlantic Bight [Skrabal, 2006] and agree with previous observations in the same region in May 2010 [Dammshäuser et al., 2011]. The spatial distributions of surface water

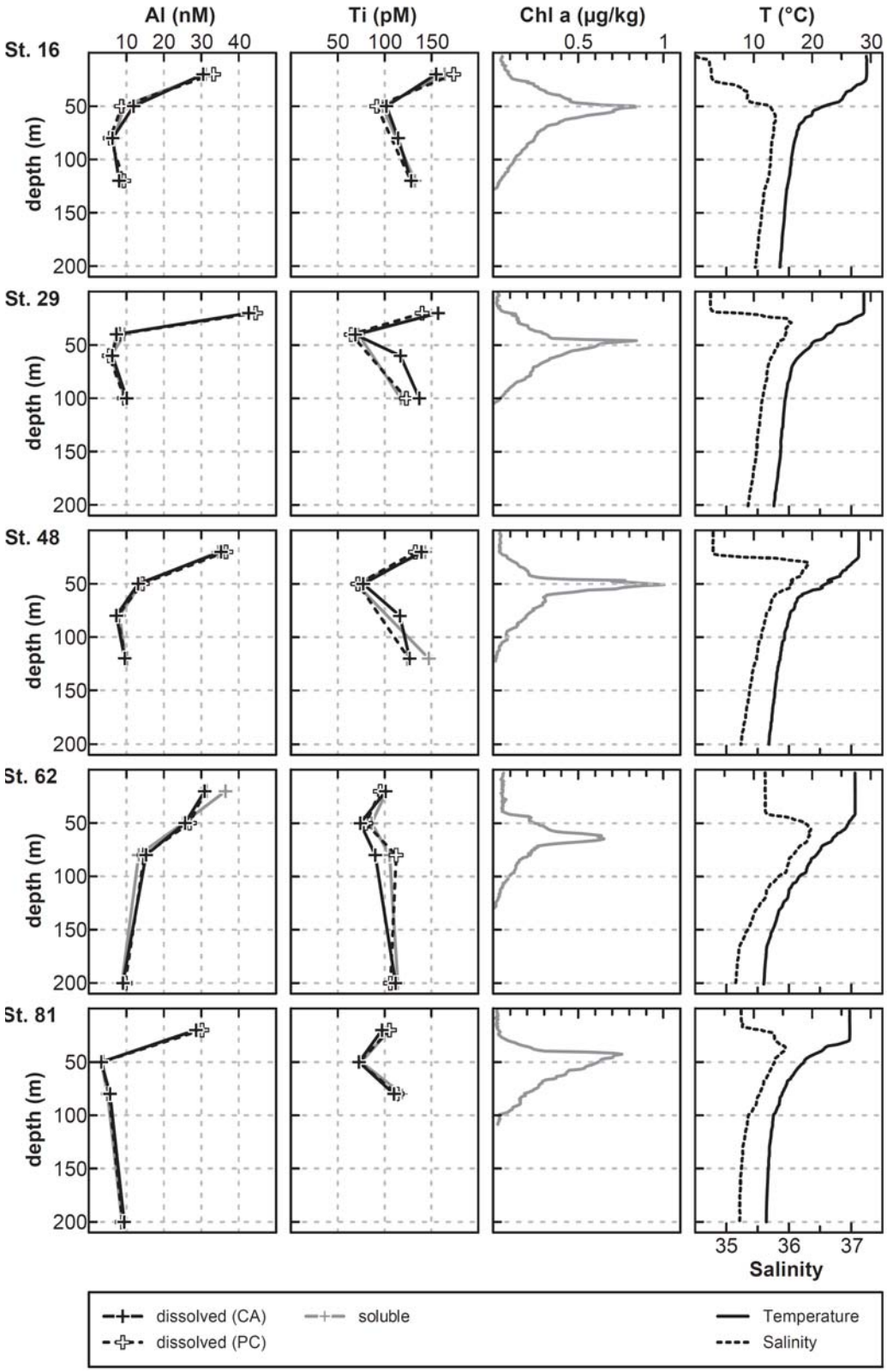

Fig. 4.4: Distributions of the dissolved and soluble concentrations of Al and Ti, chlorophyll *a* concentrations, temperature and salinity at the five sampled stations. The dissolved fraction is given as the result of two different filtration procedures (CA and PC filtrate, see section 4.2.1). The salinity, temperature and chlorophyll *a* profiles were obtained from the CTD sensor. Refer to Tables 4.1 and 4.2 for values and standard deviations.

dTi concentrations reflects the suggested pattern of dust deposition, that is pronounced at the more remote stations 48 and 62 and, during boreal winter, at the more northern station 81 [Moulin et al., 1997].

The subsurface minima of dAl and dTi indicate the removal of the dissolved metals by scavenging processes and/or biological uptake upon their atmospheric supply. The distributions of both metals are known to be strongly influenced by scavenging processes [e.g. Hydes, 1979; Orians and Bruland, 1986; Orians et al., 1990; Kramer et al., 2004], which agrees with their predominant occurrence as hydrolyzed species in seawater [Turner et al., 1981]. Aluminium and Ti are so far not known to have essential biological functions, however, biological productivity may increase the removal processes either by providing additional adsorption sites for the hydrolyzed metal species or by passive uptake by organisms. For dAl, some evidence has been found for the removal with diatoms [Deuser et al., 1983; Moran and Moore, 1988; van Bennekom et al., 1989; Moran and Moore, 1992], due to the incorporation of Al in the silicate frustules of the living or dead organisms [Gehlen et al., 2002; Koning et al., 2007]. In the case of dTi, the concurrence of the subsurface minima and the chlorophyll *a* maxima similarly suggests some relation to biological productivity. The decrease between the surface water concentrations and the subsurface minima was generally more extensive for dAl than for dTi, with 79 - 88 % of dAl compared to 20 - 49 % of dTi being removed. This indicates that dTi is less susceptible to scavenging removal and/or uptake processes than dAl. At the stations 16 and 48, the different locations of the subsurface minima of dAl and dTi suggest specific influences on the removal processes of both metals. It is possible that the sinking of

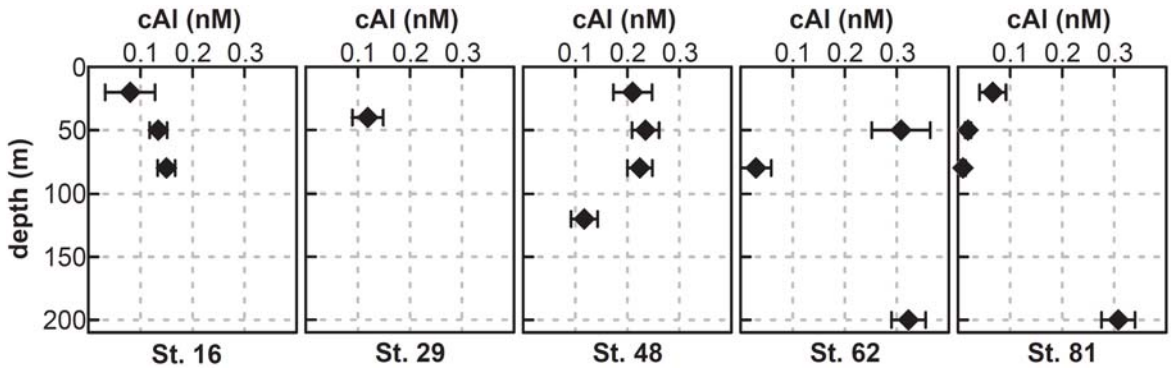

Fig. 4.5: Distributions of colloidal Al at the sampled stations. Exact values and standard deviations are given in Table 4.1.

particles below the chlorophyll *a* maxima resulted in ongoing scavenging of dAl with depth. At station 62, the less pronounced to absent subsurface minima of dAl and dTi is likely related to decreased biological productivity and lower particle abundance, as indicated by the decreased chlorophyll *a* fluorescence. A similar relationship was observed by Kramer et al. [2004], who found subsurface minima of dAl only at stations with pronounced chlorophyll *a* maxima. In addition, the deeper mixed layer at station 62 suggests more pronounced mixing processes in the upper 50 m.

The identification of trends in the distribution of cAl is limited by the small number of observations (Fig. 4.5). The concentrations of cAl showed small elevations in the region of the subsurface minima at the stations 16 and 48, which may indicate some removal of dAl via colloidal intermediates [e.g. Honeyman and Santschi, 1989; Moran and Buesseler, 1993; Moran et al., 1996; see section 4.4.3]. However, in contrast to this the cAl concentrations were decreased within the subsurface minimum of dAl at station 81. Overall, highest concentrations of cAl occurred in the samples at 200 m depth at the stations 62 and 81. These observations differ from those by Moran and Moore [1989], who found highest cAl concentrations in surface waters and decreasing colloidal fractions of Al with depth.

At all sampling stations, the elemental ratios of dAl/dTi (Fig. 4.6) in the surface waters clearly deviate from the crustal ratios (Al/Ti = 19.61) given by McLennan [2001] and show the presence of excess dAl over dTi. With depth, the ratios of dAl/dTi then approached the

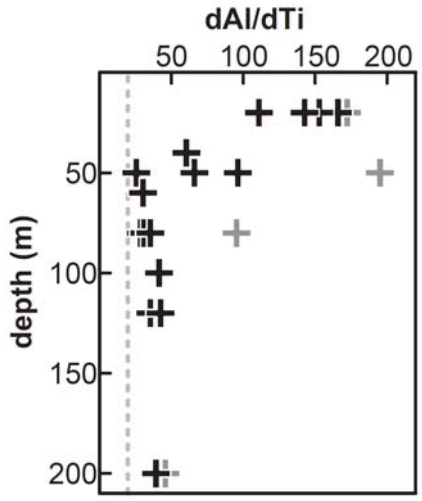

Fig. 4.6: Depth distribution of dAl/dTi (weight/weight). Displayed are the elemental ratios from all analyzed samples, grey crosses distinguish the samples from station 62. At station 62 lower biological activity is assumed (see also Fig. 4.4). The dashed grey line marks the elemental ratio given by McLennan [2001].

crustal value. The pronounced surface maxima and extensive removal of dAl in the upper water column suggest that this difference to the crustal ratio results from higher atmospheric inputs of dAl compared to dTi. Since both metals are commonly delivered with atmospheric mineral particles, this would thus imply higher soluble fractions for Al compared to Ti. The solubility of Ti from atmospheric particles is poorly studied so far. In dissolution experiments with aerosol samples and deionized water, Buck et al. [2010] indeed observed higher solubilities of Al compared to Ti, mostly by a factor of 3 - 9. Completely ascribing our observed deviation in the elemental ratios in the surface waters to differences in the solubilities yields a 5 - 7 times lower solubility of aerosol Ti in seawater.

4.4.2 Size distributions of Al and Ti in seawater

Our observations clearly show that the predominant part of the dAl and dTi occurred in the soluble form. Less than 4 % of dAl, and no detectable fraction of dTi were present in the colloidal size class between 10 kDa and 0.2 µm. Table 4.3 gives an overview of previously observed colloidal fractions of Al and Ti in different environments. Listed are results from size fractionations by ultrafiltration with membrane cut-offs from 1 to 10 kDa. In most studies the initial and permeate samples were examined, and very infrequently the retentate, and typically the colloidal concentration in the initial sample or the colloidal metal as fraction (%) of the dissolved metal concentration are reported [Moran and Moore, 1989; Reitmeyer et al., 1996; Sañudo-Wilhelmy et al., 1996]. In other studies [Bertine and Vernonclark, 1996; Guo et al., 2000], the colloidal fractions were isolated and the colloidal metals were determined as fractions of the total colloidal mass (e.g. mg/g). Our data agree well with the observation of less than 3.5 % of cAl in the North Atlantic [Moran and Moore, 1989]. In the North Pacific, slightly higher fractions (<11 %) of cAl were found using a 1 kDa membrane, however, the authors also report contamination problems and variations in the permeate concentration of Al during the filtration process [Reitmeyer et al., 1996]. For dTi, there is to our knowledge no data available on the size distribution in seawater. Some studies report Ti concentrations as fraction of the colloidal phase in seawater; however, the authors did not examine cTi or dTi concentrations in the initial seawater sample [Bertine and Vernonclark, 1996; Guo et al., 2000]. Using literature values for dTi, Bertine and Vernonclark [1996] estimated up to 100 % of Ti being present in the colloidal form. Likewise, Skrabal et al. [1992] and van den Berg et al. [1994] suggest the existence of some cTi in estuaries and in seawater. These estimations are in contrast to our

direct observations of no detectable cTi fraction in seawater. Even with the assumption that some cTi occurred in the form of nano-particulate TiO_2 that would not have been detected by the voltammetric method, our data clearly show that a considerable fraction of dTi is present in the size class smaller than 10 kDa.

In seawater, the inorganic species of Al and Ti predominantly occur in their hydrolyzed forms [Turner et al., 1981; Byrne et al., 1988] and the traditional paradigm is that strongly hydrolyzed species are highly particle reactive and should be present predominantly in the colloidal or particulate phases in the ocean. In contrast to this, our data show that both dAl and dTi are predominantly present in the soluble phase smaller than 10 kDa. Moreover, lowest colloidal fractions were observed for Ti, although highest reactivity could be expected for the hydrolyzed species of Ti, due to its quadrivalence [Li, 1991]. Bertine and Vernonclark [1996] suggested that colloidal associations are related to the specific charge of the inorganic metal species. Inorganic Ti occurs in seawater mostly as the neutral hydroxyl species $TiO(OH)_2$, whereas Al is mostly in the form of the anion $Al(OH)_4^-$ [Turner et al., 1981; van den Berg et al., 1994]. The negatively charged hydroxyl species can be expected to be less attracted to the mostly negatively charged

Table 4.3: Previously reported colloidal fractions of Al and Ti. Note that colloidal metal fractions in the lower part of the table were determined as weight (%) of the total colloidal fraction.

Study	Study area	Filter cut off	Salinity	cAl	cTi
Colloidal metal fraction given as (%) of dissolved metal fraction					
Salinity >30					
this study	tropical NE Atlantic	10 kDa	34 - 36	0.2 - 3.4	b.d. [a]
Bertine and Vernonclark, 1996	Buzzards Bay	1 kDa		1 [b]	100 [b]
Moran and Moore, 1989	Scotian Shelf	10 kDa	31 - 34	0.7 - 3.5	
Moran and Moore, 1989	Gulf Stream	10 kDa	34 - 36	0.2 - 0.8	
Reitmeyer et al., 1996	N Pacific	1 kDa		0 - 11	
Sañudo-Wilhelmy et al., 1996	San Francisco Bay	10 kDa	30 - 32	3 - 9	
Salinity <30					
Sañudo-Wilhelmy et al., 1996	San Francisco Bay	10 kDa	0.01 - 23	33 - 99	
Colloidal metal fraction given as (mg/g) of total colloidal fraction					
Guo et al., 2000	Mid-Atlantic Bight	1 kDa	~36	0.006 - 0.013	0.004 - 0.012
Guo et al., 2000	Gulf of Mexico	1 kDa	34 - 36	0.002 - 0.024	0.005 - 0.011

[a] below detection limit: colloidal fraction not statistically different from dissolved fraction
[b] estimated using literature values for dissolved concentrations

colloidal surfaces in seawater [Hunter and Liss, 1982; Hunter, 1983] and this was the basis for the estimation of high colloidal fractions of Ti and low colloidal fractions of Al by Bertine and Vernonclark [1996]. However, the considerations about the inorganic speciation and the particle reactivity of the hydroxyl species can not explain our observation of the small colloidal fractions of both Al and Ti.

In general, the ability of Al and Ti to form pure inorganic colloids is controlled by their solubility in seawater. For Al, in the form of $Al(OH)_3$ (gibbsite), the solubility is ~100 nM at the pH minimum of 6, while at the pH of seawater it is considerably higher (~1 µM) due to the formation of $Al(OH)_4^-$ [May et al., 1979]. Only a few studies have reported direct measurements of Al solubility in seawater; results from filtration experiments (0.45 µm) suggest a range between ~1.8 µM [Savenko and Savenko, 2011] and ~18.5 µM [Willey, 1975]. For Ti, to our knowledge the solubility in seawater has not been investigated so far. Recent studies in 0.1 M NaCl indicate that the solubility of crystalline TiO_2 is about 1 nM in the pH range of 3 to 11, where the neutral complex ion $Ti(OH)_4$ is predominant [Schmidt and Vogelsberger, 2009]. For amorphous TiO_2 initially formed in saturated solutions over the same pH range, higher solubilities (~3 µM) have been found [Sugimoto et al., 2002; Schmidt and Vogelsberger, 2009]. For dAl and dTi, typical seawater concentrations lay well within these solubilities ranges. This suggests that both metals generally have a low potential to form pure inorganic colloids in seawater.

The comparison of Al and Ti with Fe suggests that associations with the colloidal phase are additionally controlled by the ability to form organic complexes in seawater. Similar to Al and Ti, the inorganic speciation of Fe is dominated by the hydrolyzed form in seawater and the distribution of Fe is influenced by scavenging processes. However, in contrast to Al and Ti, Fe shows strong associations with the colloidal phase in seawater [e.g. Wu et al., 2001; Cullen et al., 2006; Bergquist et al., 2007; Thuróczy et al., 2010]. For Fe, the formation of pure inorganic colloids in seawater may be favored by the presence of Fe above its inorganic solubility level in seawater [Kuma et al., 1996; Liu and Millero, 2002]. In addition, Fe has been found to occur in strong organic complexes in both the soluble and the colloidal phases in seawater [Cullen et al., 2006; Boye et al., 2010; Thuróczy et al., 2010]. For Al and Ti, only weak evidence exists for organic complexation in seawater [van den Berg et al., 1994]. Moran and Moore [1989] found a correlation between the small amount of Al that was colloidal (0.1 - 0.5 nM) and colloidal organic carbon in seawater, possibly indicating some association of Al with organic molecules in the colloidal phase.

Studies with terrestrial fulvic acids have indicated that some Al can be bound to humics at seawater pH [Sutheimer and Cabaniss, 1997], however, under seawater conditions Ca and Mg may outcompete Al for binding sites. In the case of Ti, the existence of strongly bound organo-Ti complexes similar to Fe siderophores has been suggested [Uppal et al., 2009], but these complexes have not been examined or detected in seawater.

At low salinities, Al and Ti have high colloidal fractions similar to Fe [Table 4.3; Skrabal et al., 1992; Neal et al., 2011], and are predominantly associated with the larger colloidal phase rich in inorganic Fe-oxyhydroxides [Powell et al., 1996; Pokrovsky and Schott, 2002; Stolpe and Hassellöv, 2007; Stolpe et al., 2010]. During estuarine mixing, the colloidal fractions of Al and Ti then disappear [Skrabal et al., 1992; Sañudo-Wilhelmy et al., 1996], coinciding with the removal of this larger colloidal size class [Stolpe and Hassellöv, 2007; Stolpe et al., 2010]. In contrast to Al and Ti, Fe becomes increasingly associated with the smaller colloidal phase rich in chromophoric dissolved organic matter during estuarine mixing [Stolpe et al., 2010]. This suggests that the disappearance of the colloidal fractions of Al and Ti and the persistence of colloidal Fe are controlled by the ability to associate with organic molecules. More general, the formation of metal organic complexes with functional organic groups in colloidal matter can be expected to be a driving force for the partitioning into the colloidal phase in seawater. The low colloidal associations of Al and Ti in seawater may thus be explained by two complementary mechanisms; (1) their presence within the inorganic solubility levels and thus low tendency to form inorganic colloids and (2) the absence of organic complexes of both metals and the little affinity to functional organic groups that are present in the colloidal phase.

4.4.3 Residence times of Al and Ti in surface waters and role of the colloidal pool

We estimated residence times for Al and Ti in the upper 100 m of the water column as described in Croot et al. [2004]. The input of the trace metals was calculated from dust deposition averages given by the model composite from Jickells et al. [2005] assuming that the concentrations of Al and Ti equal the average crustal abundances of 8.04 % and 0.41 % [McLennan, 2001]. The modeled deposition fluxes range between 8 and 10 g m^{-2} a^{-1} and are in good agreement with field observations in the study region [Baker et al., 2006a; Baker et al., 2006b; Baker et al., 2007]. The soluble trace metal fluxes were calculated assuming solubilities of 3 % for Al and 0.1 % for Ti. For Al, this estimate is based on observations in Saharan dust samples [Prospero et al., 1987; Baker et al., 2006b]. For Ti, an intermediate value was chosen between results from aerosol filter leaches with

deionized water [Buck et al., 2010] and the significantly lower Ti solubilities observed in seawater incubations with Saharan dust [Dammshäuser et al., 2011]. The large variations in the observed Ti solubilities are most likely related to the different setups applied in the dissolution experiments. Given the uncertainties in the soluble aerosol fluxes, the calculated values are thus only indicative. The estimated residence times range between 1.6 and 4 years for dAl and between 14 and 17 years for dTi for the upper 100 m of the water column. These estimations are in general agreement with previously reported values for dAl [Jickells, 1999], and are somewhat longer than estimated residence times for dTi and dAl within the mixed layer in the same region [Dammshäuser et al., 2011]. However, it has to be noted that for Ti the calculated residence times strongly depend on the assumed soluble dust fractions. If the solubility of Ti is assumed to be 5 - 7 times lower than that of Al, as indicated by the elemental ratios in the surface waters (section 4.4.1), the calculated residence times for Ti lie in the order of 2 - 4 years. For dAl, our estimated residence times are clearly shorter than the estimation of 5 years that has been used in modeling approaches to calculate atmospheric inputs into the mixed layer (30 m) [e.g. Measures and Vink, 2000; Measures et al., 2005; Measures et al., 2008].

The residence time of an element in the dissolved pool is a combination of the time spent in the colloidal and in the soluble pools. The colloidal phase is assumed to behave as a transient intermediate in the transport of the soluble species to the particulate phase via coagulation processes and, therefore, in the removal of trace metals [e.g. Honeyman and Santschi, 1989; Moran and Buesseler, 1993; Moran et al., 1996]. Consequently, some relationship can be expected between the residence time of a certain trace metal and its colloidal fraction in the ocean. This concept agrees with our observation of shorter residence times and higher colloidal associations of Al compared to Ti. However, the anticipated role of the colloidal phase is in contrast to the generally short residence times of Al and Ti and their overall low colloidal associations. One explanation could be that removal also occurs via the direct adsorption of the soluble, hydrolyzed species to the surfaces of large (>0.2 μm) biogenic particles as has been suggested for Al [Moran and Moore, 1992; Koning et al., 2007]. However, the turnover time of the colloidal pool is also an important factor in the overall residence time. If the removal of dAl and dTi predominantly occurs through colloidal intermediates, the short residence times of both metals implicate rapid turnover of the small colloidal fraction in the upper water column. Evidence for such rapid turnover in the colloidal phase was found in studies on ^{234}Th, a similarly particle reactive element. In surface waters near Bermuda a residence time of

~10 days was observed for ^{234}Th in the colloidal pool [Moran and Buesseler, 1992] and in more productive coastal waters further reduced colloidal residence times were found [Moran and Buesseler, 1993].

Based on our observations we developed a simple model (Fig. 4.7) with which to examine the influence of kinetics and organic complexation on the colloidal pool and residence time of an element. Our model is based on the following steady state assumptions: 1) that the only source of the element to the dissolved phase is in the soluble form and that this is constant (k_1); 2) that the only loss term from the dissolved phase is via loss from the colloidal pool (k_3), via particulate formation; 3) that a reversible equilibrium is established between the soluble and colloidal pools via a forward reaction (k_2) dependent on the concentration of colloidal ligands [L_{Col}], and the soluble metal [Sol], while the backward reaction (k_4) is only dependent on the colloidal metal concentration [Col]. The ratio of k_2/k_4 is then analogous to a formation constant for the metal-organic complexes in the colloidal phase. The simple model indicates that the residence time for the dissolved pool and the steady state value for the colloidal fractions (%) are independent of the flux of the element into the dissolved phase (Fig. 4.7). The residence times for the soluble and colloidal pools are $\tau_{sol} = 1/(k_2)$ and $\tau_{col} = 1/(k_3+k_4)$ respectively. This indicates that the residence time in the soluble pool is controlled solely by transformation into the colloidal phase. The turnover of the colloidal pool is governed by losses to the particulate pool and the dissociation of the metal colloid complexes. The model further predicts that elements

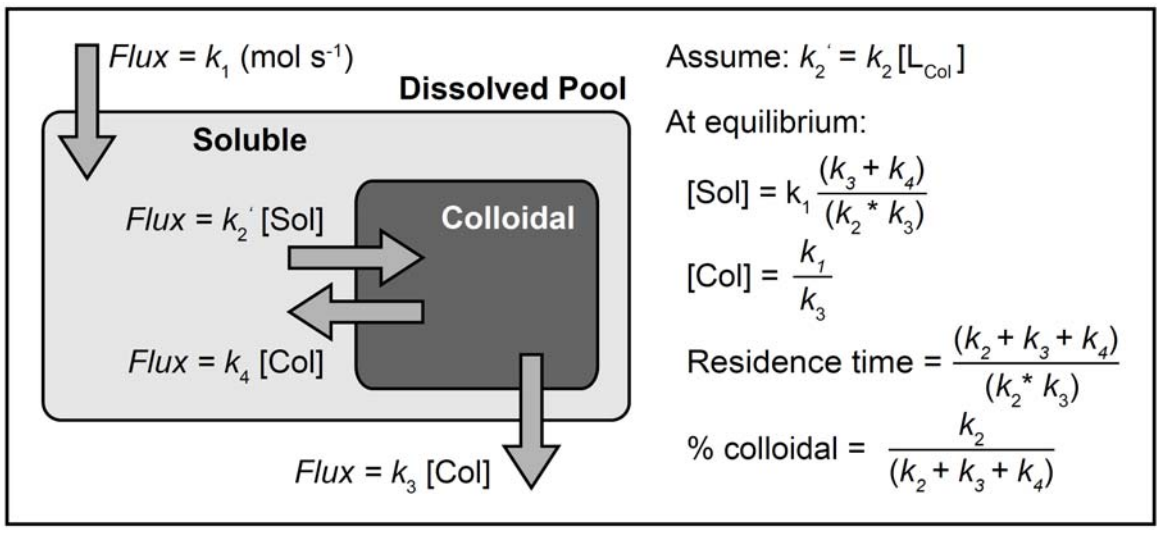

Fig. 4.7: Conceptual model of the partitioning between soluble and colloidal components for dissolved metals in the surface ocean. For explanations see section 4.4.3.

with low ratios of k_2/k_4, indicating a weak affinity for organic binding (e.g. Al and Ti), would give rise to long residence times and low colloidal fractions in the dissolved phase. In contrast, strong organic binding in the colloidal phase (e.g. Fe) results in high values of k_2/k_4, short residence times and higher colloidal fractions. Thus the model appears to retain the observed features in the soluble and colloidal distributions of Al, Ti and Fe. It should be noted, however, that our simple approach does not include the direct transfer of soluble trace metal species into the particulate fraction, e.g. due to biological uptake or adsorption onto biogenic particles. In this case, uptake rates would also be controlled to some extent by the kinetics of organic chelation. Such potential influences, as well as the links between organic complexation in the colloidal phase, residence time and the colloidal distribution need to be examined more quantitatively in future studies.

4.5 Conclusions

The size distributions of the two lithogenic metals Al and Ti were examined in the upper water column of the eastern tropical North Atlantic, a region receiving high dust inputs from the adjacent Sahara. The fractionation by ultrafiltration revealed that the major part of the dissolved fractions of Al and Ti existed in the soluble phase, defined here as smaller than 10 kDa. Associations with the colloidal phase, defined here as size fraction between 10 kDa and 0.2 µm, were smaller than 3.4 % for Al and not detectable for Ti. Our observations agree with previously reported colloidal fractions of Al but are opposed to previous assumptions for colloidal associations of Ti. The size distributions of both metals are in contrast to their predominant occurrence as hydrolyzed species and the anticipated high particle reactivity in seawater. However, the low colloidal associations of Al and Ti agree with their presence within the inorganic solubility levels and the accordingly low tendency to form inorganic colloids in seawater. In addition, little tendency can be expected for both metals to associate with functional organic groups that are present in the colloidal phase.

The spatial distribution of dAl and dTi reflects their atmospheric source and the influence of removal processes in the upper water column. Subsurface minima were found at most stations and can be ascribed to scavenging processes and/or biological uptake. In the surface waters, excess dAl over dTi was present compared to the crustal ratio, indicating higher solubility and thus elevated inputs of Al compared to Ti from atmospheric mineral particles. The dAl/dTi ratios decreased with depth, in agreement with the extensive

removal of dAl within the upper water column. Estimated residence times in the upper 100 m were 1.6 - 4 years for dAl. For dTi, residence times of 14 - 17 years were estimated, however, due to poorly constrained soluble aerosol fractions of dTi these are only indicative values. The generally short residence times of both metals and the extensive removal of dAl are in some contrast to the low colloidal associations and the anticipated important role of the colloidal phase in scavenging processes. This suggests that either the removal of dAl and dTi occurs predominantly via the direct adsorption of the dissolved, hydrolyzed species on the particulate fraction, or that rapid turnover occurs in the colloidal phase. Both, the role of the particulate phase in the removal of Al and Ti, as well as the relative input of both metals from the aerosol source need to be better constrained in further studies.

Acknowledgements: We thank the officers and crew of RV Meteor for their help and cooperation during M80-2. Special thanks are also due to our collegues O. Baars, R. Link, P. Streu and T. Wagener for their support in the shipboard and shore-based laboratory work. Chlorophyll *a* data are courtesy of T. Großkopf. This work is a contribution of the Sonderforschungsbereich 754 "Climate – Biogeochemistry Interactions in the Tropical Ocean" (www.sfb754.de). Financial support for this work was provided by the Deutsche Forschungsgemeinschaft (DFG) via grants to PLC (CR145/15-1 and SFB754 B5).

4.6 References

Baker A. R., French M. and Linge K. L. (2006a) Trends in aerosol nutrient solubility along a west-east transect of the Saharan dust plume. *Geophysical Research Letters* **33**, L07805, doi:10.1029/2005GL024764.

Baker A. R., Jickells T. D., Witt M. and Linge K. L. (2006b) Trends in the solubility of iron, aluminium, manganese and phosphorus in aerosol collected over the Atlantic Ocean. *Marine Chemistry* **98**, 43-58.

Baker A. R., Weston K., Kelly S. D., Voss M., Streu P. and Cape J. N. (2007) Dry and wet deposition of nutrients from the tropical Atlantic atmosphere: Links to primary productivity and nitrogen fixation. *Deep Sea Research Part I: Oceanographic Research Papers* **54**, 1704-1720.

Bergquist B. A., Wu J. and Boyle E. A. (2007) Variability in oceanic dissolved iron is dominated by the colloidal fraction. *Geochimica et Cosmochimica Acta* **71**, 2960-2974.

Bertine K. K. and Vernonclark R. (1996) Elemental composition of the colloidal phase isolated by cross-flow filtration from coastal seawater samples. *Marine Chemistry* **55**, 189-204.

Boncagni N. T., Otaegui J. M., Warner E., Curran T., Ren J. and Fidalgo de Cortalezzi M. M. (2009) Exchange of TiO_2 nanoparticles between streams and streambeds. *Environmental Science and Technology* **43**, 7699-7705.

Boye M., Nishioka J., Croot P. L., Laan P., Timmermans K. R., Strass V. H., Takeda S. and de Baar H. J. W. (2010) Significant portion of dissolved organic Fe complexes in fact is Fe colloids. *Marine Chemistry* **122**, 20-27.

Buck C. S., Landing W. M., Resing J. A. and Measures C. I. (2010) The solubility and deposition of aerosol Fe and other trace elements in the North Atlantic Ocean: Observations from the A16N CLIVAR/CO_2 repeat hydrography section. *Marine Chemistry* **120**, 57-70.

Buesseler K. O., Bauer J. E., Chen R. F., Eglinton T. I., Gustafsson O., Landing W. M., Mopper K., Moran S. B., Santschi P. H., Vernonclark R. and Wells M. L. (1996) An intercomparison of cross-flow filtration techniques used for sampling marine colloids: Overview and organic carbon results. *Marine Chemistry* **55**, 1-31.

Byrne R. H., Kump L. R. and Cantrell K. J. (1988) The influence of temperature and pH on trace metal speciation in seawater. *Marine Chemistry* **25**, 163-181.

Croot P. L. (2011) Rapid determination of picomolar titanium in seawater with catalytic cathodic stripping voltammetry. *Analytical Chemistry* **83**, 6395-6400.

Croot P. L., Streu P. and Baker A. R. (2004) Short residence time for iron in surface seawater impacted by atmospheric dry deposition from Saharan dust events. *Geophysical Research Letters* **31**, L23S08, doi:10.1029/2004gl020153.

Cullen J. T., Bergquist B. A. and Moffett J. W. (2006) Thermodynamic characterization of the partitioning of iron between soluble and colloidal species in the Atlantic Ocean. *Marine Chemistry* **98**, 295-303.

Dahlqvist R., Benedetti M. F., Andersson K., Turner D., Larsson T., Stolpe B. and Ingri J. (2004) Association of calcium with colloidal particles and speciation of calcium in the Kalix and Amazon rivers. *Geochimica et Cosmochimica Acta* **68**, 4059-4075.

Dammshäuser A., Wagener T. and Croot P. L. (2011) Surface water dissolved aluminum and titanium: Tracers for specific time scales of dust deposition to the Atlantic? *Geophysical Research Letters* **38**, L24601, doi:10.1029/2011gl049847.

de Jong J. T. M., den Das J., Bathmann U., Stoll M. H. C., Kattner G., Nolting R. F. and de Baar H. J. W. (1998) Dissolved iron at subnanomolar levels in the Southern Ocean as determined by ship-board analysis. *Analytica Chimica Acta* **377**, 113-124.

Deuser W. G., Brewer P. G., Jickells T. D. and Commeau R. F. (1983) Biological control of the removal of abiogenic particles from the surface ocean. *Science* **219**, 388-391.

Duce R. A., Liss P. S., Merrill J. T., Atlas E. L., Buat-Menard P., Hicks B. B., Miller J. M., Prospero J. M., Arimoto R., Church T. M., Ellis W., Galloway J. N., Hansen L., Jickells T. D., Knap A. H., Reinhardt K. H., Schneider B., Soudine A., Tokos J. J., Tsunogai S., Wollast R. and Zhou M. (1991) The atmospheric input of trace species to the World Ocean. *Global Biogeochemical Cycles* **5**, 193-259.

Gehlen M., Beck L., Calas G., Flank A. M., van Bennekom A. J. and van Beusekom J. E. E. (2002) Unraveling the atomic structure of biogenic silica: Evidence of the structural association of Al and Si in diatom frustules. *Geochimica et Cosmochimica Acta* **66**, 1601-1609.

Gehlen M., Heinze C., Maier-Reimer E. and Measures C. I. (2003) Coupled Al-Si geochemistry in an ocean general circulation model: A tool for the validation of oceanic dust deposition fields? *Global Biogeochemical Cycles* **17**, 1028, doi:10.1029/2001gb001549.

Guo L. and Santschi P. H. (2007) Ultrafiltration and its application to sampling and characterisation of aquatic colloids. In *Environmental Colloids and Particles: Behaviour, Separation and Characterisation* (eds. Wilkinson K. J. and Lead J. R.). John Wiley & Sons Ltd, Chichester, pp. 159-221.

Guo L., Santschi P. H. and Warnken K. W. (2000) Trace metal composition of colloidal organic material in marine environments. *Marine Chemistry* **70**, 257-275.

Guo L., Hunt B. J. and Santschi P. H. (2001) Ultrafiltration behavior of major ions (Na, Ca, Mg, F, Cl, and SO_4) in natural waters. *Water Research* **35**, 1500-1508.

Han Q., Moore J. K., Zender C., Measures C. I. and Hydes D. J. (2008) Constraining oceanic dust deposition using surface ocean dissolved Al. *Global Biogeochemical Cycles* **22**, GB2003, doi:10.1029/2007gb002975.

Helmers E. and Rutgers van der Loeff M. M. (1993) Lead and aluminum in Atlantic surface waters (50 °N to 50 °S) reflecting anthropogenic and natural sources in the eolian transport. *Journal of Geophysical Research* **98**, 20261-20273.

Honeyman B. D. and Santschi P. H. (1989) A Brownian-pumping model for oceanic trace metal scavenging: Evidence from Th isotopes. *Journal of Marine Research* **47**, 951-992.

Hunter K. A. (1983) The adsorptive properties of sinking particles in the deep ocean. *Deep Sea Research Part A. Oceanographic Research Papers* **30**, 669-675.

Hunter K. A. and Liss P. S. (1982) Organic matter and the surface charge of suspended particles in estuarine waters. *Limnology and Oceanography* **27**, 322-335.

Hydes D. J. (1979) Aluminum in seawater: Control by inorganic processes. *Science* **205**, 1260-1262.

Hydes D. J. and Liss P. S. (1976) Fluorimetric method for the determination of low concentrations of dissolved aluminum in natural waters. *Analyst* **101**, 922-931.

Jickells T. D. (1999) The inputs of dust derived elements to the Sargasso Sea; A synthesis. *Marine Chemistry* **68**, 5-14.

Jickells T. D., An Z. S., Andersen K. K., Baker A. R., Bergametti G., Brooks N., Cao J. J., Boyd P. W., Duce R. A., Hunter K. A., Kawahata H., Kubilay N., laRoche J., Liss P. S., Mahowald N., Prospero J. M., Ridgwell A. J., Tegen I. and Torres R. (2005) Global iron connections between desert dust, ocean biogeochemistry, and climate. *Science* **308**, 67-71.

Koning E., Gehlen M., Flank A. M., Calas G. and Epping E. (2007) Rapid post-mortem incorporation of aluminum in diatom frustules: Evidence from chemical and structural analyses. *Marine Chemistry* **106**, 208-222.

Kormann C., Bahnemann D. W. and Hoffmann M. R. (1988) Preparation and characterization of quantum-size titanium dioxide. *The Journal of Physical Chemistry* **92**, 5196-5201.

Kramer J., Laan P., Sarthou G., Timmermans K. R. and de Baar H. J. W. (2004) Distribution of dissolved aluminium in the high atmospheric input region of the subtropical waters of the North Atlantic Ocean. *Marine Chemistry* **88**, 85-101.

Kremling K., Andreae M. O., Brügmann L., van den Berg C. M. G., Prange A., Schirmacher M., Koroleff E. and Kuss J. (2007) Determination of trace elements. In *Methods of Seawater Analysis* (eds. Grasshoff K., Ehrhardt M. and Kremling K.). Wiley-VCH Verlag GmbH, pp. 253-364.

Kuehner E. C., Alvarez R., Paulsen P. J. and Murphy T. J. (1972) Production and analysis of special high-purity acids purified by subboiling distillation. *Analytical Chemistry* **44**, 2050-2056.

Kuma K., Nishioka J. and Matsunaga K. (1996) Controls on iron(III) hydroxide solubility in seawater: The influence of pH and natural organic chelators. *Limnology and Oceanography* **41**, 396-407.

Li Y.-H. (1981) Ultimate removal mechanisms of elements from the ocean. *Geochimica et Cosmochimica Acta* **45**, 1659-1664.

Li Y.-H. (1991) Distribution patterns of the elements in the ocean: A synthesis. *Geochimica et Cosmochimica Acta* **55**, 3223-3240.

Liu X. and Millero F. J. (2002) The solubility of iron in seawater. *Marine Chemistry* **77**, 43-54.

Luo C., Mahowald N. and del Corral J. (2003) Sensitivity study of meteorological parameters on mineral aerosol mobilization, transport, and distribution. *Journal of Geophysical Research* **108**, 4447, doi:10.1029/2003jd003483.

May H. M., Helmke P. A. and Jackson M. L. (1979) Gibbsite solubility and thermodynamic properties of hydroxy-aluminum ions in aqueous solution at 25 °C. *Geochimica et Cosmochimica Acta* **43**, 861-868.

McLennan S. M. (2001) Relationships between the trace element composition of sedimentary rocks and upper continental crust. *Geochemistry Geophysics Geosystems* **2**, 1021, doi:10.1029/2000gc000109.

Measures C. I. (1995) The distribution of Al in the IOC stations of the eastern Atlantic between 30 °S and 34 °N. *Marine Chemistry* **49**, 267-281.

Measures C. I. and Vink S. (2000) On the use of dissolved aluminum in surface waters to estimate dust deposition to the ocean. *Global Biogeochemical Cycles* **14**, 317-327.

Measures C. I., Brown M. T. and Vink S. (2005) Dust deposition to the surface waters of the western and central North Pacific inferred from surface water dissolved aluminum concentrations. *Geochemistry Geophysics Geosystems* **6**, Q09M03, doi:10.1029/2005gc000922.

Measures C. I., Landing W. M., Brown M. T. and Buck C. S. (2008) High-resolution Al and Fe data from the Atlantic Ocean CLIVAR-CO2 repeat hydrography A16N transect: Extensive linkages between atmospheric dust and upper ocean geochemistry. *Global Biogeochemical Cycles* **22**, GB1005, doi:10.1029/2007gb003042.

Moran S. B. and Buesseler K. O. (1992) Short residence time of colloids in the upper ocean estimated from ^{238}U - ^{234}Th disequilibria. *Nature* **359**, 221-223.

Moran S. B. and Buesseler K. O. (1993) Size-fractionated ^{234}Th in continental shelf waters off New England: Implications for the role of colloids in oceanic trace metal scavenging. *Journal of Marine Research* **51**, 893-922.

Moran S. B. and Moore R. M. (1988) Evidence from mesocosm studies for biological removal of dissolved aluminum from sea water. *Nature* **335**, 706-708.

Moran S. B. and Moore R. M. (1989) The distribution of colloidal aluminum and organic carbon in coastal and open ocean waters off Nova Scotia. *Geochimica et Cosmochimica Acta* **53**, 2519-2527.

Moran S. B. and Moore R. M. (1992) Kinetics of the removal of dissolved aluminum by diatoms in seawater: A comparison with thorium. *Geochimica et Cosmochimica Acta* **56**, 3365-3374.

Moran S. B., Yeats P. A. and Balls P. W. (1996) On the role of colloids in trace metal solid-solution partitioning in continental shelf waters: A comparison of model results and field data. *Continental Shelf Research* **16**, 397-408.

Moulin C., Lambert C. E., Dulac F. and Dayan U. (1997) Control of atmospheric export of dust from North Africa by the North Atlantic Oscillation. *Nature* **387**, 691-694.

Neal C., Jarvie H., Rowland P., Lawler A., Sleep D. and Scholefield P. (2011) Titanium in UK rural, agricultural and urban/industrial rivers: Geogenic and anthropogenic colloidal/sub-colloidal sources and the significance of within-river retention. *Science of The Total Environment* **409**, 1843-1853.

Orians K. J. and Bruland K. W. (1986) The biogeochemistry of aluminum in the Pacific Ocean. *Earth and Planetary Science Letters* **78**, 397-410.

Orians K. J. and Boyle E. A. (1993) Determination of picomolar concentrations of titanium, gallium and indium in sea water by inductively coupled plasma mass spectrometry following an 8-hydroxyquinoline chelating resin preconcentration. *Analytica Chimica Acta* **282**, 63-74.

Orians K. J., Boyle E. A. and Bruland K. W. (1990) Dissolved titanium in the open ocean. *Nature* **348**, 322-325.

Pokrovsky O. S. and Schott J. (2002) Iron colloids/organic matter associated transport of major and trace elements in small boreal rivers and their estuaries (NW Russia). *Chemical Geology* **190**, 141-179.

Powell R. T., Landing W. M. and Bauer J. E. (1996) Colloidal trace metals, organic carbon and nitrogen in a southeastern U.S. estuary. *Marine Chemistry* **55**, 165-176.

Prospero J. M., Nees R. T. and Uematsu M. (1987) Deposition rate of particulate and dissolved aluminium derived from Saharan dust in precipitation at Miami, Florida. *Journal of Geophysical Research* **92**, 14723-14731.

Reitmeyer R., Powell R. T., Landing W. M. and Measures C. I. (1996) Colloidal aluminum and iron in seawater: An intercomparison between various cross-flow ultrafiltration systems. *Marine Chemistry* **55**, 75-91.

Reyes-Coronado D., Rodríguez-Gattorno G., Espinosa-Pesqueira M. E., Cab C., de Coss R. and Oskam G. (2008) Phase-pure TiO_2 nanoparticles: Anatase, brookite and rutile. *Nanotechnology* **19**, 145605, doi:10.1088/0957-4484/19/14/145605.

Rijkenberg M. J. A., Powell C. F., Dall'Osto M., Nielsdottir M. C., Patey M. D., Hill P. G., Baker A. R., Jickells T. D., Harrison R. M. and Achterberg E. P. (2008) Changes in iron speciation following a Saharan dust event in the tropical North Atlantic Ocean. *Marine Chemistry* **110**, 56-67.

Sañudo-Wilhelmy S. A., Rivera-Duarte I. and Russell Flegal A. (1996) Distribution of colloidal trace metals in the San Francisco Bay estuary. *Geochimica et Cosmochimica Acta* **60**, 4933-4944.

Savenko A. V. and Savenko V. S. (2011) Aluminum hydroxide's solubility and the forms of dissolved aluminum's occurrence in Seawater. *Oceanology* **51**, 231-234.

Schlosser C. and Croot P. L. (2008) Application of cross-flow filtration for determining the solubility of iron species in open ocean seawater. *Limnology and Oceanography-Methods* **6**, 630-642.

Schmidt J. and Vogelsberger W. (2006) Dissolution kinetics of titanium dioxide nanoparticles: The observation of an unusual kinetic size effect. *Journal of Physical Chemistry B* **110**, 3955-3963.

Schmidt J. and Vogelsberger W. (2009) Aqueous long-term solubility of titania nanoparticles and titanium(IV) hydrolysis in a sodium chloride system studied by adsorptive stripping voltammetry. *Journal of Solution Chemistry* **38**, 1267-1282.

Skrabal S. A. (2006) Dissolved titanium distributions in the Mid-Atlantic Bight. *Marine Chemistry* **102**, 218-229.

Skrabal S. A., Ullman W. J. and Luther III G. W. (1992) Estuarine distributions of dissolved titanium. *Marine Chemistry* **37**, 83-103.

Stolpe B., Guo L., Shiller A. M. and Hassellöv M. (2010) Size and composition of colloidal organic matter and trace elements in the Mississippi River, Pearl River and the northern Gulf of Mexico, as characterized by flow field-flow fractionation. *Marine Chemistry* **118**, 119-128.

Stolpe B. and Hassellöv M. (2007) Changes in size distribution of fresh water nanoscale colloidal matter and associated elements on mixing with seawater. *Geochimica et Cosmochimica Acta* **71**, 3292-3301.

Sugimoto T., Zhou X. and Muramatsu A. (2002) Synthesis of uniform anatase TiO_2 nanoparticles by gel-sol method: 1. Solution chemistry of $Ti(OH)_n^{(4-n)+}$ complexes. *Journal of Colloid and Interface Science* **252**, 339-346.

Sutheimer S. H. and Cabaniss S. E. (1997) Aluminum binding to humic substances determined by high performance cation exchange chromatography. *Geochimica et Cosmochimica Acta* **61**, 1-9.

Thuróczy C. E., Gerringa L. J. A., Klunder M. B., Middag R., Laan P., Timmermans K. R. and de Baar H. J. W. (2010) Speciation of Fe in the eastern North Atlantic Ocean. *Deep Sea Research Part I: Oceanographic Research Papers* **57**, 1444-1453.

Turner D. R., Whitfield M. and Dickson A. G. (1981) The equilibrium speciation of dissolved components in freshwater and sea water at 25°C and 1 atm pressure. *Geochimica et Cosmochimica Acta* **45**, 855-881.

Uppal R., Israel H. P., Incarvito C. D. and Valentine A. M. (2009) Titanium(IV) complexes with N,N'-dialkyl-2,3-dihydroxyterephthalamides and 1-hydroxy-2(1H)-pyridinone as siderophore and tunichrome analogues. *Inorganic Chemistry* **48**, 10769-10779.

van Bennekom A. J., Fred Jansen J. H., van der Gaast S. J., van Iperen J. M. and Pieters J. (1989) Aluminium-rich opal: An intermediate in the preservation of biogenic silica in the Zaire (Congo) deep-sea fan. *Deep Sea Research Part A. Oceanographic Research Papers* **36**, 173-190.

van den Berg C. M. G., Boussemart M., Yokoi K., Prartono T. and Campos M. L. A. M. (1994) Speciation of aluminium, chromium and titanium in the NW Mediterranean. *Marine Chemistry* **45**, 267-282.

Wen L.-S., Santschi P. H., Gill G. A. and Paternostro C. (1999) Estuarine trace metal distributions in Galveston Bay: Importance of colloidal forms in the speciation of the dissolved phase. *Marine Chemistry* **63**, 185-212.

Wen L.-S., Stordal M. C., Tang D., Gill G. A. and Santschi P. H. (1996) An ultraclean cross-flow ultrafiltration technique for the study of trace metal phase speciation in seawater. *Marine Chemistry* **55**, 129-152.

Willey J. D. (1975) Reactions which remove dissolved alumina from seawater. *Marine Chemistry* **3**, 227-240.

Wu J., Boyle E. A., Sunda W. G. and Wen L.-S. (2001) Soluble and colloidal iron in the oligotrophic North Atlantic and North Pacific. *Science* **293**, 847-849.

5 Particulate and Dissolved Aluminium and Titanium in the Upper Water Column of the Atlantic Ocean

Anna Dammshäuser[1], Thibaut Wagener[1, 2], Carl-Dieter Garbe-Schönberg[3], Peter Croot[1, 4, 5]

Manuscript in preparation for submission to
Deep Sea Research Part I: Oceanographic Research Papers

Abstract

In order to better constrain the oceanic behavior of the lithogenic trace elements Al and Ti, dissolved and particulate fractions of both metals were determined in the upper 200 m of the Atlantic Ocean. Sampling was conducted during an E-W transect in the eastern tropical North Atlantic (December 2009) and along a meridional Atlantic transect (April - May 2010). The surface water distributions of particulate and dissolved Al and Ti reflected the anticipated pattern of atmospheric inputs into the Atlantic Ocean. Vertical distributions of Al and Ti were characterized by elevated surface concentrations of the dissolved and particulate metals, in agreement with their predominant input from atmospheric sources. Subsurface minima at stations with pronounced fluorescence maxima suggest links with biological productivity on the removal of both dissolved and particulate Al and Ti. This may include uptake mechanisms, adsorption and aggregation processes on biogenic

[1] Helmholtz Centre for Ocean Research Kiel (GEOMAR), Germany

[2] now at: Mediterranean Institute of Oceanography (MIO), UMR 7294 - CNRS - Univ. Aix-Marseille - IRD, Marseille, France

[3] Institute of Geosciences, University of Kiel, Germany

[4] Plymouth Marine Laboratory, PML, United Kingdom

[5] now at: Earth and Ocean Sciences, National University of Ireland - Galway, NUIG, Ireland

particle surfaces, and the formation of large, fast sinking biogenic particles (e.g. fecal pellets). Residence times in the tropical and subtropical North Atlantic were estimated to range in the order of days to weeks in the particulate phases (Al: 3 - 22 days, Ti: 4 - 37 days) and were 0.9 - 3.8 years for Al and 10 - 31 years for Ti in the dissolved phases. Longer residence times in both size fractions in the South Atlantic agree with lower biological productivity, suggesting decreased removal rates. In the upper water column, Al was predominantly present in the dissolved form, whereas Ti mostly occurred in the particulate form. Largest deviations in the partitioning coefficients were found in the surface waters, together with excess dissolved Al and excess particulate Ti compared to the crustal ratio, and likely reflect elevated dissolution of Al compared to Ti from atmospheric mineral particles. Minima of the partitioning coefficients in the region of the fluorescence maxima suggest that here the removal of particulate trace Al and Ti exceeds the transfer from the dissolved into the particulate phase.

5.1 Introduction

The input of atmospheric mineral particles (also referred to as dust) can supply essential nutrients into the surface ocean [e.g. Duce et al., 1991; Jickells et al., 2005; Baker et al., 2010] and may thus strongly influence biological processes in the open ocean. However, dust inputs to the ocean are yet poorly quantified. Surface water concentrations of dissolved Al (dAl), and more recently dissolved Ti (dTi) have been suggested as tracers to estimate dust inputs into the open ocean [e.g. Measures and Vink, 2000; Gehlen et al., 2003; Han et al., 2008; Dammshäuser et al., 2011]. Both metals are abundant elements in the earth's crust [McLennan, 2001] and their supply into the open ocean occurs predominantly via the deposition of atmospheric mineral particles [Orians and Bruland, 1986; Orians et al., 1990]. However, the assessment of dust inputs from surface water concentrations of dAl and dTi requires knowledge of their oceanic behavior. For Al, spatial and temporal variations in the residence times have been found to complicate the quantification of dust inputs [Han et al., 2008; Dammshäuser et al., 2011]. In the case of Ti, few studies report surface water concentrations and very little is known about surface water residence times yet.

In seawater, dAl and dTi are mostly present as highly particle reactive, hydrolyzed species [Turner et al., 1981; Li, 1991]. Thus, upon their atmospheric delivery the oceanic distributions of dAl and dTi are strongly influenced by scavenging removal from the upper

water column [Hydes, 1979; e.g. Orians et al., 1990]. The process of scavenging generally includes the transfer from the dissolved to the particulate phase via surface adsorption and aggregation mechanisms, followed by the settling of the particles through the water column [e.g. Turekian, 1977; Li, 1981; Fowler and Knauer, 1986; Whitfield and Turner, 1987; Li, 2011]. Both processes are to some extent controlled by the general abundance of suspended particulate matter (SPM) that provides surface adsorption and aggregation sites. Biological productivity may enhance the removal of trace metals through uptake mechanisms and through the production of SPM and/or large, fast sinking biogenic particles, e.g. fecal pellets [Lal, 1977; Whitfield and Turner, 1987]. Active or passive biological uptake may occur in the case of Al, as evidence has been found for the incorporation of Al into the silicate frustules of diatoms [Gehlen et al., 2002; Koning et al., 2007].

In the upper water column of the open ocean, the particulate phase controls both the input (via dissolution of atmospheric mineral particles) and the removal (via scavenging) of dAl and dTi. For the particulate trace metals, short residence times can be expected, whereas longer residence times occur in the dissolved phase [e.g. Jickells, 1999]. Thus, the oceanic behavior of Al and Ti is closely related to their distributions between the dissolved and the particulate phase. However, so far very few studies report distributions of the particulate Al (pAl) and particulate Ti (pTi) fractions in the open ocean, or combine observations of the trace metals in both the particulate and dissolved size fractions [Sherrell and Boyle, 1992; Helmers, 1996; Kuss and Kremling, 1999].

In this study, the concentrations of the dissolved and particulate phases of Al and Ti were determined in the upper water column of the Atlantic Ocean. Samples were taken along an E-W transect in the tropical North Atlantic in December 2009 and along a meridional Atlantic transect in April - May 2010. The study regions are characterized by large variations in the supply of atmospheric mineral particle, and thus specific input signals and removal processes can be expected for Al and Ti. This study is complementary to two previous studies that focused on the potential suitability of dAl and dTi as complementary dust tracers [Dammshäuser et al., 2011] and on the size distributions (soluble - colloidal) of both metals within the dissolved phase [Dammshäuser and Croot, submitted to Geochimica et Cosmochimica Acta]. The aim of this study was to better constrain the oceanic behavior of both trace metals upon their supply via dust deposition. The particular focus is in identifying the role of particulate associations in the removal processes of dAl and dTi. A deeper understanding of the oceanic behavior of Al and Ti will eventually help to constrain

their complementary utilization as tracers for the supply of atmospheric mineral particles to the open ocean.

5.2 Methods

Sampling for this study was conducted during two cruises in the Atlantic Ocean. Seawater samples from the eastern tropical North Atlantic were collected aboard RV Meteor during the SFB 754 cruise M80-2 (Mindelo - Dakar) in November and December 2009. In addition, a meridional Atlantic transect was sampled aboard RV Polarstern (ANTXXVI-4, Punta Arenas - Bremerhaven) in April - May 2010. The sampled stations are displayed in Fig. 5.1, locations and sampling dates are given in the Tables 5.1 and 5.2.

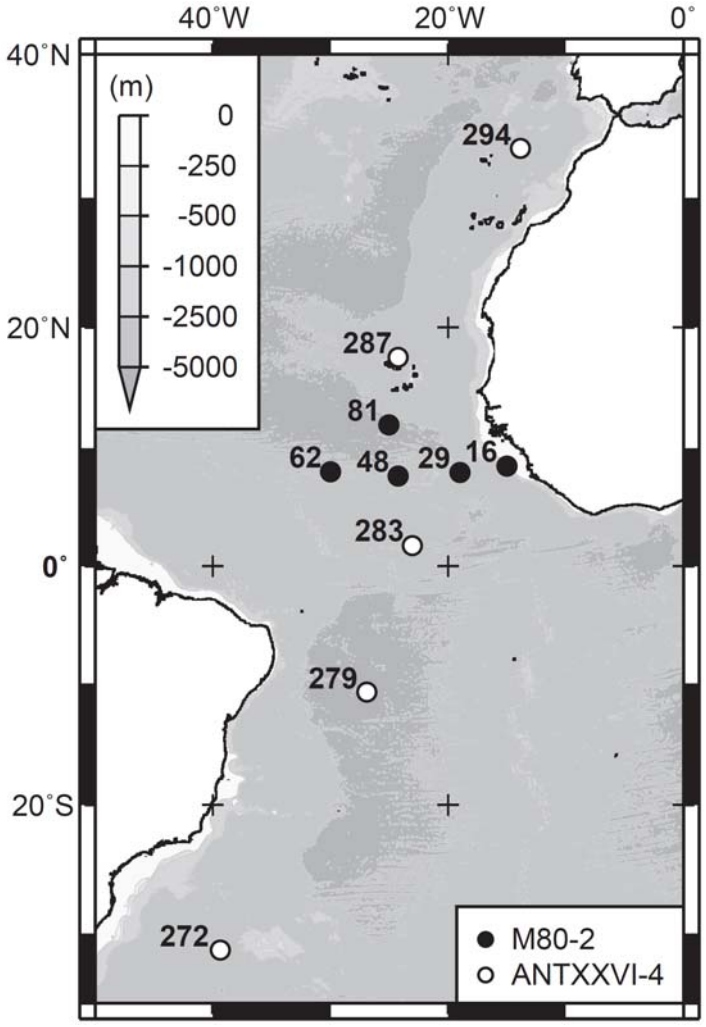

Fig. 5.1: Sampled stations during M80-2 (black circles) in December 2009, and during ANTXXVI-4 (open circles) in April - May 2010.

5.2.1 Dissolved fractions

The collection of seawater and the analysis of the dissolved fractions was conducted exactly as given in Dammshäuser et al. [2011] and Dammshäuser and Croot [submitted to Geochimica et Cosmochimica Acta]. In short, the samples were collected in PTFE coated 8 l GO-FLO bottles (General Oceanics) and transferred into a sea-going clean van (ISO 5, class 100). For the analysis of the dissolved fractions, samples were filtered in-line through 0.2 µm cartridge filters (Sartobran® P, Sartorius) by applying nitrogen overpressure, and acidified with sub-boiled quartz distilled HCl to pH <2 for at least 24 h before analysis. Dissolved Al concentrations were determined by a slightly modified version of the fluorometric method described by Hydes and Liss [1976]. The detection limit ranged between 0.1 and 0.3 nM, the blank values between 0.4 and 0.6 nM at the different days of analysis. The analysis of the SAFe reference seawater S1 gave 1.81 ± 0.24 nM of Al (n = 4) during M80-2 and 1.70 ± 0.21 nM of Al (n = 14) during ANTXXVI-4 (consensus value of 1.74 ± 0.09 nM). Dissolved Ti concentrations were determined using the voltammetric method described by Croot [2011]. The detection limit was 9 pM and the blank value was 24 ± 3 pM for Ti.

5.2.2 Particulate fractions

The particulate fractions of Al and Ti (pAl, pTi) were collected on 0.2 µm track-etched polycarbonate membrane disk filters (Nuclepore™, Whatman). Prior to filtration, the polycarbonate filters were repeatedly cleaned in diluted HCl (1 M) and rinsed with deionized water. The filtration was conducted in-line by attaching PFA filter holders and tubing (Savillex) directly to the GO-FLO bottles and applying slight nitrogen overpressure (0.2 bar). The filtration time typically ranged around 1 h and about 2 l of seawater were filtered. The loaded filters were placed in Petri dishes (Analyslide®, Pall Corporation) and stored at -20 °C until digestion in the shore-based laboratory.

The digestion procedure was conducted according to the sample-handling protocols for GEOTRACES cruises [GEOTRACES Standards and Intercalibration Committee, 2010]. The filters were cut in two halves, placed around the walls of an acid cleaned Teflon vial, and 1 ml of subboiled quartz distilled concentrated HNO_3, 900 µl of deionized water, and 100 µl of HF (trace metal clean grade) were added. The samples were then heated for 4 h at 130 °C, which allowed the acid to reflux within the Teflon vials without the filters being immersed fully in hot acid. Subsequently, the acid solution was reduced at 130 °C, and

Table 5.1: Sampled stations and determined concentrations of particulate and dissolved Al and Ti during M80-2. Standard deviations are given in parentheses.

Station	Lat.	Lon.	Date	Depth (m)	pAl (nM)	dAl (nM)	pAl/dAl	pTi (pM)	dTi (pM)	pTi/dTi
16	8.50	-15.00	2009-12-01	20	3.39	30.52 (0.07)	0.11	202.9	155.0 (10.9)	1.31
16	8.50	-15.00	2009-12-01	50	0.59	11.93 (0.11)	0.05	63.6	101.9 (10.7)	0.62
16	8.50	-15.00	2009-12-01	80	1.62	6.32 (0.02)	0.26	79.7	114.4 (12.7)	0.70
16	8.50	-15.00	2009-12-01	120	4.49	8.05 (0.06)	0.56	154.2	128.3 (12.9)	1.20
29	7.96	-18.00	2009-12-05	20	17.71	42.68 (0.27)	0.42	586.1	157.3 (7.0)	3.73
29	7.96	-18.00	2009-12-05	40	2.10	7.36 (0.1)	0.29	181.4	68.7 (7.4)	2.64
29	7.96	-18.00	2009-12-05	60	2.32	6.26 (0.08)	0.37	190.3	116.8 (12.8)	1.63
29	7.96	-18.00	2009-12-05	100	7.00	10.10 (0.27)	0.69	260.1	137.2 (8.3)	1.90
48	7.67	-24.23	2009-12-10	20	14.11	35.26 (0.17)	0.40	486.4	139.2 (10.8)	3.49
48	7.67	-24.23	2009-12-10	50	2.67	13.16 (0.1)	0.20	92.8	77.0 (6.3)	1.20
48	7.67	-24.23	2009-12-10	80	4.01	7.31 (0.12)	0.55	158.9	116.3 (13.8)	1.37
48	7.67	-24.23	2009-12-10	120	8.30	9.55 (0.09)	0.87	442.8	126.7 (6.8)	3.49
48	7.67	-24.23	2009-12-10	160	8.91	9.87 (0.13)	0.90	293.1	131.9 (5.2)	2.22
48	7.67	-24.23	2009-12-10	200	9.66	7.04 (0.08)	1.37	385.1	94.6 (3.9)	4.07
62	8.02	-29.98	2009-12-14	20	3.04	30.93 (0.41)	0.10	152.7	101.1 (6.3)	1.51
62	8.02	-29.98	2009-12-14	50	2.42	25.66 (0.45)	0.09	47.5	74.1 (6.6)	0.64
62	8.02	-29.98	2009-12-14	80	2.52	15.24 (0.29)	0.17	95.4	90.2 (9.1)	1.06
62	8.02	-29.98	2009-12-14	120	4.39	10.62 (0.18)	0.41	127.2	95.6 (8.2)	1.33
62	8.02	-29.98	2009-12-14	160	9.74	7.90 (0.04)	1.23	250.6	106.0 (5.4)	2.37
62	8.02	-29.98	2009-12-14	200	13.90	9.09 (0.05)	1.53	393.6	111.7 (4.9)	3.52
81	12.00	-25.00	2009-12-18	20	2.46	28.58 (0.24)	0.09	221.1	97.1 (5.5)	2.28
81	12.00	-25.00	2009-12-18	50	1.85	3.30 (0.06)	0.56	41.0	72.7 (4.6)	0.56
81	12.00	-25.00	2009-12-18	80	2.72	5.59 (0.05)	0.49	313.7	110.2 (6.1)	2.85
81	12.00	-25.00	2009-12-18	120	7.67	7.65 (0.04)	1.00	493.3	131.0 (4.0)	3.77
81	12.00	-25.00	2009-12-18	160	7.66	8.39 (0.12)	0.91	197.1	121.5 (4.7)	1.62
81	12.00	-25.00	2009-12-18	200	9.37	9.42 (0.05)	1.00	181.1	134.8 (5.1)	1.34

Table 5.2: Sampled stations and determined concentrations of particulate and dissolved Al and Ti during ANTXXVI-4. Standard deviations are given in parentheses.

Station	Lat.	Lon.	Date	Depth (m)	pAl (nM)	dAl (nM)	pAl/dAl	pTi (pM)	dTi (pM)	pTi/dTi
272	-31.21	-39.37	2010-04-17	20	1.08	7.04 (0.16)	0.15	66.3	34.7 (5.6)	1.91
272	-31.21	-39.37	2010-04-17	40	2.51	5.72 (0.06)	0.44	70.0	51.0 (3.2)	1.37
272	-31.21	-39.37	2010-04-17	60	1.69	6.12 (0.16)	0.28	139.3	50.9 (3.6)	2.74
272	-31.21	-39.37	2010-04-17	80	0.62	6.32 (0.08)	0.10	281.1	62.3 (5.4)	4.51
272	-31.21	-39.37	2010-04-17	100	0.67	5.16 (0.12)	0.13	66.1	72.6 (4.2)	0.91
272	-31.21	-39.37	2010-04-17	200	1.85	8.87 (0.13)	0.21	98.3	53.1 (5.2)	1.85
279	-10.71	-26.93	2010-04-24	25	1.68	15.17 (0.22)	0.11	97.0	57.3 (11.2)	1.69
279	-10.71	-26.93	2010-04-24	50	2.33	15.79 (0.31)	0.15	161.6	67.0 (4.8)	2.41
279	-10.71	-26.93	2010-04-24	75	0.93	10.84 (0.12)	0.09	33.1	79.5 (3.5)	0.42
279	-10.71	-26.93	2010-04-24	100	0.65	10.06 (0.22)	0.07	77.6	56.9 (5.5)	1.36
279	-10.71	-26.93	2010-04-24	130	0.52	7.38 (0.06)	0.07	86.7	61.2 (4.9)	1.42
279	-10.71	-26.93	2010-04-24	200	0.83	2.99 (0.08)	0.28	65.8	75.9 (4.9)	0.87
283	1.78	-23.00	2010-04-28	20	6.96	26.68 (0.34)	0.26	290.3	90.6 (6.7)	3.20
283	1.78	-23.00	2010-04-28	40	8.27	24.37 (0.15)	0.34	498.6	99.2 (4.3)	5.03
283	1.78	-23.00	2010-04-28	60	2.26	13.78 (0.13)	0.16	139.2	65.3 (5.1)	2.13
283	1.78	-23.00	2010-04-28	80	2.40	4.89 (0.02)	0.49	141.2	72.4 (6.2)	1.95
283	1.78	-23.00	2010-04-28	100	4.10	4.80 (0.12)	0.85	189.0	58.0 (4.8)	3.26
283	1.78	-23.00	2010-04-28	200	16.05	6.13 (0.09)	2.62	553.7	77.2 (5.9)	7.17
287	17.59	-24.26	2010-05-04	20	4.12	12.66 (0.28)	0.33	155.8	104.5 (7.8)	1.49
287	17.59	-24.26	2010-05-04	40	2.27	13.15 (0.10)	0.17	71.4	96.1 (4.9)	0.74
287	17.59	-24.26	2010-05-04	60	0.35	8.74 (0.10)	0.04	27.8	50.2 (3.3)	0.55
287	17.59	-24.26	2010-05-04	80	0.61	7.34 (0.12)	0.08	47.9	59.9 (6.6)	0.80
287	17.59	-24.26	2010-05-04	100	0.54	7.73 (0.11)	0.07	151.2	99.6 (7.2)	1.52
287	17.59	-24.26	2010-05-04	200	5.65	10.16 (0.02)	0.56	248.6	136.5 (5.6)	1.82
294	33.59	-13.86	2010-05-09	20	1.07	13.08 (0.25)	0.08	157.4	59.2 (5.2)	2.66
294	33.59	-13.86	2010-05-09	40	1.20	9.00 (0.05)	0.13	89.0	61.0 (5.0)	1.46
294	33.59	-13.86	2010-05-09	60	1.57	10.42 (0.13)	0.15	230.8	61.5 (7.3)	3.75
294	33.59	-13.86	2010-05-09	80	2.32	9.63 (0.11)	0.24	120.1	36.4 (4.5)	3.30
294	33.59	-13.86	2010-05-09	100	4.46	10.32 (0.12)	0.43	265.4	35.1 (3.5)	7.57
294	33.59	-13.86	2010-05-09	200	6.66	19.08 (0.08)	0.35	432.3	73.9 (5.9)	5.85

100 µl of HNO_3 were added just before dryness to ensure complete HF removal. The samples were then again reduced to near dryness, redissolved in 3 ml of 0.2 M HNO_3 and heated for 1 h at 60 °C. Finally, the digested samples were transferred into acid cleaned PE vials (Zinsser Polyvials®) and stored until analysis.

The concentrations of Al and Ti in the digested samples were determined by ICP-MS (Agilent 7500cs) at the CAU Institute of Geosciences. Sample introduction was conducted via an APEX (ESI Inc., USA) desolvating nebulizer device. The ICP-MS was operated under standard mode conditions with the APEX set to 140 °C desolvating, and 2 °C condensation temperature. A 2.5 µg/l Be and In spike was used for internal standardisation. Further details of instrument setup and calibration strategies can be found in Garbe-Schönberg [1993]. Analytical precision for Al and Ti as estimated from duplicate sample measurements was 7 and 6 %RSD, respectively. Filter blanks were determined by digesting process blank filters from both cruises. The determined blank values were 0.518 ± 0.055 nmol of Al and 101 ± 26 pmol of Ti per filter (n = 7). During the sampling, the filter loads were 1.6 - 50 nmol for Al and 262 pmol - 1.8 nmol for Ti.

As no certified reference material is available for suspended oceanic particulate matter, the accuracy of the results was monitored by digestion and analyses of the international certified reference material BIR-1 (Icelandic basalt, USGS) and an international laboratory comparison standard "Koelln Loess" [GeoPT13, IAG; Potts et al., 2003]. The loess standard was chosen based on the assumption that in our samples a large fraction of the particulate Al and Ti occurs in the form of deposited atmospheric mineral particles. For Al the recovery was 95. 8 % in the BIR-1 and 96.2 % in the GeoPT13, for Ti 99.9 % were found in the BIR-1 and 60.8 % in the GeoPT13 (n = 6). In the loess samples, small mineral grains were still visible after the digestion procedure. This suggests that the low recovery of Ti is associated with the presence of hardly soluble Ti bearing mineral phases. Bowie et al. [2010] report even lower recoveries (<8 %) of Ti in marine sediments using a different digestion method. The authors also found very low recoveries of Al during digestions with pure HNO_3 that increased to values around 80 % when HF:HNO_3 (1:1) was used. Our digestion method included a much smaller fraction of HF but a nearly complete recovery of Al was achieved. Furthermore, our observed pTi concentrations are in good agreement with previously reported values in the same region (see section 5.4.1) that have been determined after a more rigorous digestion procedure at higher temperatures using pressure bombs and an 1:3:3 mixture of nitric acid, hydrofluoric acid and perchloric acid [Kuss and Kremling, 1999]. For Ti, Kuss and Kremling [1999] report accuracies for sediment

standards within three standard deviations of the certified values. Given the agreement in the observed Ti values and the fact that our digestion procedure was conducted as suggested by the GEOTRACES Standards and Intercalibration Committee [2010], we thus assume that for Ti a more complete recovery was achieved in the filter digestions compared to the loess reference standard.

5.2.3 Ancillary data

Supporting oceanographic data including fluorescence measurements were obtained from the CTD system. Data for ANTXXVI-4 are available in the Pangaea data management system [Rohardt and Bracher, 2011]. Fluorescence data for ANTXXVI-4 are given as uncalibrated raw data and thus serve to locate and compare the chlorophyll *a* maxima among the different stations, rather than to determine absolute concentrations. During M80-2, the fluorescence sensor data were calibrated with individual measurements of chlorophyll *a* from the Niskin bottles and concentrations are given.

5.3 Results

The observed concentrations of particulate and dissolved Al and Ti are given in Tables 5.1 and 5.2 and are displayed together with supporting oceanographic data in Figs. 5.2 and 5.3. The vertical distributions of dissolved Al and Ti in the eastern tropical North Atlantic (M80-2), and surface water distributions of the dissolved fractions during the Atlantic transect (ANTXXVI-4) have already been described and discussed in two previous publications [Dammshäuser et al., 2011; Dammshäuser and Croot, submitted to Geochimica et Cosmochimica Acta]. The new data presented in this study comprise vertical distributions of Al and Ti during the Atlantic transect in April - May 2010, as well as the distributions of both metals in the particulate phase.

5.3.1 Aluminium

Particulate Al concentrations were elevated in the surface waters at three stations in the eastern tropical North Atlantic. Highest pAl concentrations of 14 - 18 nM were found at 8 °N, between 19 °W and 24 °W in December 2009. During the Atlantic transect in April - May 2010, highest surface water concentrations of 7 nM of pAl were observed at 2 °N, 23 °W. At the remaining stations, the surface water concentrations of pAl ranged between 1 and 4 nM. With depth, at most stations in the tropical North Atlantic, the concentrations

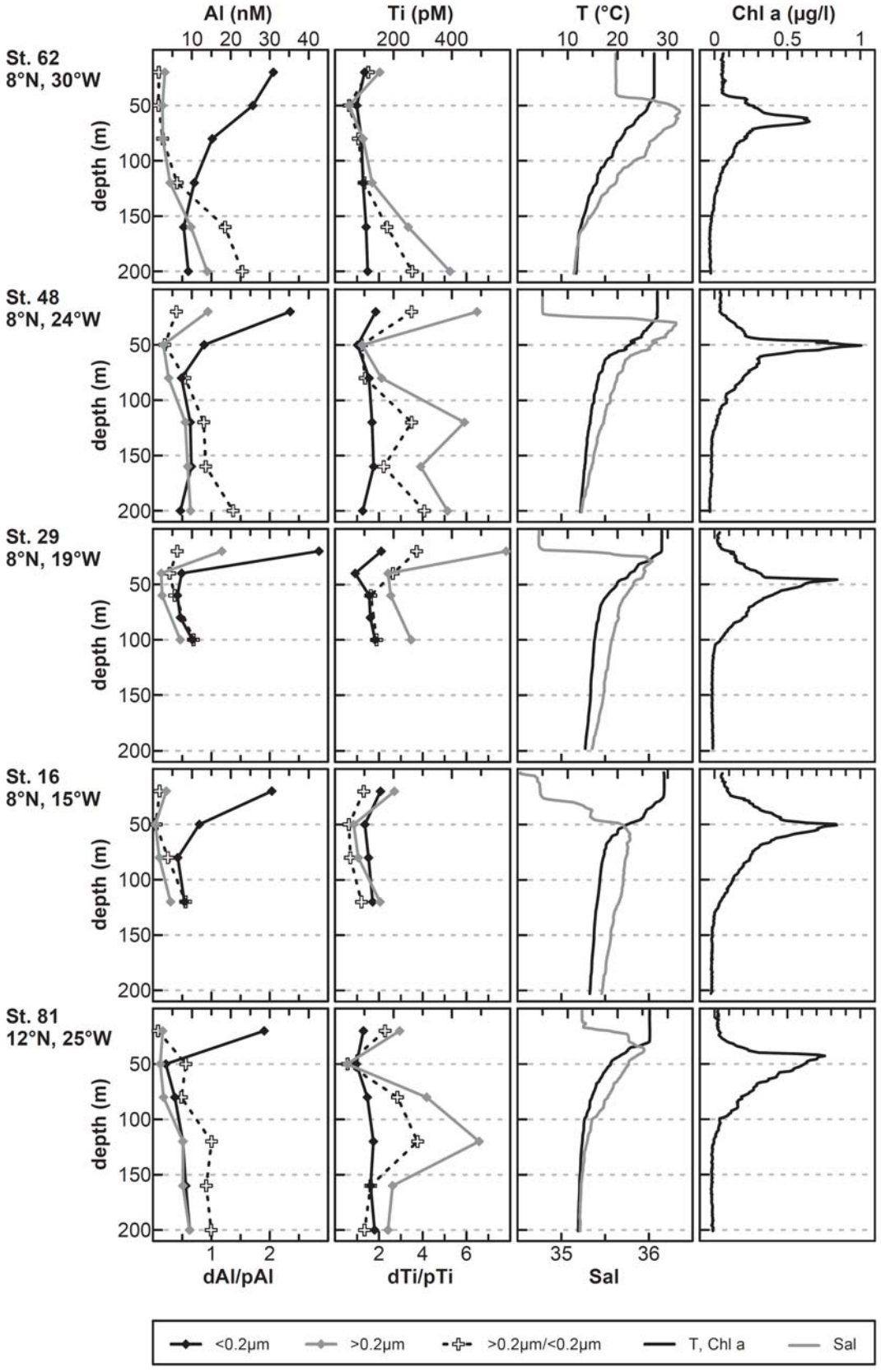

Fig. 5.2: Depth distributions of particulate (>0.2 µm) and dissolved (<0.2 µm) Al and Ti, as well as temperature, salinity and chlorophyll *a* concentrations during M80-2. Also shown are the coefficients of partitioning between the particulate and the dissolved fractions for Al and Ti (crosses and dotted lines).

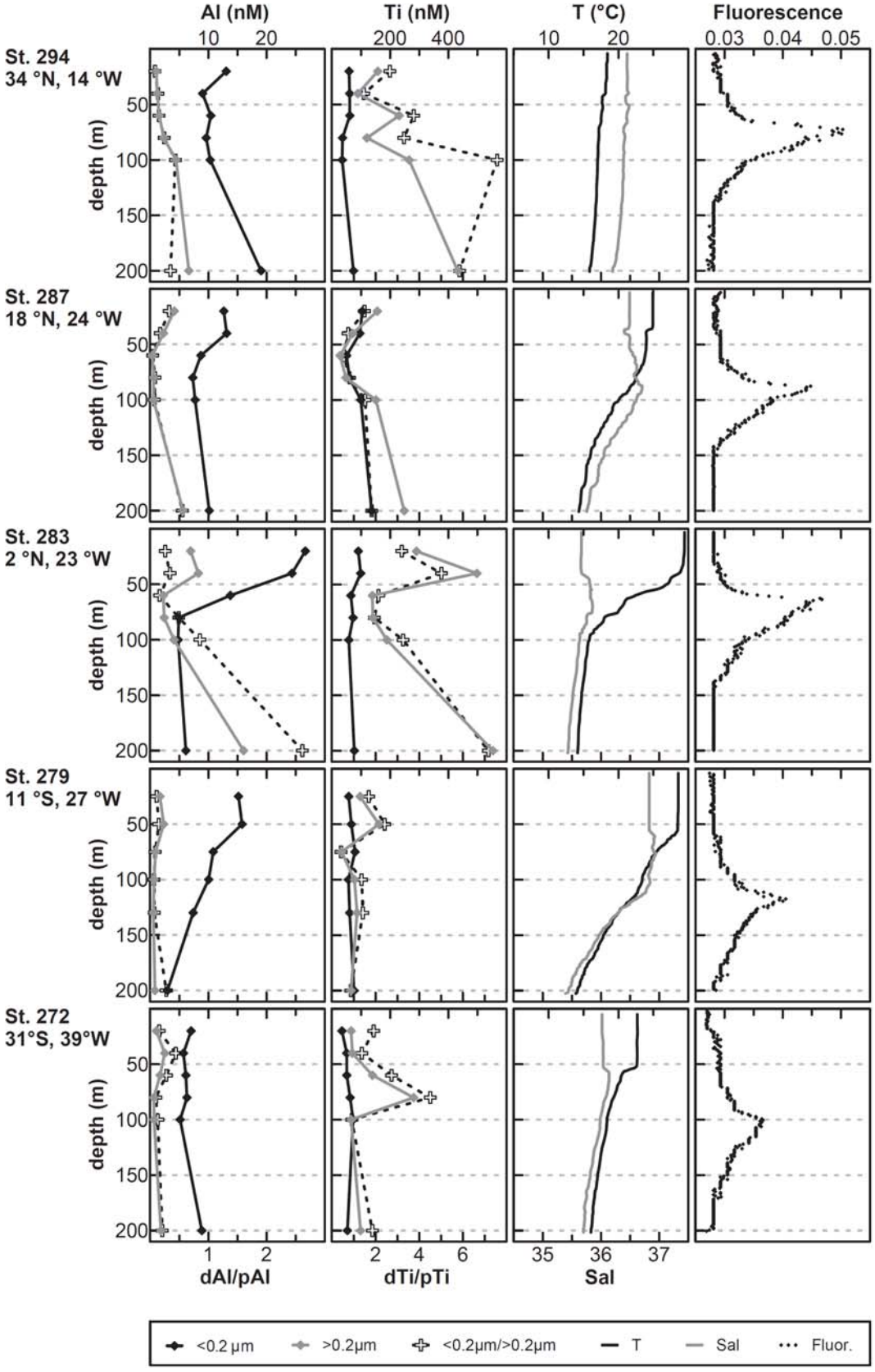

Fig. 5.3: Depth distributions of particulate (>0.2 µm) and dissolved (<0.2 µm) Al and Ti, as well as temperature, salinity and fluorescence during ANTXXVI-4. Also shown are the coefficients of partitioning between the particulate and the dissolved fractions for Al and Ti (crosses and dotted lines).

of pAl decreased from surface maxima to subsurface minima and again increased with depth. Surface elevations were absent at 8 °N, 30 °W and at 12 °N, 25 °W in December 2009. At these stations the concentrations of pAl ranged between 2 and 3 nM in the upper 80 m of the water column and then increased with depth to 9 - 14 nM. A similar distribution with slightly lower abundance of pAl was observed at 34 °N, 14 °W in April - May 2010. At the stations in the South Atlantic, the concentrations of pAl were generally lower compared to the stations in the North Atlantic, with maximal 2.5 nM of pAl.

The depth distributions of dAl showed some similarities to those of dAl. At most stations in the eastern tropical North Atlantic, the dAl concentrations decreased to subsurface minima of 3 - 7 nM and again increased further below to concentrations of 5 - 10 nM. The subsurface minima of dAl were mostly located close to the fluorescence maxima. In the subtropical North Atlantic (34 °N, 14 °W) the dAl concentrations increased more pronouncedly with depth to up to 19 nM at 200 m. The distributions of dAl in the South Atlantic differed from those in the North Atlantic. At 31 °S, 39 °W, lowest surface water concentrations were observed and dAl was quite uniformly distributed around 5 - 9 nM in the upper water column. At 11 °S, 37 °W, the dAl concentrations constantly decreased with depth, from 15 nM at the surface to 3 nM at 200 m depth.

5.3.2 Titanium

The surface water concentrations of pTi were elevated at three stations in the tropical North Atlantic, similar to those of pAl. In December 2009, highest pTi concentrations of up to 590 pM occurred at 8 °N, between 19 °W and 24 °W. During the Atlantic transect in April - May 2010, highest surface water concentrations of 290 pM of pTi were found at 2 °N, 23 °W. At this station, the pTi concentrations further increased to 500 pM at the lower boundary of the mixed layer (40 m). At the remaining stations in the tropical and subtropical North Atlantic, the surface water concentrations of pTi were 150 - 220 pM. In the South Atlantic, lower surface water pTi concentrations of 70 - 100 pM were observed. The depth distributions of pTi were characterized by subsurface minima close to the fluorescence maxim at all station in the North Atlantic, with minimum pTi concentrations of 28 - 139 pM. Below the subsurface minima, the pTi concentrations again increased, to 250 - 550 pM at 200 m depth. At two stations in the tropical North Atlantic (8 °N, 24 °W and 12 °N, 25 °W), pTi maxima were observed below the subsurface minimum at 120 m depth, with pTi concentrations of 440 - 490 pM. In the South Atlantic, at 31 °S, 39 °W, the pTi concentrations showed a subsurface maximum with 280 pM of pTi at 80 m depth and

again decreasing concentrations of pTi to 66 - 100 pM further below. At 11 °S, 27 °W, the pTi concentrations increased from 97 to 162 pM between 20 and 50 m depth and were 33 - 87 pM further below.

The depth distributions of dTi showed some similarities to those of pTi. Subsurface minima occurred near the fluorescence maxima at all stations in the tropical and subtropical North Atlantic, with dTi concentrations of 50 - 100 pM. In the subtropical North Atlantic (34 °N, 14 °W), the dTi concentrations ranged uniformly around 60 pM to 60 m depth and then decreased to around 35 pM in the subsurface minima. Below the subsurface minima, the dTi concentrations increased to 74 - 137 pM. In the South Atlantic, no subsurface minima were found and the dTi concentrations were more uniformly distributed between 50 and 80 pM.

5.4 Discussion

5.4.1 Distributions of Al and Ti in the Atlantic Ocean

Surface water distributions

The surface water distributions of dAl and dTi during the two cruises were already discussed in different contexts in separate publications [Dammshäuser et al., 2011; Dammshäuser and Croot, submitted to Geochimica et Cosmochimica Acta]. The dissolved concentrations of both metals generally reflected the pattern of dust deposition into the Atlantic (Fig. 5.4). However, along the meridional Atlantic transect, specific relations to dust inputs were found for dAl and dTi. Whereas dTi concentrations agreed with the general pattern of average annual dust deposition [Jickells et al., 2005], the distribution of dAl indicates increased supply with wet deposition in the Inter-Tropical Convergence Zone (ITCZ) [Dammshäuser et al., 2011].

Similar to the dissolved fractions, the surface water distributions of pAl and pTi reflected their predominant input from atmospheric sources and the expected pattern of atmospheric inputs into the Atlantic Ocean [Duce et al., 1991; Jickells et al., 2005]. Figure 5.4 displays the surface water concentrations of pAl and pTi versus latitude between 40 °W and 14 °W (23 °W - 24 °W in the tropical North Atlantic). Highest concentrations of pAl and pTi were found in the surface waters of the tropical North Atlantic, in agreement with the increased dust deposition in this region. By contrast, much lower surface water concentrations were found in the region of the South Atlantic Gyre, where low dust deposition occurs [Duce et

al., 1991; Jickells et al., 2005]. For pTi, to our knowledge only one previous study reports surface water concentrations in our study region. Kuss and Kremling [1999] found ~100 pM of pTi in the Northeast Atlantic, which is slightly lower than our observed pTi concentrations of 158 pM. The observed pAl concentrations agree well with previous results in Atlantic surface waters [Krishnaswami and Sarin, 1976; Sherrell and Boyle, 1992; Helmers, 1996; Kuss and Kremling, 1999].

Clearly elevated surface water concentrations of pAl and pTi were found between 2 °N (May 2010) and 8 °N (December 2009; Fig. 5.4). Similar to our results, Helmers [1996] observed pAl concentrations of around 7 nM at 4 °N in May 1990. The increased concentrations of pAl around 2 - 4 °N are most likely associated to wet deposition of atmospheric mineral particles within the ITCZ. Our observed pAl concentrations at 8 °N, 30 °W in December 2009 (3 nM) also agree closely with previous finding in the same

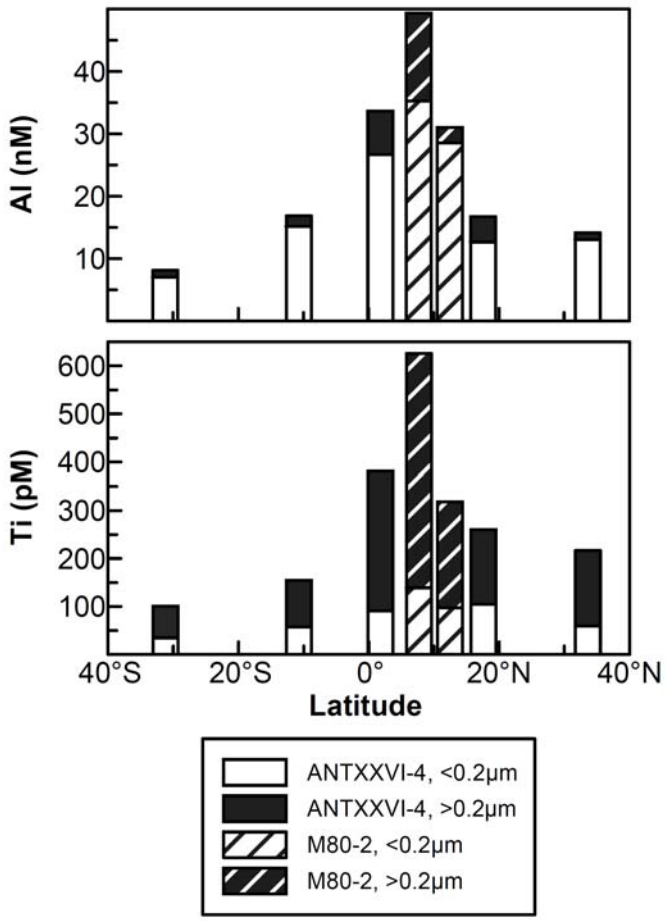

Fig. 5.4: North - South transect of surface water concentrations of dissolved and particulate Al and Ti. Black and white bars indicate sampling stations during ANTXXVI-4 (April - May 2010) the shaded bars those during M80-2 (December 2009). Sampling stations in the tropical North Atlantic were located between 23 °W and 24 °W.

region [Helmers, 1996]. However, our observed pAl concentrations of 18 nM at 8 °N, 18 °W in December 2009 (no sampling of SPM in May 2010), clearly exceed the previously reported pAl concentrations of 1- 4 nM in the same region in May 1990 [Helmers, 1996]. In general, the increasing concentrations of pAl and pTi along the 8 °N transect between 30 °W and 18 °W (Fig. 5.2) agree well with the distribution of desert dust optical depth in boreal winter [Moulin et al., 1997]. This suggests that the elevated pAl and pTi concentrations at 8 °N, 18 °W in December 2009 compared to May 1990 resulted from increased total (dry and/or wet) deposition.

In contrast to the general trend between 18 °W and 30 °W, decreased surface water concentrations of particulate and dissolved Al and Ti were found further east at 8.5 °N, 15 °W, although highest atmospheric inputs would be expected for this station. Our observation agrees with results by Bory and Newton [2000], who found more efficient down column transport of lithogenic material at a more remote mesotrophic station compared to an oligotrophic station close to the shelf in the tropical North Atlantic. This suggests that the decreased Al and Ti concentrations result from increased scavenging of the particulate phase, most likely associated with increased biological productivity [Wallace et al., 1981; Chester, 1982; Deuser et al., 1983] at the station closest to the shelf (8.5 °N, 15 °W). The removal processes and residence times of particulate and dissolved Al and Ti at the different stations are discussed in more detail below.

Vertical distributions

The vertical distributions of dAl and dTi in the tropical North Atlantic have already been discussed in a previous publication [data from M80-2; Dammshäuser and Croot, submitted to Geochimica et Cosmochimica Acta]. This section thus focuses on the particulate fractions, as well as on the additional stations in the North and South Atlantic.

Particulate and dissolved Al and Ti concentrations were elevated in the upper 20 - 40 m of the water column at those stations where increased atmospheric inputs can be expected (Figs. 5.2 and 5.3). The observed surface water elevations in the particulate phase were more pronounced for Ti than for Al, whereas for Al more pronounced surface elevations occurred in the dissolved phase. This is in agreement with the anticipated higher solubility of Al from the mineral particles [Baker et al., 2006b; Buck et al., 2010; Dammshäuser et al., 2011] and the generally stronger abundance of Al in the dissolved phase in the surface waters compared to Ti. At stations where low atmospheric inputs can be expected, depleted particulate fractions of Al and Ti were found in the surface waters. With depth, the

concentrations in both size fractions frequently decreased to subsurface minima close to the fluorescence maxima. For pAl, the observed depth distributions agree well with previously reported data in different study regions. Depleted surface water concentrations similar to our profiles in the South Atlantic and at 33 °N have been found in regions that receive low atmospheric inputs, e.g. near Bermuda [Sherrell and Boyle, 1992] and in the North Pacific [Orians and Bruland, 1986]. Surface elevations of pAl around 5 nM have been reported for stations in the Gulf Stream [Wallace et al., 1981] and in the eastern subtropical North Atlantic [29 °N; Von Oppen, 2005]. For pTi, to our knowledge no other publication reports depth distributions in the open Atlantic Ocean so far.

In the both size fractions, the observed depletion in the region of the fluorescence maxima indicates that the removal process is linked to biological productivity. In the dissolved phase, this relation could be due to active or passive biological uptake. For dAl, observations of incorporation into the silicate frustules of living or dead diatoms suggest biological uptake mechanisms [Gehlen et al., 2002; Koning et al., 2007]. However, biological productivity may also indirectly increase the removal of Al and Ti via scavenging. In the region of the fluorescence maxima, the high abundance of biogenic particles provides additional surfaces for adsorption mechanisms and thus may enhance the transfer of dissolved Al and Ti into the particulate phase. In the particulate phase, the removal generally occurs via the aggregation of suspended particulate matter to larger particles that subsequently sink through the water column. Biological productivity may increase the removal process by the formation of large biogenic particles, e.g. fecal pellets [Lal, 1977; Fowler and Knauer, 1986; Whitfield and Turner, 1987]. In the case of pAl, previous studies suggested a biological control on the removal process, based on observed removal and down column transport rates [Wallace et al., 1981; Chester, 1982], as well as seasonal variations in surface water pAl concentrations [Deuser et al., 1981; Deuser et al., 1983]. The removal of Al and Ti from the dissolved phase generally results in increasing particulate fractions. However, both size fractions were depleted in the region of the fluorescence maxima. This suggests that two steps of the scavenging mechanisms concur: 1) the transport from the dissolved into the particulate phase, likely via adsorption onto or incorporation into suspended biogenic particles and 2) the aggregation into larger particles that rapidly sink through the water column. The slightly deeper location of subsurface minima of dAl compared to pAl at some stations the tropical North Atlantic (2 - 8 °N) may result from continuing adsorption of the dissolved trace metal phases onto sinking particles. With depth the particulate and dissolved fractions of Al and Ti again increased at

most stations. This increase may result from some breakup of larger particles during the recycling of particulate organic material, and, in the particulate phase, from the continuing transfer of the dissolved trace metals.

At 33 °N, the distributions of the dAl concentrations clearly differed from any other station. Here, the subsurface dAl concentrations were elevated and up to 19 nM of dAl were found at 200 m. The dAl concentrations in the upper 100 m agree very well with previous observations by Kramer et al. [2004] at 33 °N, 13 °W. Dissolved Al concentrations above 18 nM in water depths between 100 and 400 m were also reported by Measures et al., [2008] at 20 - 35 °N, 20°W. The elevated concentrations of dAl in this region have been attributed to the propagation of Al-rich subtropical mode water from the western Atlantic basin, in agreement with previous observations of dAl concentrations of up to 40 nM in the source region [Measures et al., 2008]. In contrast to dAl, dTi concentrations were not elevated at 33 °N. This difference may result from different input mechanisms of dAl and dTi, similar to our observations in the tropical North Atlantic [Dammshäuser et al., 2011]. The western North Atlantic receives increased inputs of wet precipitation [Yuan and Miller, 2002] and the elevated solubility of aerosol Al in rainwater [Prospero et al., 1987] potentially results in excess input of dAl over dTi in this region. Indeed, Orians et al. [1990] report surface water dTi concentrations at 32 °N, 64 °W that are similar to our observations at 33 °N, 14 °W. However, more detailed information on the distribution of dTi in the western Atlantic basin would be necessary to evaluate potential differences in the supply of dAl and dTi to the eastern North Atlantic.

5.4.2 Residence times

In order to evaluate the role of the particulate and dissolved fractions in the removal processes of Al and Ti, we estimated residence time for the upper 100 m of the water column at each sampling station. For the calculation it was assumed that input solely occurs via dust deposition and that input and removal processes are in steady state. The residence time is thus given as quotient between the atmospheric flux and the inventory of the dissolved metal. The inventory was estimated as integrated metal concentration in the upper 100 m of the water column. The atmospheric flux was estimated from the average annual dust deposition given in the model composite by Jickells et al. [2005 and references therein]. For the tropical North Atlantic, the modeled deposition fluxes range between 8 and 10 g m^{-2} a^{-1} and are in good agreement with field observations [Baker et al., 2006a; Baker et al., 2006b; Baker et al., 2007]. The flux of dAl and dTi was calculate assuming

dust concentrations of 8.04 % and 0.41 % for Al and Ti [McLennan, 2001] and solubilities of 3 % and 0.1 % respectively. For Al, the solubility estimate is based on observations in Saharan dust samples [Prospero et al., 1987; Baker et al., 2006b]. For Ti, an intermediate value was chosen between results from aerosol filter leaches with deionized water [Buck et al., 2010] and significantly lower Ti solubilities of <0.01 % that had been observed in seawater incubations with Saharan dust [Dammshäuser et al., 2011]. The utilized value of 0.1 % agrees well with most recent observations of 0.08 % Ti solubility (0.03 - 0.18 %; n = 7) in Saharan dust (R. Shelley, P. Morton and W. M. Landing, personal communication). However, the assumed solubilities are key uncertainties in the residence time calculation. The estimated inventories and residence times for particulate, dissolved and total Al and Ti are given in Table 5.3.

The residence times in the particulate phase were 3 - 22 days for pAl and 4 - 37 days for pTi in the tropical and subtropical North Atlantic. For pAl, these values agree well with previous observations in the eastern subtropical North Atlantic [Bory and Newton, 2000; Von Oppen, 2005]. In the South Atlantic, longer residence times were found for both metals, with 56 - 61 days for pAl and 125 - 171 days for pTi. The longer residence times are most likely associated with reduced biological activity and thus less pronounced aggregation and removal of suspended particulate matter at these stations (see section 5.4.1). For pAl, the observed residence times in the South Atlantic are in agreement with estimations of 54 days in the Gulf stream [Wallace et al., 1981] and of up to 80 days in the Sargasso Sea [Deuser et al., 1983] that were based on pAl fluxes to depth. The observed residence times of pAl and pTi are broadly in the same range and show similar spatial variations. This suggests a close relation in the removal of pAl and pTi that is likely associated with general particle dynamics in the upper water column. The slightly shorter residence times of pAl may result from more pronounced transfer of Al from the particulate into the dissolved phase due to higher solubility of Al from atmospheric mineral particles compared to Ti.

The residence times of the dissolved fractions are clearly higher than those of the particulate fractions, about one to two orders of magnitude in the case of Al and two to three orders of magnitude in the case of Ti. In the tropical and subtropical North Atlantic the residence times were 0.9 - 3.8 years for dAl and 10 - 31 years for dTi. In the South Atlantic, the residence times in the dissolved phase were 14 - 28 years for dAl and 190 - 236 years for dTi. The spatial differences are similar to our observations for the particulate fractions and likely result from lower scavenging rates and/or uptake due to

Table 5.3: Inventories and residence times for Al and Ti in the upper 100 m of the water column. Residence times of the total trace metals (particulate + dissolved, tAl and tTi) were calculated from total deposition fluxes, those of the particulate and dissolved trace metal fractions (dAl and dTi) from the assumed particulate and soluble deposition fluxes.

				Inventories (Al: µmol m^{-2}, Ti: nmol m^{-2})				Residence times					
Station	Lat.	Lon.	Deposition (g m^{-2} a^{-1})	pAl	dAl	pTi	dTi	pAl (d)	pTi (d)	dAl (a)	dTi (a)	tAl (d)	tTi (d)
16	8.5	-15.0	9.90	222	1665	12.5	12.6	3	5	1.1	15	23	11
29	8.0	-19.00	8.76	783	1818	32.1	12.3	11	16	1.4	16	36	22
48	7.7	-24.2	8.39	757	1907	28.2	11.4	11	14	1.5	16	39	20
62	8.0	-30.0	7.69	286	2340	10.4	9.0	5	6	2.0	14	42	11
81	12.0	-25.0	10.09	286	1316	21.7	9.6	3	9	0.9	11	19	13
272	-31.2	-39.4	0.31	136	626	12.5	5.1	56	171	14	190	300	240
279	-10.7	-26.9	0.32	153	1361	9.5	6.5	61	125	28	236	575	212
283	1.8	-23.0	3.03	508	1709	26.2	8.0	22	37	3.8	31	90	48
287	17.6	-24.3	9.60	193	1041	9.1	8.3	3	4	0.7	10	16	8
294	33.6	-13.9	2.42	179	1077	16.2	5.3	10	28	3.0	26	63	38

smaller biological productivity and abundance of biogenic particles at the stations in the South Atlantic. For dAl, the observed residence times lay in the same range as previously reported values of 0.5 - 1 years in the eastern subtropical North Atlantic [Von Oppen, 2005], of ~4 years for the central Pacific Ocean [Orians and Bruland, 1986], of 4.5 - 13 years for the Sargasso Sea [Orians and Bruland, 1986; Jickells, 1999], and as results from modeling approaches for different regions in the Atlantic [Gehlen et al., 2003; Han et al., 2008]. The shorter residence times of dAl compared to dTi indicate higher reactivity of dAl in the upper water column. This also agrees with the more pronounced removal of dAl between the surface waters and the subsurface minima observed at most stations (Figs. 5.2 and 5.3), and suggests more pronounced scavenging of dAl compared to dTi. A higher susceptibility to scavenging processes is also indicated by observed higher colloidal associations of Al compared to Ti [Dammshäuser and Croot, submitted to Geochimica et Cosmochimica Acta] and Al/Ti ratios in sediments [Murray and Leinen, 1996; Dymond et al., 1997; Timothy and Calvert, 1998].

Considering the total (particulate + dissolved) trace metals (tAl and tTi) in the upper 100 m of the water column, residence times of 16 - 90 days for tAl and 8 - 48 days for tTi were estimated in the tropical and subtropical North Atlantic. Again the residence times are

clearly higher in the South Atlantic. Previous estimations of tAl residence times of 235 - 255 days in the Sargasso Sea [Jickells, 1999] lie well in between our observations for the different regions. The observation of shorter residence times for tTi compared to tAl is in contrast to the findings for the particulate and dissolved fractions. This difference can be explained by the higher association of Ti with the particulate phase. The residence times of tTi are thus mostly controlled by the fast removal of the particulate phase, whereas the residence times of tAl are rather determined by the slower removal processes in the dissolved phase.

5.4.3 Partitioning between the particulate and dissolved fractions

The coefficients of partitioning between the particulate and the dissolved phase for Al and Ti are given in Tables 5.1 and 5.2 and displayed in Figs. 5.2 and 5.3 (dotted lines). Overall, the major fraction of Al was present in the dissolved phase, whereas Ti predominantly occurred in the particulate form. On average, 75 % (28 - 96 %) of the total Al and 36 % (12 - 71 %) of the total Ti were dissolved. Thus, the partitioning coefficients ([particulate]/[dissolved]) were mostly lower for Al (pAl/dAl = 0.04 - 2.62) than for Ti (pTi/dTi = 0.42 - 7.57). The observed differences generally agree with the predicted higher particle reactivity of Ti compared to Al due to its occurrence as quadrivalent ion ($TiO(OH)_2$) in seawater [Li, 1981; Li, 2011].

The partitioning coefficients of Al and Ti showed characteristic vertical distributions (Figs. 5.2 and 5.3). For Al, the partitioning coefficients increased with depth at most stations, as a result of decreasing dAl and slightly increasing pAl concentrations. This distribution reflects the considerable input of dAl via dissolution of atmospheric mineral particles into the surface waters, and the subsequent removal of dAl via scavenging mechanisms in subsurface waters. In contrast to Al, the partitioning coefficients of Ti mostly lay in the same range at the surface and at 200 m depth. Largest deviations between the partitioning coefficients of Al and Ti were observed in the surface waters. This difference between both metals agrees with the assumed lower solubility of Ti from atmospheric mineral particles compared to Al (see residence time calculation in section 5.4.2) and the prevailing input of Ti in the particulate form.

The specific partitioning of Al and Ti between the particulate and the dissolved fraction is also reflected in the depth distributions of Al/Ti ratios (Fig. 5.5). In the surface waters, Al/Ti ratios in the dissolved phase were elevated (dAl/dTi = 60.5 - 147.7) compared to the crustal ratio (Al/Ti = 19.61) given by McLennan [2001]. By contrast, lower Al/Ti ratios

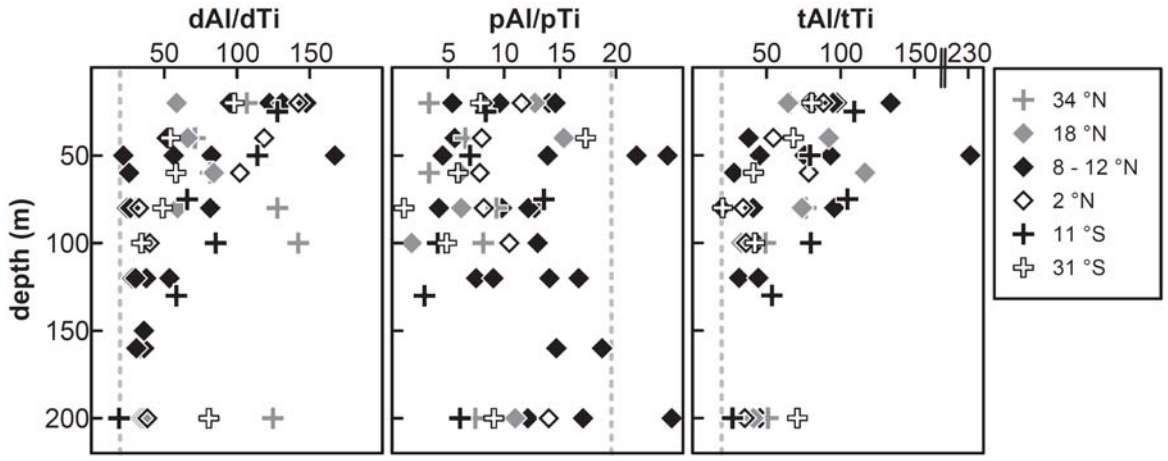

Fig. 5.5: Depth distributions of dissolved, particulate and total Al/Ti ratios (weight/weight) from all analyzed samples. The sampled stations during ANTXXVI-4 are distinguished by latitude; those from M80-2 are grouped as black diamonds. The dashed grey line marks the elemental ratio given by McLennan [2001].

compared to the crustal source were found in the particulate phase (pAl/pTi = 5.4 - 14.6). These deviations agree with the perception that excess Al over Ti is supplied in the dissolved phase via the dissolution of atmospheric mineral particles. With depth, the Al/Ti ratios in both the particulate and the dissolved phase approached the crustal ratio [McLennan, 2001]. This is in agreement with the scavenging removal of dAl in the subsurface waters and thus the (re-)transfer of dAl from the dissolved into the particulate phase. The distributions of dAl/dTi and pAl/pTi ratios indicate that the scavenging process is more pronounced for dAl compared to dTi. Similar to the dissolved fractions, the elemental ratios of the total trace metals (tAl/tTi) were clearly elevated at the surface and decreased with depth to values close to the crustal ratio (Fig. 5.5). This agrees with the clearly longer residence times of both Al and Ti in the dissolved compared to the particulate phase, and the stronger partitioning of Al into the dissolved phase in the surface waters. Thus, upon the atmospheric delivery Ti seems to be rapidly removed via scavenging of the particulate phase, whereas Al partitions into the dissolved phase and accumulates in the upper water column.

For both trace metals, the partitioning coefficients frequently showed subsurface minima close to the fluorescence maxima. In previous studies, an inverse relationship has been observed between partitioning coefficients and particle concentrations [Honeyman et al., 1988; Balls, 1989]. Similarly, our observed low partitioning coefficients may be associated to high particle abundances in the region of the fluorescence maxima. The decreasing

partitioning coefficients can mostly be ascribed to pronounced decreases in the particulate compared to the dissolved fractions. Thus, in the region of the subsurface minima the removal of pAl and pTi appears to exceed the removal of dAl and dTi, which agrees with the longer residence times of Al and Ti in the dissolved compared to the particulate phase. This indicates that the removal of pAl and pTi via aggregation and sinking mechanisms occurs faster than the transfer of dAl and dTi into the particulate phase.

5.5 Conclusions

The spatial and vertical distributions of particulate and dissolved Al and Ti in the upper water column of the Atlantic Ocean reflect their predominant supply via the deposition of atmospheric mineral particles and their removal via scavenging mechanisms. Surface water concentrations of Al and Ti were in agreement with the expected pattern of dust inputs. The depth distributions were mostly characterized by elevated surface concentrations and subsurface minima close to the fluorescence maxima in both size fractions of Al and Ti. Subsurface minima occurred at stations with pronounced fluorescence maxima, suggesting that biological productivity controls the removal of the dissolved and particulate metals. The removal of dissolved Al and Ti from the dissolved phase may be directly associated to biological productivity due to uptake mechanisms, or indirectly via adsorption and aggregation processes on biogenic particle surfaces. In the particulate phase, removal processes may be increased via the formation of large, fast sinking biogenic particles (e.g. fecal pellets). The depletion of both particulate and dissolved fractions of Al and Ti near the fluorescence maxima suggests that the transfer from the dissolved into the particulate phase concurs with the transfer of SPM into larger particles that rapidly sink through the water column.

Estimated residence times in the particulate phase were 3 - 22 days for pAl and 4 - 37 days for pTi in the tropical and subtropical North Atlantic. In the dissolved phase the residence times were 0.9 - 3.8 years for dAl and 10 - 31 years for dTi. In both size fractions clearly longer residence times were found in the South Atlantic, likely associated to lower biological productivity and decreased removal processes in this region. Broadly similar residence times of particulate Al and Ti suggest that the removal is controlled by general particle dynamics in the upper water column. In the dissolved phase, shorter residence times of Al indicate higher susceptibility to scavenging removal compared to Ti.

The partitioning between the dissolved and the particulate phase differed for Al and Ti.

The major fraction of Al was present in the dissolved form (pAl/dAl = 0.04 - 2.62), whereas Ti mostly occurred in the particulate form (pTi/dTi = 0.42 - 7.57). Largest deviations in the partitioning coefficients occurred in the surface waters, where also excess dAl and excess pTi compared to the crustal ratio were present. This indicates elevated atmospheric supply of Al in the dissolved form, whereas Ti is predominantly supplied in the particulate form. With depth, increasing partitioning coefficients for Al agree with the scavenging removal of dAl. Minima of the partitioning coefficients in the region of the fluorescence maxima suggest that the removal of pAl and pTi via aggregation and sinking mechanisms exceeds the transfer from the dissolved into the particulate phase.

Acknowledgements: We thank the crews of RV Meteor and RV Polarstern for their support during M80-2 and ANTXXVI-4. Thanks are also due to our collegues O. Baars, D. Gaiero and M. Heller for their help during the sampling and shipboard laboratory work, and to U. Westernströer for the ICP-MS analyses. The Financial support for this work was provided by SOPRAN (BMBF FKZ 03F0462A and 03F0611A), and the DFG via grants to P. Croot (CR145/15-1 and CR145/18-1). T. Wagener was supported by a Marie Curie IEF (Grant agreement No.: PIEF-GA-2009-236694, DAPOP).

5.6 References

Baker A. R., French M. and Linge K. L. (2006a) Trends in aerosol nutrient solubility along a west-east transect of the Saharan dust plume. *Geophysical Research Letters* **33**, L07805, doi:10.1029/2005GL024764.

Baker A. R., Jickells T. D., Witt M. and Linge K. L. (2006b) Trends in the solubility of iron, aluminium, manganese and phosphorus in aerosol collected over the Atlantic Ocean. *Marine Chemistry* **98**, 43-58.

Baker A. R., Weston K., Kelly S. D., Voss M., Streu P. and Cape J. N. (2007) Dry and wet deposition of nutrients from the tropical Atlantic atmosphere: Links to primary productivity and nitrogen fixation. *Deep Sea Research Part I: Oceanographic Research Papers* **54**, 1704-1720.

Baker A. R., Lesworth T., Adams C., Jickells T. D. and Ganzeveld L. (2010) Estimation of atmospheric nutrient inputs to the Atlantic Ocean from 50 °N to 50 °S based on large-scale field sampling: Fixed nitrogen and dry deposition of phosphorus. *Global Biogeochemical Cycles* **24**, GB3006, doi:10.1029/2009gb003634.

Balls P. W. (1989) The partition of trace metals between dissolved and particulate phases in European coastal waters: A compilation of field data and comparison with laboratory studies. *Netherlands Journal of Sea Research* **23**, 7-14.

Bory A. J. M. and Newton P. P. (2000) Transport of airborne lithogenic material down through the water column in two contrasting regions of the eastern subtropical North Atlantic Ocean. *Global Biogeochemical Cycles* **14**, 297-315.

Bowie A. R., Townsend A. T., Lannuzel D., Remenyi T. A. and van der Merwe P. (2010) Modern sampling and analytical methods for the determination of trace elements in marine particulate material using magnetic sector inductively coupled plasma-mass spectrometry. *Analytica Chimica Acta* **676**, 15-27.

Buck C. S., Landing W. M., Resing J. A. and Measures C. I. (2010) The solubility and deposition of aerosol Fe and other trace elements in the North Atlantic Ocean: Observations from the A16N CLIVAR/CO_2 repeat hydrography section. *Marine Chemistry* **120**, 57-70.

Chester R. (1982) Particulate aluminium fluxes in the eastern Atlantic. *Marine Chemistry* **11**, 1-16.

Croot P. L. (2011) Rapid determination of picomolar titanium in seawater with catalytic cathodic stripping voltammetry. *Analytical Chemistry* **83**, 6395-6400.

Dammshäuser A., Wagener T. and Croot P. L. (2011) Surface water dissolved aluminum and titanium: Tracers for specific time scales of dust deposition to the Atlantic? *Geophysical Research Letters* **38**, L24601, doi:10.1029/2011gl049847.

Deuser W. G., Brewer P. G., Jickells T. D. and Commeau R. F. (1983) Biological control of the removal of abiogenic particles from the surface ocean. *Science* **219**, 388-391.

Deuser W. G., Ross E. H. and Anderson R. F. (1981) Seasonality in the supply of sediment to the deep Sargasso Sea and implications for the rapid transfer of matter to the deep ocean. *Deep Sea Research Part A. Oceanographic Research Papers* **28**, 495-505.

Duce R. A., Liss P. S., Merrill J. T., Atlas E. L., Buat-Menard P., Hicks B. B., Miller J. M., Prospero J. M., Arimoto R., Church T. M., Ellis W., Galloway J. N., Hansen L., Jickells T. D., Knap A. H., Reinhardt K. H., Schneider B., Soudine A., Tokos J. J., Tsunogai S., Wollast R. and Zhou M. (1991) The atmospheric input of trace species to the World Ocean. *Global Biogeochemical Cycles* **5**, 193-259.

Dymond J., Collier R., McManus J., Honjo S. and Manganini S. (1997) Can the aluminium and titanium contents of ocean sediments be used to determine the paleoproductivity of the oceans? *Paleoceanography* **12**, 586-593.

Fowler S. W. and Knauer G. A. (1986) Role of large particles in the transport of elements and organic compounds through the oceanic water column. *Progress In Oceanography* **16**, 147-194.

Garbe-Schönberg C.-D. (1993) Simultaneous determination of thirty-seven trace elements in twenty-eight international rock standards by ICP-MS. *Geostandards Newsletter* **17**, 81-97.

Gehlen M., Beck L., Calas G., Flank A. M., van Bennekom A. J. and van Beusekom J. E. E. (2002) Unraveling the atomic structure of biogenic silica: Evidence of the structural association of Al and Si in diatom frustules. *Geochimica et Cosmochimica Acta* **66**, 1601-1609.

Gehlen M., Heinze C., Maier-Reimer E. and Measures C. I. (2003) Coupled Al-Si geochemistry in an ocean general circulation model: A tool for the validation of oceanic dust deposition fields? *Global Biogeochemical Cycles* **17**, 1028, doi:10.1029/2001gb001549.

Han Q., Moore J. K., Zender C., Measures C. I. and Hydes D. J. (2008) Constraining oceanic dust deposition using surface ocean dissolved Al. *Global Biogeochemical Cycles* **22**, GB2003, doi:10.1029/2007gb002975.

Helmers E. (1996) Trace metals in suspended particulate matter of Atlantic Ocean surface water (40 °N to 20 °S). *Marine Chemistry* **53**, 51-67.

Honeyman B. D., Balistrieri L. S. and Murray J. W. (1988) Oceanic trace metal scavenging: The importance of particle concentration. *Deep Sea Research Part A. Oceanographic Research Papers* **35**, 227-246.

Hydes D. J. (1979) Aluminum in seawater: Control by inorganic processes. *Science* **205**, 1260-1262.

Hydes D. J. and Liss P. S. (1976) Fluorimetric method for the determination of low concentrations of dissolved aluminum in natural waters. *Analyst* **101**, 922-931.

Jickells T. D. (1999) The inputs of dust derived elements to the Sargasso Sea; A synthesis. *Marine Chemistry* **68**, 5-14.

Jickells T. D., An Z. S., Andersen K. K., Baker A. R., Bergametti G., Brooks N., Cao J. J., Boyd P. W., Duce R. A., Hunter K. A., Kawahata H., Kubilay N., laRoche J., Liss P. S., Mahowald N., Prospero J. M., Ridgwell A. J., Tegen I. and Torres R. (2005) Global iron connections between desert dust, ocean biogeochemistry, and climate. *Science* **308**, 67-71.

Koning E., Gehlen M., Flank A. M., Calas G. and Epping E. (2007) Rapid post-mortem incorporation of aluminum in diatom frustules: Evidence from chemical and structural analyses. *Marine Chemistry* **106**, 208-222.

Kramer J., Laan P., Sarthou G., Timmermans K. R. and de Baar H. J. W. (2004) Distribution of dissolved aluminium in the high atmospheric input region of the subtropical waters of the North Atlantic Ocean. *Marine Chemistry* **88**, 85-101.

Krishnaswami S. and Sarin M. M. (1976) Atlantic surface particulates: Composition, settling rates and dissolution in the deep sea. *Earth and Planetary Science Letters* **32**, 430-440.

Kuss J. and Kremling K. (1999) Spatial variability of particle associated trace elements in near-surface waters of the North Atlantic (30 °N / 60 °W to 60 °N / 2 °W), derived by large volume sampling. *Marine Chemistry* **68**, 71-86.

Lal D. (1977) The oceanic microcosm of particles. *Science* **198**, 997-1009.

Li Y.-H. (1981) Ultimate removal mechanisms of elements from the ocean. *Geochimica et Cosmochimica Acta* **45**, 1659-1664.

Li Y.-H. (1991) Distribution patterns of the elements in the ocean: A synthesis. *Geochimica et Cosmochimica Acta* **55**, 3223-3240.

Li Y.-H. (2011) Partition of elements between solid and liquid phases in aquatic environments. *Aquatic Geochemistry* **17**, 697-725.

McLennan S. M. (2001) Relationships between the trace element composition of sedimentary rocks and upper continental crust. *Geochemistry Geophysics Geosystems* **2**, 1021, doi:10.1029/2000gc000109.

Measures C. I. and Vink S. (2000) On the use of dissolved aluminum in surface waters to estimate dust deposition to the ocean. *Global Biogeochemical Cycles* **14**, 317-327.

Measures C. I., Landing W. M., Brown M. T. and Buck C. S. (2008) High-resolution Al and Fe data from the Atlantic Ocean CLIVAR-CO2 repeat hydrography A16N transect: Extensive linkages between atmospheric dust and upper ocean geochemistry. *Global Biogeochemical Cycles* **22**, GB1005, doi:10.1029/2007gb003042.

Moulin C., Lambert C. E., Dulac F. and Dayan U. (1997) Control of atmospheric export of dust from North Africa by the North Atlantic Oscillation. *Nature* **387**, 691-694.

Murray R. W. and Leinen M. (1996) Scavenged excess aluminum and its relationship to bulk titanium in biogenic sediment from the central equatorial Pacific Ocean. *Geochimica et Cosmochimica Acta* **60**, 3869-3878.

Orians K. J., Boyle E. A. and Bruland K. W. (1990) Dissolved titanium in the open ocean. *Nature* **348**, 322-325.

Orians K. J. and Bruland K. W. (1986) The biogeochemistry of aluminum in the Pacific Ocean. *Earth and Planetary Science Letters* **78**, 397-410.

Potts P. J. P., Thompson M., Chenery S. R. N., Webb P. C. and Kasper H. U. (2003), GeoPT13 - An international proficiency test for analytical geochemistry laboratories - Report on round 13 / July 2003 (Köln Loess), International Association of Geoanalysts. www.geoanalyst.org/geopt/GeoPT13Report.pdf.

Prospero J. M., Nees R. T. and Uematsu M. (1987) Deposition rate of particulate and dissolved aluminium derived from Saharan dust in precipitation at Miami, Florida. *Journal of Geophysical Research* **92**, 14723-14731.

Rohardt G. and Bracher A. (2011), Physical oceanography during POLARSTERN cruise ANT-XXVI/4, Alfred Wegener Institute for Polar and Marine Research, Bremerhaven, doi:10.1594/PANGAEA.758127.

Sherrell R. M. and Boyle E. A. (1992) The trace metal composition of suspended particles in the oceanic water column near Bermuda. *Earth and Planetary Science Letters* **111**, 155-174.

Timothy D. A. and Calvert S. E. (1998) Systematics of variations in excess Al and Al/Ti in sediments from the central Equatorial Pacific. *Paleoceanography* **13**, 127-130.

Turekian K. K. (1977) The fate of metals in the oceans. *Geochimica et Cosmochimica Acta* **41**, 1139-1144.

Turner D. R., Whitfield M. and Dickson A. G. (1981) The equilibrium speciation of dissolved components in freshwater and sea water at 25 °C and 1 atm pressure. *Geochimica et Cosmochimica Acta* **45**, 855-881.

Von Oppen C. (2005) Zum Kreislauf der Spurenmetalle Aluminium, Eisen und Mangan im subtropischen Ostatlantik (Kanarische Inseln): Vertikaltransport und Wechselwirkungen zwischen Partikeln und Lösung. PhD Thesis, Universität Bremen.

Wallace G. T., Mahoney O. M., Dulmage R., Storti F. and Dudek N. (1981) First-order removal of particulate aluminium in oceanic surface layers. *Nature* **293**, 729-731.

Whitfield M. and Turner D. R. (1987) The role of particles in regulating the composition of seawater. In *Aquatic Surface Chemistry* (ed. Stumm W.). John Wiley & Sons, Inc., New York, pp. 457-493.

Yuan J. and Miller R. L. (2002) Seasonal variation in precipitation patterns to the global ocean: An analysis of the GPCP version 2 data set. *Global Biogeochemical Cycles* **16**, 1103, doi: 10.1029/2001gb001458.

6 Synthesis

This thesis focused on the distributions and the behavior of the lithogenic trace elements Al and Ti in the upper water column of the Atlantic Ocean. The potential utilization of Al and Ti as dust tracers was evaluated. Furthermore, principal processes were constrained that occur after the atmospheric supply of both metals, in order to lay a basis for the successful application of Al and Ti as dust tracers.

Chapter 3 dealt with the specific relationships of surface water dissolved Al and Ti concentrations to dust deposition estimates along a meridional Atlantic transect. A novel finding is that Ti may serve as complementary dust tracer to Al, with both metals reflecting different time scales of dust deposition. Whereas dissolved Al concentrations may serve to trace seasonal variations in the dust deposition, dissolved Ti concentrations reflect variations in the dust deposition over longer time scales. However, any calculation of dust inputs from surface water concentrations requires an accurate knowledge of the solubilities of Al and Ti from mineral dust and their residence times in the upper water column. Here, evidence was presented for increased dissolution of Al during wet deposition and for significant spatial variations in the residence times of both metals that preclude a simple calculation.

Chapter 4 dealt with the role of colloidal associations in the removal of Al and Ti from the upper water column of the eastern tropical North Atlantic. Despite the hydrolyzed speciation and high particle reactivity of Al and Ti that suggest high colloidal associations, the predominant part of both metals was found in the soluble phase (smaller than 10 kDa). Thess size distributions can be explained by low tendencies to form organic or inorganic colloids, as both metals occurred within their inorganic solubility levels and are not known to form organic complexes in seawater. Given the high susceptibility of Al and Ti to scavenging and the anticipated role of colloidal species as intermediate in the scavenging process, the results indicate two potential mechanisms for the transfer from the soluble into the particulate phase: a) rapid turnover and thus short residence times of the colloidal phase, and/or b) direct adsorption of the hydrolyzed species on the particulate fraction.

The role of the particulate phase in the scavenging removal of Al and Ti was dealt with in Chapter 5. The distributions of both metals indicate that two steps of the scavenging process concur; the transfer from the dissolved into the particulate phase and the transfer of

suspended particulate matter into larger particles that rapidly sink through the water column. For both sub-processes, a relation to biological productivity has been identified. In the dissolved phase, this relation is likely based on adsorption and aggregation processes on biogenic particle surfaces. In the particulate phase, biological productivity may increase the formation of large and fast sinking biogenic particles.

Estimated residence times in the particulate phase ranged between 3 and 22 days for Al and between 4 and 37 days for Ti. In the dissolved phase, the residence times ranged between 0.9 and 3.8 years for Al and between 10 and 31 years for Ti. In agreement with the anticipated lower biological activity, clearly longer residence times were estimated in the South Atlantic Gyre. The broad similarity in the residence times in the particulate phase suggests a combined removal process for particulate Al and Ti, whereas larger deviations in the dissolved phase indicate a higher susceptibility to scavenging removal for dissolved Al compared to dissolved Ti.

A major finding of this work is the potential suitability of surface water dissolved Ti concentrations as dust tracer. The combined consideration of both Al and Ti could allow a more precise estimation of dust deposition into the surface ocean via a multi-tracer approach. So far, such an application has been limited by the lack of information on both the distribution and the processes of Ti in the surface ocean. The present study helps to overcome this gap and gives detailed insights into removal processes and residence times of Al and Ti in regions that largely vary in their dust inputs and biological productivity. The findings may thus provide the basis for further estimations of dust inputs from Ti and Al concentrations, e.g. in modeling approaches. However, the seawater soluble fractions of both metals in atmospheric mineral particles remain a major uncertainty in the relationship between surface water concentrations and dust inputs. During this work, solubilities of both metals were indirectly assessed from elemental ratios in the surface waters of the tropical and subtropical Atlantic, and evidence was found for higher solubility of Al compared to Ti. A major aim for future studies is to better constrain the fractional dissolution of Al and Ti from sampled atmospheric mineral particles.

Acknowledgements

This PhD project was realized under the supervision of Dr. Peter Croot. I would like to thank him for making this work possible and for his support during the period of my PhD.
Prof. Dr. Arne Körtzinger took over the supervision of my PhD project after the leaving of Dr. Croot and Prof. Dr. Douglas Wallace, and agreed to act as referee for this study. I am grateful for his support and strategic advice during the final period of my PhD.
I would like to thank Prof. Dr. Douglas Wallace for acting as co-referee, even after his leave to Halifax.
My sincere thanks are also due to Prof Dr. Martin Frank, for constructive comments during the thesis committee meetings, for providing the laboratory facilities for the filter digestions, and for his encouragement during critical periods in the past three years.
During the work for my PhD project I benefited from the support and the experiences of many colleagues. I am deeply grateful for this help and for the enjoyable working atmosphere both at the institute and during the research cruises I participated in.
In particular, I would like to thank Thibaut Wagener for the pleasant cooperation and his encouragements during ANTXXVI-4, for fruitful discussion on the different manuscripts, and for proof reading parts of this thesis.
I am also grateful to Oliver Baars for diverting conversations and his help during virtually endless filtration night shifts during M80-2.
Peter Streu is thanked for his support and for sharing his experience during the laboratory work in Kiel.
I am much obliged to Dieter Garbe-Schönberg and Ulrike Westernströer for their successful efforts with the ICP-MS measurements.
I sincerely thank Harald Schunck and Janine Flöter for relaxing coffee breaks, stimulating discussions, Matlab support and their dog sitting services in the last months.
I am deeply grateful for the consistent confidence of my parents Lothar and Birgit Dammshäuser.
Finally, my affectionate thanks are due to Florian Scholz for accepting my moods and for supporting and encouraging me in any possible way.

Anna Dammshäuser

Saarbrückenstraße 26
24114 Kiel
+49 (0)431 60831143
adammshaeuser@geomar.de
Date of birth: 03.06.1982
Place of birth: Gießen

Curriculum Vitae

Since 09/2008	**Research associate** at the Helmholtz Centre for Ocean Research Kiel (GEOMAR), Department of Chemical Oceanography
05/2008 - 06/2008	**Research associate** at the Leibniz Institute for Baltic Sea Research Warnemünde (IOW), Department of Marine Chemistry
05/2008	Diploma thesis at the Leibniz Institute for Baltic Sea Research Warnemünde (IOW), Department of Marine Chemistry: **„Distribution and behavior of atrazine and its degradation products in coastal waters of the lagoon Mundaú-Manguaba, Brazil“**
09/2004 - 07/2005	Studies of **„Ciências do meio aquático“** („aquatic environmental sciences“) at the University of Porto, Portugal
10/2001 - 05/2008	Studies of **„Geoökologie“** at the University of Karlsruhe (TH)

Kiel, January 2012